School of Electronic, Electrical and Systems Engineering

UNIVERSITY OF BIRMINGHAM

Decarbonisation Cost Optimisation for Diesel Railway Traction System Conversion

A thesis submitted to the University of Birmingham for the degree of

DOCTOR OF PHILOSOPHY

Supervisors: Prof. Clive Roberts

Prof. Stuart Hillmansen

Student Name: Yizhe Zhang

Date Submitted: 2023-12-12

Abstract

In the field of transportation, especially with trains, lowering carbon emissions is a very important problem. This thesis introduces a novel approach centred on cost optimisation for converting from diesel-powered trains to more environmentally sustainable alternatives. It combines different new green power technologies like electrification, hydrogen fuel cells, and batteries, with the goal to reduce carbon emissions and also keeping in mind the cost. A significant aspect of this research involves the development of a multi-mode train simulator. This innovation in railway technology enables accurate calculations of energy consumption and efficient management of various power systems in different operational scenarios. Its capability to handle train operation strategies is important, enabling more accurate assessments of the cost-effectiveness in decarbonisation strategies.

The study includes a detailed economic analysis over a period of 40 years. This analysis focuses mainly on the costs involved, including replacing diesel parts, installing new power systems, and their maintenance over a long time. This deep cost analysis gives important understanding about the money aspects of changing to green power in trains. Also, the research uses advanced methods like the Genetic Algorithm and Particle Swarm Optimisation to accurately change important things such as how long the electrification should be and how powerful the energy systems need to be. These methods are used to find the best ways to save costs, showing a new way of looking at costs in making railways more eco-friendly.

The results of the study about saving money are obvious. The research shows that using trains with different modes could make the costs go down by 40.4% compared to normal diesel trains, as seen in the example of the train route from London St. Pancras to Leicester. This shows the financial good points of using different kinds of green power in trains. The study also looks at

how trains powered by hydrogen might be used in the future. Right now, they are not as cost-saving as other choices, but the study says they might become better as the price of hydrogen goes down. This part of the research shows how new green power can change the way we think about making trains more eco-friendly in the future, especially about the costs.

In summary, this study is very important for making trains more eco-friendly, focusing a lot on saving costs. By bringing together new technologies and ways of doing things, it deals with environmental problems while also thinking a lot about how much things cost. The ideas and ways used in this study are very useful for making future plans and policies in trains, leading to a future that is both more sustainable and saves money.

Publication

Zhang, Y., Tian, Z., Roberts, C., Hillmansen, S. and Chen, M., 2022. Cost optimization of multi-mode train conversion for discontinuously electrified routes. International Journal of Electrical Power & Energy Systems, 138, p.107993.

Kamel, T., Amor, P., Polater, N., Zhang, Y., Tian, Z., Hillmansen, S. and Tricoli, P., 2023. Development of a smart hybrid drive system with advanced logistics for railway applications. International Journal of Hydrogen Energy.

Acknowledgement

Firstly, I would like to express my sincere gratitude to my supervisors, Prof. Clive Roberts and Prof. Stuart Hillmansen, for their encouragement and valuable guidance in my studies and for their care in my daily life. They led me into the railway industry and taught me a lot. They have not only given feedback and suggestions but also motivated me for the research.

Secondly, I would like to say a special thank you to Dr Zhongbei Tian, Dr Ning Zhao, and Dr Jie Tang. Without their valuable knowledge and thoughtful guidance, I could not have completed all my work successfully. Thanks to all my colleagues in BCRRE, I got a deeper and broader understanding of the railway system every time I discussed it with them. Our discussion is located everywhere in my thesis, with many thanks to my friends, who enhanced my daily life and shared the enjoyable experience.

Last but not least, I want to thank my family. Especially thanks to my parents for their unwavering support and trust in me during my PhD study. Words cannot express my gratitude for their love. They are always the best teammates in my life.

Table of Contents

List of Figures

List of Tables

List of Abbreviations

Term	Explanation
AC	Alternating Current
AT	Autotransformer
BCRRE	Birmingham Centre for Railway Research and Education
BF	Brute Force
BT	Booster Transformer
CC	Constant Current
CV	Constant Voltage
DC	Direct Current
DOD	Depth of Discharge
ESSDs	Energy Storage System Devices
GA	Genetic Algorithm
GB	Great Britain (England, Scotland, and Wales)
GSA	Global Sensitivity Analysis

Term	Explanation
HFC	Hydrogen Fuel Cell
LSA	Local Sensitivity Analysis
MML	Midland Main Line
NPV	Net Present Value
OAT	One-at-a-Time
OHL	Overhead Line
PSAT	Powertrain System Analysis Toolkit
PSO	Particle Swarm Optimisation
PVB	Present Value of Benefits
PVC	Present Value of Costs
RIA	Railway Industry Association
RSSB	Rail Safety and Standards Board
SA	Sensitivity Analysis
SOC	State of Charge
STK	Single Track Kilometre
STM	Single Track Mile
STS	Single-Train Simulator
TDNS	Traction Decarbonisation Network Strategy

Term	Explanation
TF	Time Factor
TPS	Train Performance Simulation
UK	United Kingdom (Great Britain and Northern Ireland)

1 Introduction

1.1 Background

Climate change is a global concern that threatens humans and the environment in which we live. In December 2015, 195 countries adopted the first universal, legally binding global climate deal, the Paris Agreement. The agreement's central aim is to strengthen the global response to the threat of climate change by keeping the global temperature rise this century well below 2 °C above pre-industrial levels and to pursue efforts to limit the temperature increase to 1.5 °C. The Paris Agreement is a bridge between today's policies and climate neutrality before the end of the century. On 18 November 2016, the United Kingdom (UK) government announced that it had ratified the Paris Agreement. This was recognised globally with the adoption of the Paris Climate Agreement, which created a legally binding aim for mitigating the effects of global warming and associated climate change. On 12 February 2018, Minister for Trains Jo Johnson MP urged the rail sector to take bolder measures toward a greener future. He pushed the industry, in particular, to phase out "all diesel-only trains by 2040" and to offer "a clear, long-term strategy with consistent objectives and incentives" that included "ambitious and bold plans on decarbonising the whole rail sector".

Table 1 Modal share in England, 2022 [1]

	Walk	Car or van	Bus	Rail	Cycle	Other
Trips	30.9%	58.2%	4.4%	2.6%	1.8%	2.1%
Distance	4.1%	78.0%	3.5%	9.8%	1.1%	2.8%

Rail is one of the greenest transport modes in the UK [2]. Rail offers a mass transport solution with relatively low emissions (especially on electrified railways) with one of the lowest emissions per passenger rates in transport and a 76% emission reduction for freight compared

with road [3, 4]. As the National Travel Survey showed in 2022, the railway takes 9.8% of total travel distance while the number of trips by railway is only 2.6% as shown in Table 1. That means most railway trips are long-distance trips. Long-distance trips with less acceleration are the key reason why railway has relatively low energy consumption. Overall, rail contributes less than 1% of the annual greenhouse gas emissions of the UK, and rail is one of the greenest modes of transport available. As a result, rail has massive potential for decarbonisation of the economy by increasing the volume of goods and people transported by rail in the UK due to a modal shift to rail. Similarly, while some of the reduction in industrial emissions is due to the decrease in manufacturing in the UK since 1990, significant effort has been made by the industry sector as a whole, with significant emissions reductions achieved through more efficient energy use and several industries transitioning to onsite renewable energy generation [5].

1.2 Problem description and trend

The UK's goal to reduce carbon emissions to net-zero by 2050 brings a significant challenge to its railway sector. This goal requires moving away from traditional diesel trains to greener alternatives. However, this change is not straightforward, as shown by recent difficulties in UK rail electrification projects.

Several important electrification projects in the UK, such as in Wales, the Midlands, and the North of England, were cancelled [6]. These cancellations, often due to high costs and technical issues, underline the challenges in updating the UK's railway system to be more environmentally friendly. Areas with limited electrification continue to depend on diesel trains, which conflicts with the UK's environmental goals.

The financial aspect of moving to green railway technologies is also a major challenge [7]. The high initial cost of new technologies, along with installation, operation, and maintenance expenses, needs careful consideration. This financial factor is important for the success and acceptance of decarbonisation efforts.

Moreover, current strategies in railway decarbonisation often focus on single technology solutions. There is a lack of integrated approaches that combine different technologies, like electrification, hydrogen fuel cells, and batteries, in one system. The effectiveness of these green strategies also varies based on location. Different regions may require different approaches due to varying route characteristics and climate conditions. This calls for flexible and region-specific solutions.

In conclusion, the UK's railway decarbonisation faces multiple challenges, including technical feasibility, economic costs, and the need for region-specific strategies. These challenges must be addressed to help the railway sector meet the UK's net-zero emissions target and move towards a more sustainable future.

1.3 Research Gap

Despite considerable progress in railway decarbonisation research, there are still some gaps in the field. Existing studies primarily focus on single green power technologies like electrification or hydrogen fuel cells [8-10]. However, there's limited research on integrating these technologies in a unified approach. The potential synergies and trade-offs among various green power solutions within a multi-mode railway system remain largely unexplored.

Secondly, most studies focus on the technical feasibility of green technologies but often overlook the long-term economic implications [11, 12]. There is a lack of thorough economic

analyses that consider the entire lifecycle of these technologies, including installation, operation, and maintenance costs.

Additionally, the application of advanced optimisation algorithms in railway decarbonisation strategies is still in its infancy. The use of such algorithms to enhance the cost-effectiveness of multi-mode green power technologies has not been sufficiently addressed [13]. This gap in optimisation research represents a key area where further exploration could yield significant benefits.

Lastly, the contextual applicability of these technologies in different geographical and operational settings remains under-researched. The effectiveness and viability of decarbonisation strategies may vary based on specific route characteristics, climatic conditions, and operational demands, an area that needs more focused attention.

1.4 Scope

The scope of this study is designed to address the research gaps. It will primarily focus on the integration of multiple green power technologies, including electrification, hydrogen fuel cells, and batteries, in a multi-mode railway system. The study will explore the synergies and potential trade-offs between these technologies, providing a holistic view of railway decarbonisation.

A full economic analysis will form an important part of this study, covering the entire lifecycle of the proposed green power solutions. This analysis will not only consider the initial installation costs but also explore the long-term operational, maintenance, and decommissioning expenses. Such an approach will offer a more complete understanding of the economic practicability of these technologies.

Furthermore, the study will utilise advanced optimisation algorithms, such as the Genetic Algorithm and Particle Swarm Optimisation, to refine the deployment strategies of these technologies. This will help in identifying the most cost-effective and efficient solutions for railway decarbonisation.

In terms of geographical applicability, the study will use the route from London St. Pancras to Leicester as a case study. This specific route will provide a practical context to evaluate the effectiveness of the proposed solutions, considering the unique operational and climatic conditions of this region.

1.5 Research aims and objectives

This research specifically targets the cost optimisation of the railway power system, aiming to develop a strategy for modernising the system in an economically viable manner to facilitate decarbonisation and develop a strategy for modernising the railway power supply system that minimises total costs, encompassing both the upgrading process and future operations. This involves evaluating various upgrade options through an overall cost function that integrates both the railway traction and power supply systems. A key aspect of this study is the use of sensitivity analysis to identify which parameters most significantly affect the outcomes. By fine-tuning these sensitive parameters, the research seeks to pinpoint the most economically efficient solution, which achieves decarbonisation with minimal impact on journey times. To accomplish these aims, the study will address several specific objectives:

- The literature on railway power systems and sensitivity analysis evaluations assists in optimising the upgrade process. Three major upgrading approaches are contrasted, and their corresponding field studies demonstrate how each method might improve performance or efficiency. The research process begins with a discussion of the

characteristics of each approach. The study strategy details the hypothesis, modelling, parameter analysis, and optimisation.

- This investigation will need the development of a multi-mode train simulator. This study is based on a railway system simulator. It is required to replicate a train's performance and condition during the route and enable it to be powered by various power supply systems, either synchronously or asynchronously. The train's status must be updated in dynamic to allow for management of the train's operating strategy at any point throughout the operation.
- A cost function is necessary to assess the train's lifetime performance. In contrast to the qualitative comparison used in the literature study, a more precise quantitative comparison is the primary criterion for decision-making. This assessment should be conducted regarding the entire cost, including the initial investment and subsequent operating costs. Additionally, there is a general negative association between trip duration and energy use when energy expenditure is considered. A time penalty must be included in the assessment to minimise lengthy journey situations.
- Sensitivity analysis is required to determine the optimisation priority and choose the most influential parameter for the cost function. This approach aims to quantify the sensitivity of each investigated parameter. Furthermore, the variables to be optimised might be those having a highly sensitive value.
- The ultimate goal is to optimise the total cost using the most sensitive parameters identified via sensitivity analysis. Two distinct changed optimisation algorithms are compared to optimise both progress and outcomes to arrive at the ideal option for upgrading railway power systems.

1.6 Justification

The justification for this study lies in its potential to fill critical gaps in the existing research on railway decarbonisation and contribute significantly to the field. While previous studies have made considerable progress in exploring individual green power technologies and their application in railway systems, there remains a clear need for a more integrated and comprehensive approach. This study addresses this by examining the combined use of electrification, hydrogen fuel cells, and battery technology in a multi-modal railway system, a perspective that has been notably absent in current research.

The economic aspects of railway decarbonisation have often been sidelined in favour of technical feasibility and environmental impact. This study responds to this oversight by conducting a detailed economic analysis that spans the entire lifecycle of green power technologies. Such an approach is important for understanding the long-term economic sustainability of these technologies and for providing a more holistic view of their viability.

Furthermore, the application of advanced optimisation algorithms in railway decarbonisation is an emerging field with significant potential. This study's exploration of Genetic Algorithms and Particle Swarm Optimisation for optimising the deployment of green technologies offers a novel contribution to the field. It stands to enhance the cost-effectiveness and efficiency of decarbonisation strategies, thereby providing practical solutions that can be implemented in real-world scenarios.

Additionally, the geographical context and operational specificity of railway decarbonisation strategies have been relatively underexplored in existing research. By focusing on the route from London St. Pancras to Leicester as a case study, this study provides valuable insights into the applicability and effectiveness of green power technologies in specific settings. This

approach helps in understanding the varying impacts of decarbonisation strategies across different geographical and operational contexts.

In summary, this study is important because it looks at many parts of railway decarbonisation that have not been given much attention before. It tries to connect ideas from research with reality uses, offering solutions that are good for the environment, can save money, and are practical to use. The results of this research will be very helpful in making future decisions and plans for the railway industry, helping it become more sustainable and efficient.

1.7 Thesis structure

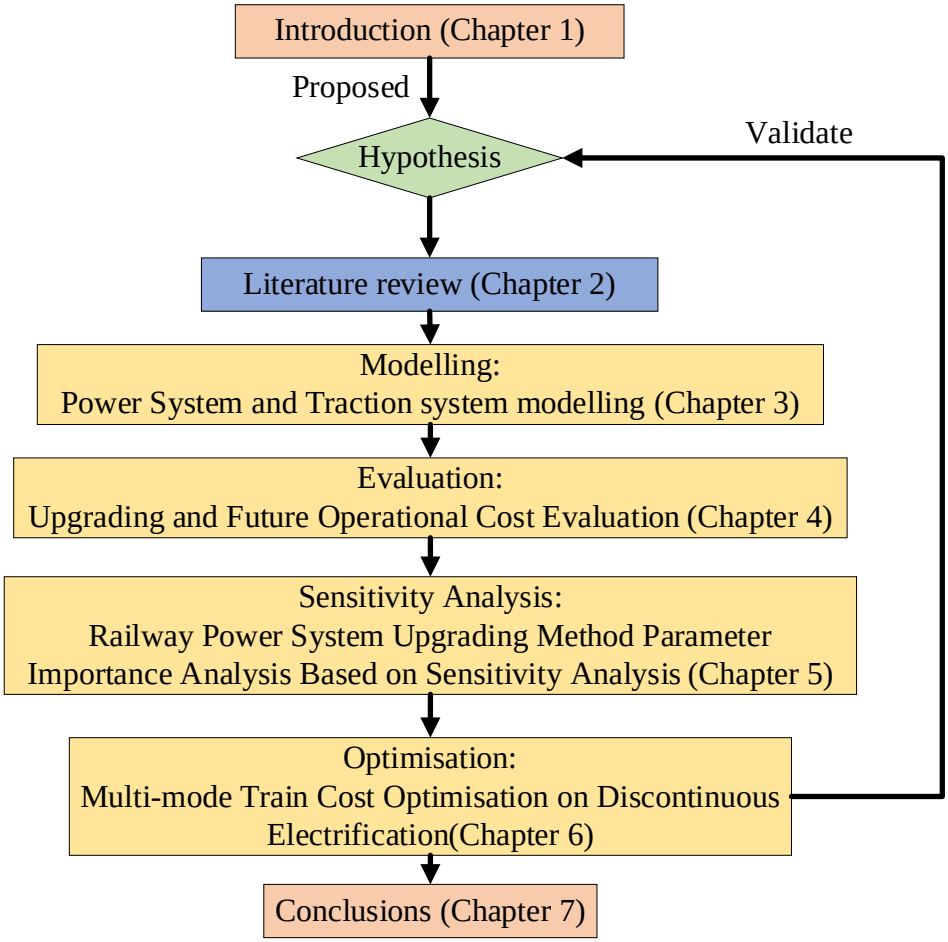

Figure 1 Thesis structure

This thesis is split into seven parts to demonstrate the whole research development; the details are shown in Figure 1 above.

Chapter 1 introduces the urgent issue of decarbonising the railway industry, addressing the challenges in shifting from diesel-powered trains towards more sustainable alternatives. It sets the scene for the research, outlining the thesis's objectives and laying the groundwork for the study, emphasising the need for efficient and environmentally friendly railway systems.

A full literature review is presented in Chapter 2, covering self-powered traction systems, including diesel, hydrogen fuel cells, battery-powered, and hybrid trains, as well as overhead line railway traction systems. This chapter critically analyses these systems, identifying gaps in current research and setting the foundation for the thesis.

Chapter 3 discusses the development of the Train Performance Simulator (TPS), a significant tool for modelling railway power systems. The TPS, designed to simulate a range of systems including diesel engines and hydrogen fuel cells, marks a major advancement in railway system simulation, enhancing the accuracy and applicability of these models.

Chapter 4 focuses on the financial and environmental aspects of transitioning railway systems, this chapter presents methodologies for assessing economic impacts and includes a practical case study. It provides insights into the feasibility and long-term benefits of adopting sustainable power systems in railways.

In Chapter 5, an in-depth sensitivity analysis of railway system parameters is conducted, using both local and global methods to pinpoint key influencing factors. A case study applies these methods in a practical scenario, highlighting the importance of understanding dynamic railway system interactions for effective optimisation.

Chapter 6 addresses optimising multi-mode railway trains, exploring various energy management strategies and their impact on performance. A case study demonstrates the application of these optimisation techniques, showcasing potential improvements in efficiency and sustainability.

The final chapter synthesises the research findings, reflecting on the contributions and innovations of the thesis, including the development of the TPS and new economic and environmental assessment methodologies. It concludes with future research recommendations, pointing towards continued advancements in sustainable railway transportation.

2 Literature review

2.1 Introduction

Railway traction power systems supply the energy necessary for vehicles to move. Traction systems vary in features and specifications depending on the supply source. Since the climate has shifted and decarbonisation targets have been established, the government and railway sector have looked for an environmentally beneficial alternative to the present diesel-powered trains [14]. Particularly after 2022, when energy prices have increased dramatically, and more people are concerned about future energy price fluctuations, cycling between new and old traction systems is critical. On the other hand, optimisation of energy consumption is a important aspect of the railway business since it directly impacts the financial costs associated with traction operation. Considerable evidence indicates that the substantial energy costs may considerably affect operational performance and train design [15, 16]. While most research has focused on railway system optimisation, a limited body of literature is devoted to parameter sensitivity analysis. These analyses provide researchers with a novel method for selecting variables before optimisation, which improves the efficiency of the optimisation process.

This chapter summarises the relevant literature on various power traction systems. Each section includes the basic principle, state-of-the-art research, and the limitations of those research. Power traction systems are divided into self-powered traction and contact wire-connected electric power systems. The last section of this chapter proposes a hypothesis to examine the link between various power supply systems' distribution designs.

2.2 Self-powered traction systems

Network Rail's Traction Decarbonisation Network Strategy advised the use of hydrogen-powered trains for 6% (900 single track kilometres, STK) of the network that is not yet electrified, battery-powered trains for 3% (400 STK), and further analysis of 15% (2300 STK)

of the network that is not yet electrified [17]. This section discusses the principles and new research about self-powered trains.

2.2.1 Diesel power traction systems

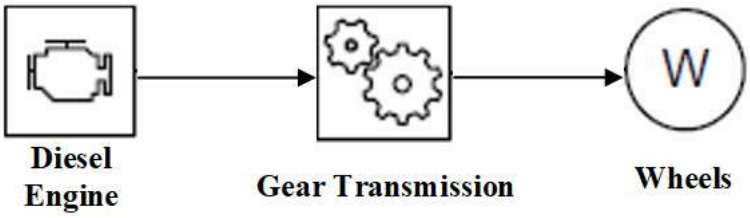

Figure 2 Diesel-mechanical locomotive structure [17]

The early generation of diesel train is an all-diesel traction train. Because this train is mechanically driven, the components are essentially those shown in Figure 2, but the train's performance is restricted. The majority of diesel-mechanical trains are limited to a maximum speed of 160 kilometres per hour (100 mph). The transmission through gearboxes and the engine is incapable of meeting high power and torque demands. The engine's power output is modified in response to the driver's power demand. The transmission's transfer ratio is changed to provide enough torque to the wheels while maintaining the train's speed.

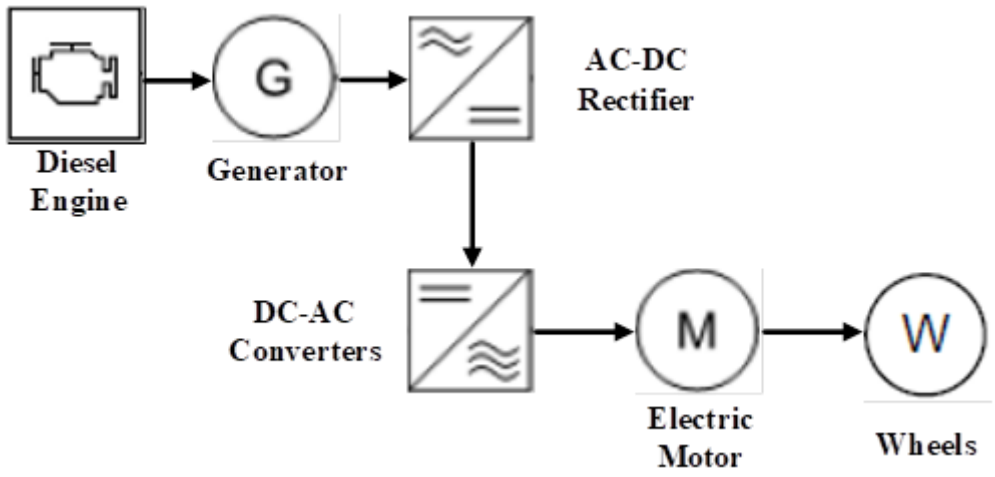

Figure 3 Diesel-electric locomotive structure [17]

The majority of current diesel trains are diesel-electric locomotives. As with the older diesel-mechanical locomotives, the diesel-electric train's diesel engine burns diesel fuel. The distinction is that a diesel-mechanical locomotive converts chemical energy to mechanical energy and then transmits it to the wheel through a transmission. Additionally, the diesel-electric train converts mechanical energy to electricity. Following that, converters (rectifiers and inverters) process the energy and deliver higher-rated power, either DC or AC electric motor, as shown in Figure 3. Electric traction provides a number of benefits over conventional transmission. The most significant performance improvement is the operating speed, which has been increased to 200 kilometres per hour (125 mph) from 160 kilometres per hour for diesel-mechanical trains (100 mph).

In the UK, over 50% of railway routes are not electrified and use a self-powered traction system to ensure railway operation. A diesel multiple-unit simulator has been built, and it considers specific curvature resistance and, wind speed and direction, which other modelling

does not include [18]. Diesel-electric locomotive fuel consumption has been researched using a hybrid powertrain, which adds the battery pack. It shows the hybrid train can save 11% energy and improve journey time by 0.7% [19]. Technical and economic feasibility studies on employing regeneration in railway systems have shown its significant value [20]. Further research indicates that modernisation of diesel-electric locomotives can lead to a decrease in energy consumption [21]. Additionally, the use of two different optimisation algorithms to determine the optimal energy savings for a system incorporating a lithium-ion battery and double-layer capacitor revealed that the optimal solution closely matches the outcomes of a specific case study [22]. Smart switching controls are employed in diesel and hybrid trains. The results show that smart switching controls can save up to 6% energy compared to auto-switching [23].

2.2.2 Hydrogen fuel cell trains

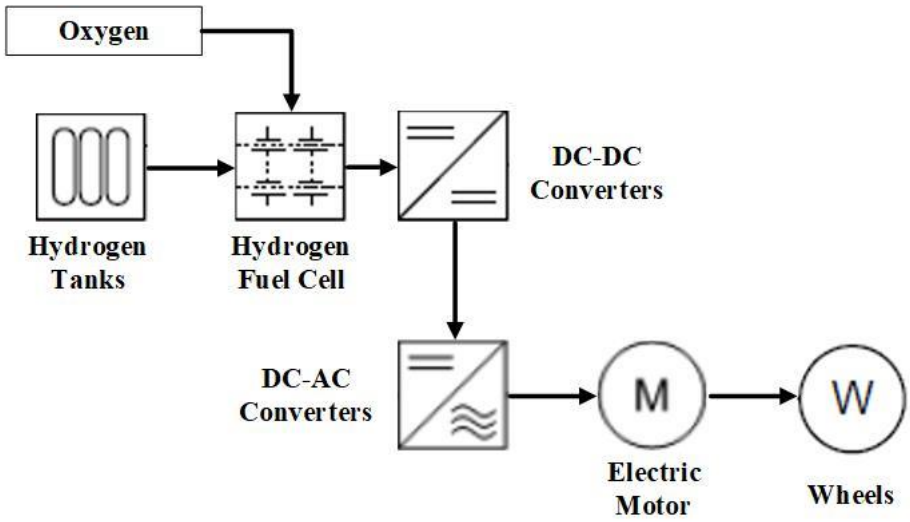

Figure 4 Hydrogen locomotive structure [17]

Hydrogen is a unique carbon-free energy source being explored for use on trains and across the economy. Alstom launched the world's first hydrogen passenger service train in September 2020 on four lines in Lower Austria, Vienna, and Styria. Porterbrook and the University of

Birmingham in the UK developed the HydroFLEX train, which has not yet been put into passenger service. Hydrogen fuel has the advantage of being zero-emission at the time of use, as hydrogen reacts with oxygen to create energy, heat, and water [24]. A hydrogen-powered train is as silent as an electric traction train but unlike electrified trains does not need considerable trackside infrastructure.

Like a diesel-electric train, a hydrogen train consumes fuel to produce power. Among the various hydrogen storage methods, the most widely used is 350 bar high-pressure composite cylinders [25]. The hydrogen fuel cell replaces the diesel engine as the energy supply system in a hydrogen train. The energy supply system creates electricity directly via the electrochemical reaction of hydrogen and oxygen within the fuel cell, and the conversion of fuel energy to electrical energy is more straightforward than with a diesel-electric train, as seen in Figure 4. Following conversion using converters, the power is sent to an electrical motor in the same manner as in a diesel-electric train. Compared to a diesel internal combustion engine traction train, the hydrogen fuel cell train is far quieter due to the lack of visibly moving components in the traction system, except cooling systems. However, due to hydrogen's low energy density, the hydrogen train can only go around 1000 kilometres on a single refuelling; diesel trains with the same amount of stored energy go eight times as far as hydrogen trains. Moreover, the peak speed remains modest, between 144 and 160 kilometres per hour (80–100 mph). As a result, hydrogen trains have the potential to replace medium-speed, medium-power, reasonably long-distance diesel trains completely.

2.2.3 Battery-powered trains

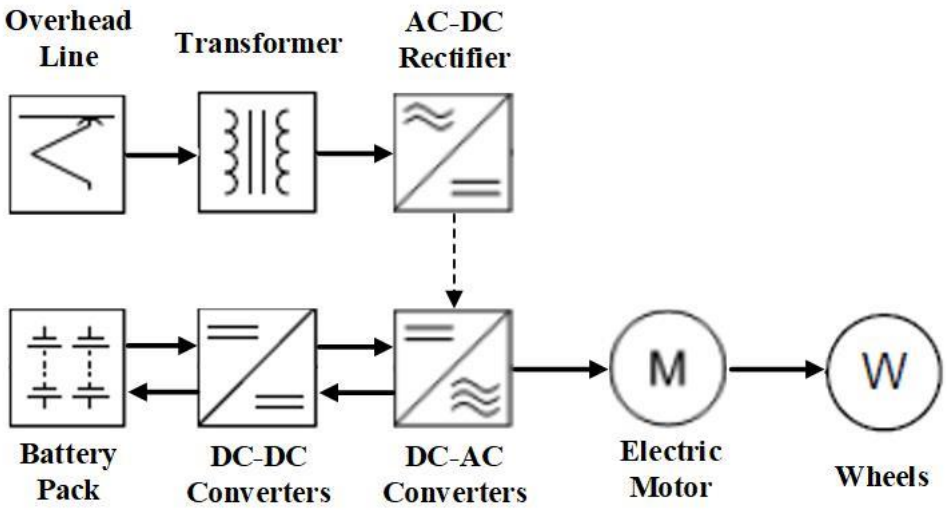

Figure 5 Battery train system (overhead wire charging) [17]

In general, the most straightforward method of storing electrical energy onboard is via the use of battery packs. Battery packs, as energy storage system devices, may receive and transmit energy by charging and discharging. Two stages must be considered to include batteries in a railway system: charging and discharging. The charging stage of the battery is where it obtains energy. Typically, this is through an overhead line, third rail, or other engine/motor, as seen in Figure 5.

The discharging portion is where the battery's chemical energy is converted to electricity and sent to the electrical traction system. The primary benefit of a battery-powered train is that it is a highly efficient train with a self-contained power supply. Additionally, it can run on the present continuously electrified track with zero emissions by harvesting power from overhead lines on the electrified section and dragging the train on the unelectrified segment using the energy stored in the battery. In comparison to the last two train types, the most significant disadvantage is the operating range. Batteries have a lower energy density and a range of 60–

80 kilometres when ultimately charged. Additionally, the peak speed is relatively modest, 120–160 km/h (75–100 mph), comparable to a hydrogen fuel cell train.

For the aims of decarbonisation, a new self-powered supply system driven by greener energy should be used to replace diesel power. Several researchers have shown the ability of energy storage technologies, such as batteries and hydrogen fuel cells, to replace diesel power. A battery-electric multiple-unit simulator was developed [26]. This research introduces a simulator for battery-electric trains. It's quite important for understanding how these trains work and for improving them. It's very interesting because it looks at how trains can use electricity better and be more environmentally friendly. This research provides valuable insights into battery-electric trains, but it notably overlooks the potential of hydrogen fuel cells, an alternative energy source in rail transport. This might limit the applicability of the simulator in environments where hydrogen fuel cells are being considered or implemented. A full review of energy storage devices, focusing on batteries and fuel cells, was conducted to compare their characteristics [27]. They looked at different ways to store energy, like batteries and fuel cells. It's very helpful for figuring out which one is best for different trains. It's really important for making trains better and choosing the right technology. This review offers a full comparison but may lack in-depth analysis of rapidly evolving technologies. Some research has concentrated on the battery pack; for example, a battery pack is employed to store regenerative energy generated during electrical braking to improve the railway’s total energy efficiency [28-30]. These studies talk about using battery packs in trains, especially for saving energy when trains brake. This is a good idea because it saves energy and makes trains use less power. The focus on battery packs highlights their potential, but there's a lack of discussion on the challenges of integrating such technology, especially in older railway systems. An optimisation method for maximising recovered energy through reversible substations and a wayside storage

system was demonstrated, featuring controlled charging and discharging between the train and a wayside battery pack [31]. They came up with a new way to save more energy in trains, using special substations and batteries. The way they control the batteries is very smart and helps to save a lot of energy. However, it does not consider the integration of hydrogen fuel cells, which are increasingly recognised for their potential in sustainable rail transport. This exclusion could limit the scope of the technique, particularly in contexts where hydrogen fuel cells might offer a more viable or efficient alternative to battery-only systems. An energy management strategy for battery packs was suggested to optimise energy storage system utilisation by adjusting charging and discharging threshold voltages, specifically for electrified routes [32]. This is about managing the energy in battery packs on electrified train routes. They change how the batteries charge and discharge to use the energy better. It's quite useful for making sure the trains don't waste electricity. The strategy effectively addresses energy management for battery packs in electrified routes. However, it doesn't fully consider scenarios involving discontinuous electrification, a common situation in many rail networks. This oversight could limit its practicality in rail systems where continuous electrification isn't available or feasible, thereby affecting the strategy's overall adaptability and efficiency in practical applications. Research about catenary-free electric trains with lithium batteries shows that speed optimisation can increase the battery train’s running distance on an unelectrified route. However, it also shows that the battery can rarely be the only power source for trains over 100 tonnes [33]. The disadvantage of employing a battery pack as an autonomous power supply system is its low-capacity limitations.

2.2.4 Hybrid trains

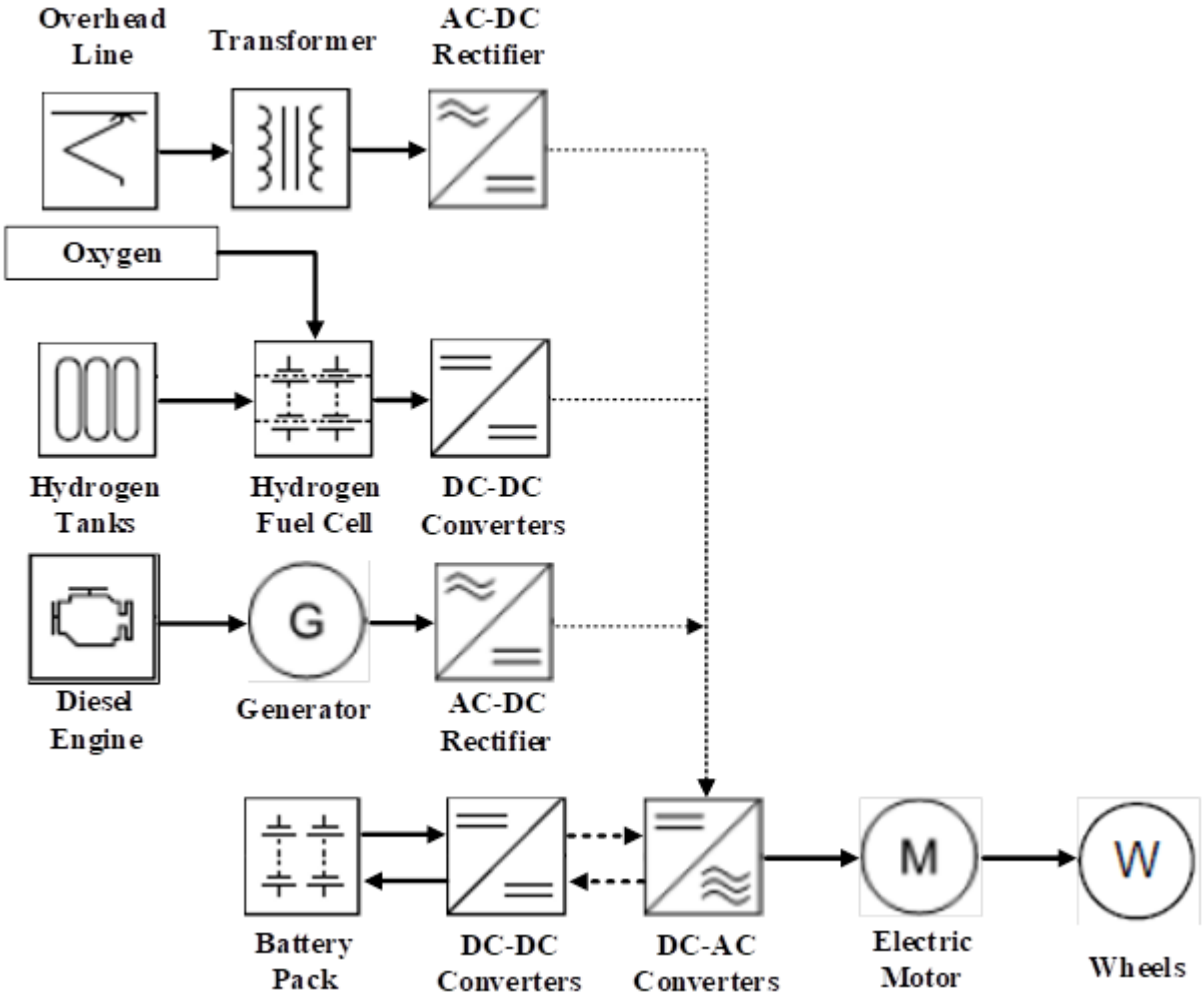

Figure 6 Hydrogen/diesel-battery hybrid train structure [17]

For the literature on hybrid trains combining battery packs with fuel cells offers a solution to capacity issues. However, this approach might face challenges in integration and cost efficiency [25, 34-37]. The research focused on hydrogen production and consumption efficiency [30] is an important aspect of developing sustainable railway systems. While it provides essential insights into the efficient use of hydrogen, the study might not fully consider the evolving nature of hydrogen technologies or their practical implementation challenges in railway [10]. The study using AI for hydrogen supply chain prediction shows promise, but practical application challenges remain [9]. The hybrid vehicle simulator marks significant

progress, though practical applicability might be limited by the assumptions of model [38]. The feasibility study comparing different energy supply systems provides valuable insights but lacks consideration of regeneration [39]. The investigation into hydrogen vs. battery transportation is critical for future decisions but concludes without a definitive preference because hydrogen fuel cell offers benefits like faster refuelling and higher range whereas Battery-powered vehicles have advantages in terms of higher energy efficiency but longer charging times and range limitations [40]. Analysis of hydrogen fuel cell trains for intercity services shows potential, especially with low-carbon hydrogen, but requires further exploration in different operational contexts [41]. The implementation of new control techniques for reducing hydrogen use in hybrid trams is innovative, but its broader impact on system efficiency needs evaluation [34, 42]. The time-based co-optimisation model offers a cost-effective approach but its adaptability to variances is yet to be tested [43]. Simulations of the bi-mode train indicate CO2 emission reduction potential, but the study is limited as it only considers diesel-electric options and not hydrogen-electric trains [44]. Research on optimising hydrogen consumption by altering the power output shows a decrease in consumption by 15%, but does not address potential impacts on journey times, important for operational efficiency[45]. This research changes the power supply to minimise the energy consumption without discussing the journey time changes resulting from power changes.

2.2.5 Challenges and research opportunities

Although previous diesel train studies have focused on energy-saving technology or strategies, the use of diesel trains is a potential problem. For the aims of carbon neutrality, almost all diesel trains need to be replaced, including replacing pure diesel trains by 2040 and achieving net-zero before 2050 [17]. However, there are still some research gaps which have not been considered:

- Previous studies on energy storage have not addressed the possibility of combining it with electrification, which has a far better energy efficiency; doing so might further reduce energy costs.
- Thus, most of the battery research only considers battery use as a mechanism for conserving regenerative energy in the absence of an overhead line connection. Not much hydrogen train research considers the energy cost of hydrogen trains, only thinking about the energy consumption.
- Researchers know that even though hydrogen trains have better energy transmission efficiency compared to diesel trains, the hydrogen energy cost is still higher than for diesel trains due to its high energy price in kWh.

2.3 Overhead line railway traction systems

Compared with those self-powered trains, electric trains have many advantages [46]:

- **Easier maintenance:** For train maintenance, the cost of the electric trains is approximately 30% less than diesel trains and 50% less than diesel bi-mode trains.
- **More seats:** For trains of the same length, electric trains have more space than other trains, such as diesel, bi-mode, and hydrogen trains, because there is no requirement to install an energy storage system and fuel tank. The saved space can be used for seat allocation.
- **Less journey time:** Electric trains can accelerate and brake faster than other trains due to the higher traction and braking power supply. That means they need less time in the acceleration and braking stages and spend more time in the full-speed stage.
- **Better reliability:** Long-term passenger rolling stock strategy research indicates that an electric train's reliability is 100% more than that of a diesel train.

The classic electric train is the only train type that does not carry fuel inside the train. Because there is no power generator mounted on the board, and it often does not need additional energy storage devices, the mass is typically less than in other systems. However, some battery packs are mounted in specially built electric trains, as in Figure 7. These battery packs act as a backup power source, providing electricity to the auxiliary system or traction motor to reduce the load on the overhead line power. Mainly, these batteries gain electricity from the overhead wires and during energy regeneration. Usually, most of the energy stored in the battery pack comes from the electrical braking process. A noticeable disadvantage of electric trains is the very high cost associated with the extensive length of overhead line equipment. The figure also shows the component differences between AC and DC trains, including their power supply infrastructure. An AC train is heavier than an DC train because it carries more equipment on board, especially power electronics devices to step down the overhead line voltage. However, the DC overhead wire does not take high-voltage electricity due to more step-down transformers in the substation. Hence, the relatively low voltage transmission results in increased losses in the wire.

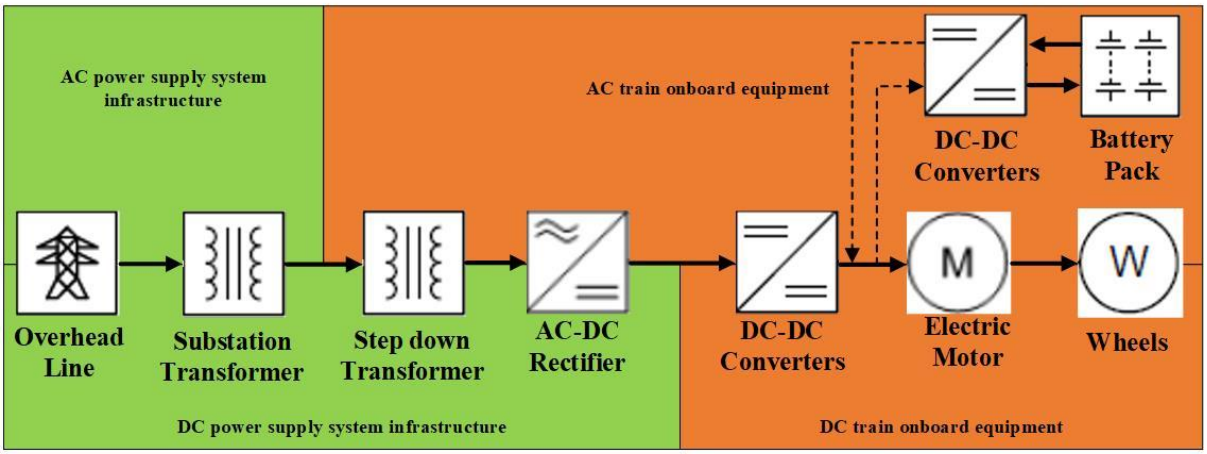

Figure 7 Electric train structure [17]

2.3.1 AC power systems

Large-scale electrification initiatives have improved the network's coverage of 25 kV electrified routes, adding about 700 kilometres since 2017. Table 2 summarises the total route kilometres operated electrically since 2011/12 [46, 47].

Table 2 The UK's railway operation route and electrified route [47]

	Route opens for traffic [km]	Of which electrified [km]	Track kilometres [track km]	Of which electrified [track km]	New electrification projects [track km]
2013	15,757	5,265	31,075	12,810	10
2014	15,755	5,268	31,092	12,887	65
2015	15,764	5,272	31,120	13,034	177
2016	15,804	5,331	31,194	13,063	7
2017	15,814	5,374	31,220	13,167	0
2018	15,846	5,483	31,038	14,129	291
2019	15,853	6,012	31,091	14,059	883
2020	15,899	6,049	31,218	14,256	252
2021	15,935	6,045	31,250	14,314	182
2022	15,873	6,042	31,209	14,321	2
2023	15,846	6,065	31,203	14,360	62

Table 2 shows data from 2013 to 2023 on total and electrified railway route and track kilometres. Over these years, there's a steady growth in both total route and electrified track lengths, indicating ongoing development in railway electrification. Certain years, especially 2018 and 2019, show significant new electrification projects, highlighting focused efforts to expand the electrified network. some years like 2016, 2017, and 2022 show minimal growth in new electrification projects. In particular, 2017 stands out with no new projects, indicating a possible pause or slowdown in electrification efforts, for example, the electrification cancellation between Cardiff and Swansea.

(1) Simple connection

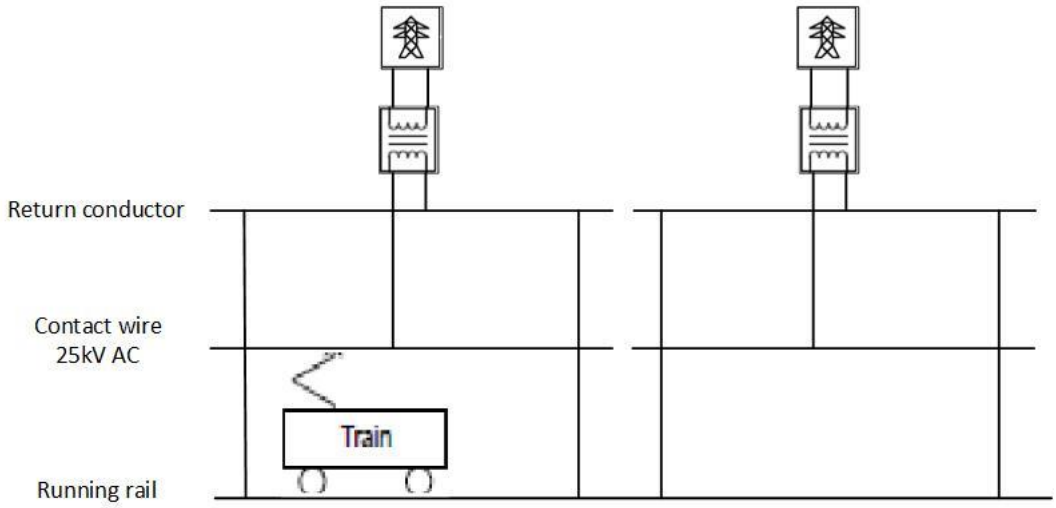

Figure 8 Simple connection system diagram

The transmission system is a straightforward catenary feeding arrangement, as seen in Figure 8. It forms a circuit when the train connects with the overhead line and the rail. The current passes through the train from the pantograph and is then sent back to the substation via the rail. For simple connection system, the biggest issue in this system is the electricity that escapes from the rails. Therefore, it's very important to reduce this electricity leakage in railway power supply systems for keeping safety, efficiency, reliability, and the life of the railway infrastructure. Moreover, when the train is operating, a large difference in voltage happens along the rail, which can cause harm to people and others nearby.

(2) Booster transformer (BT) system

Figure 9 illustrates an alternating current supply system that utilises a BT to drive rail current back to the BT and then to the substation via a feeder wire. Numerous existing transmission networks continue to be BT-fed. However, owing to the 25 kV 50 Hz power supply, BT feeding systems continue to have large transmission line power losses.

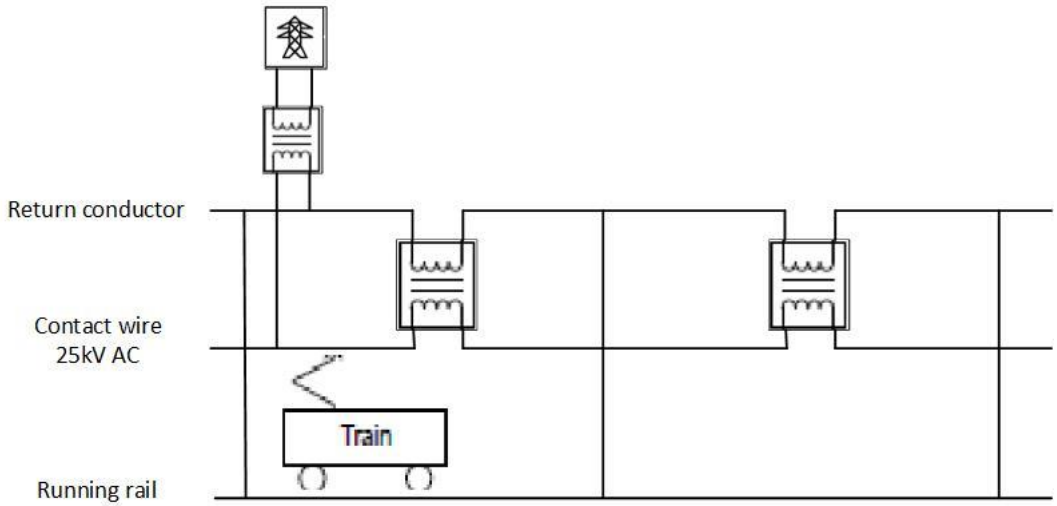

Figure 9 BT diagram

(3) Autotransformer (AT) system

The AT feeding system is a newly created system for power traction, and its construction is shown in Figure 10. Compared to a BT, it provides double the voltage, 50 kV 50 Hz AC power, and half the transmission line current of a BT or simple feeding system. Additionally, ATs may partially improve voltage, masking the evident voltage decreases in catenary wires.

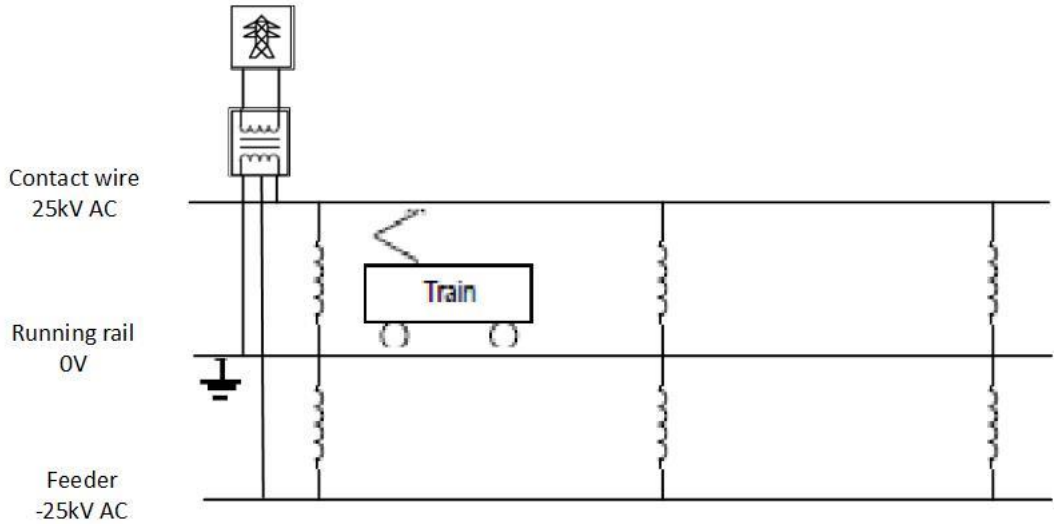

Figure 10 AT diagram

2.3.2 DC power systems

A DC system's power supply voltage is usually 750 V, 1500 V, and 2000 V, much less than that of a 25 kV AC system. This results in more transmission loss at the same rated power. DC traction substations are often fitted with transformers and rectifiers to absorb power from local distribution networks on contemporary trains. Direct current power is often employed in metros, light trains, and suburban railways. There is insufficient room for the installation of transformers and other equipment.

2.3.3 Discontinuous electrification

A railway route without full electrification is said to have discrete electrification or discontinuous electrification. Discrete electrification is when specific line segments are electrified while others are not. The gaps between electrified parts are usually significant. The number of gaps between electrified segments is expected to be restricted with discrete electrification. A train powered only by electricity is unlikely to span gaps between parts of the electrified network safely. In non-electrified segments, it will not be able to stop and start. Electrically discontinuous electrification, such as at an earthed portion via an overbridge, is known as discontinuous electrification. This is particularly likely to happen in areas like old bridges, tunnels, and other barriers. In contrast to discrete electrification, discontinuous electrification is more likely to have far more frequent, much shorter interruptions on severely limited segments of track. A train powered entirely by electricity may cross gaps reliably using momentum alone, albeit this introduces operational risks or uses limited energy storage, such as a battery. On non-electrified segments, it is doubtful that the trains will be able to stop and start again. In this thesis, both discrete electrification and discontinuous electrification are collectively referred to as discontinuous electrification for simplification.

2.3.4 Research on electric trains

In the review of electric train power systems, various strategies are discussed for reducing energy consumption and enhancing efficiency to reach the decarbonisation by 2024 [17]. It explores methods such as modifying regeneration strategies and optimising driving strategies for different traction modes, while noting that these may not fully address railway operation complexities [48-50]. The section highlights advancements in energy management in power systems and motor traction control , with proposals for stabilising overhead wire voltage using onboard energy storage systems do not point out the need for further research on their long-term reliability [51, 52]. They also compared the differential evolution optimisation results with those obtained using a Genetic Algorithm and said the Genetic Algorithm optimisation result is not as good as the differential evolution results [53]. The potential of inverting substations to improve regenerative braking efficiency is explored, but their practicality and economic feasibility across railway networks are questioned [8]. The integration of train timetabling with driving strategies for improved energy efficiency is also discussed [49], saying challenges in application due to dynamic schedules and passenger demands [54]. The use of Monte Carlo algorithms for energy consumption assessment and methods to utilise recovered DC energy for AC loads are considered promising but require testing in various operational scenarios [55-57]. However, most UK railways are intermittently electrified due to historical and economic The shift towards bi-mode trains in the UK is presented as a practical approach to intermittent electrification, but concerns are raised about their long-term sustainability due to diesel dependency [11, 12]. Studies on battery-electric trains in discontinuous electrification routes show potential for energy savings, yet require further exploration of their impact on network efficiency and operational flexibility [58]. Finally, the research on charging battery-electric trains from renewable sources is highlighted as a important step towards sustainable railway systems. However, the focus on battery performance alone, without considering overall system

optimisation, might not yield the most efficient solutions. The section advocates for integrated approaches that consider the entire energy system, including renewable sources, storage, and train operations, to maximise the benefits of railway electrification [59].

2.3.5 Limitations of electric traction systems and research opportunities

The majority of electrification energy efficiency research is conducted on fully electrified routes, and the majority of hybrid train research is conducted on current diesel hybrid trains. Hence, there are more factors that need to be considered out of the ideal situation.

- Most railway routes are discontinuously electrified, and it is impossible to fully electrify those partly electrified routes in a short time. So, the research based on full electrification can only be used on newly built electrified railways.
- The research on battery-electric trains is also limited by the battery specifications. If only employing a battery as the power supply in a long electrification gap, train performance is limited due to the battery's capacity.
- It is impossible to apply battery-powered traction in a long-distance heavy train; the energy stored in the battery will run out faster in this situation. So, extending railway electrification and battery application at the same time would solve the issues.
- However, in some cases it is hard to electrify the route, so a hydrogen fuel cell may also be applied in the railway as a multi-mode train instead of a diesel hybrid train.

2.4 Discussion and research design

Most previous studies have not considered the combination and distribution of novel power supply systems and train operation in hybrid train research. When discussing train conversion, most researchers think only about the capability of the power system but not the conversion cost. This thesis aims to demonstrate a financially effective plan for converting diesel engine trains and route electrification during an operation period. Three different kinds of energy

supply systems are combined as the new supply system to power trains on discontinuously electrified routes. This thesis proposes that multi-mode trains may reduce the entire railway cost during its lifetime under cost optimisation. The idea is validated using a cost model that estimates the total cost of the route reconstruction and new train upgrades over time. Railway modernisation includes a variety of alternative energy sources and traction technologies. The energy distribution and consumption determine the energy transmission flow of each traction type. Sensitivity analysis directs the optimisation factors to choose the appropriate kind of railway. Two optimisation techniques are used to choose the most influential parameters for optimisation. Particle Swarm Optimisation and Genetic Algorithm are compared to highlight the difference in optimisation progress in this complicated railway cost model.

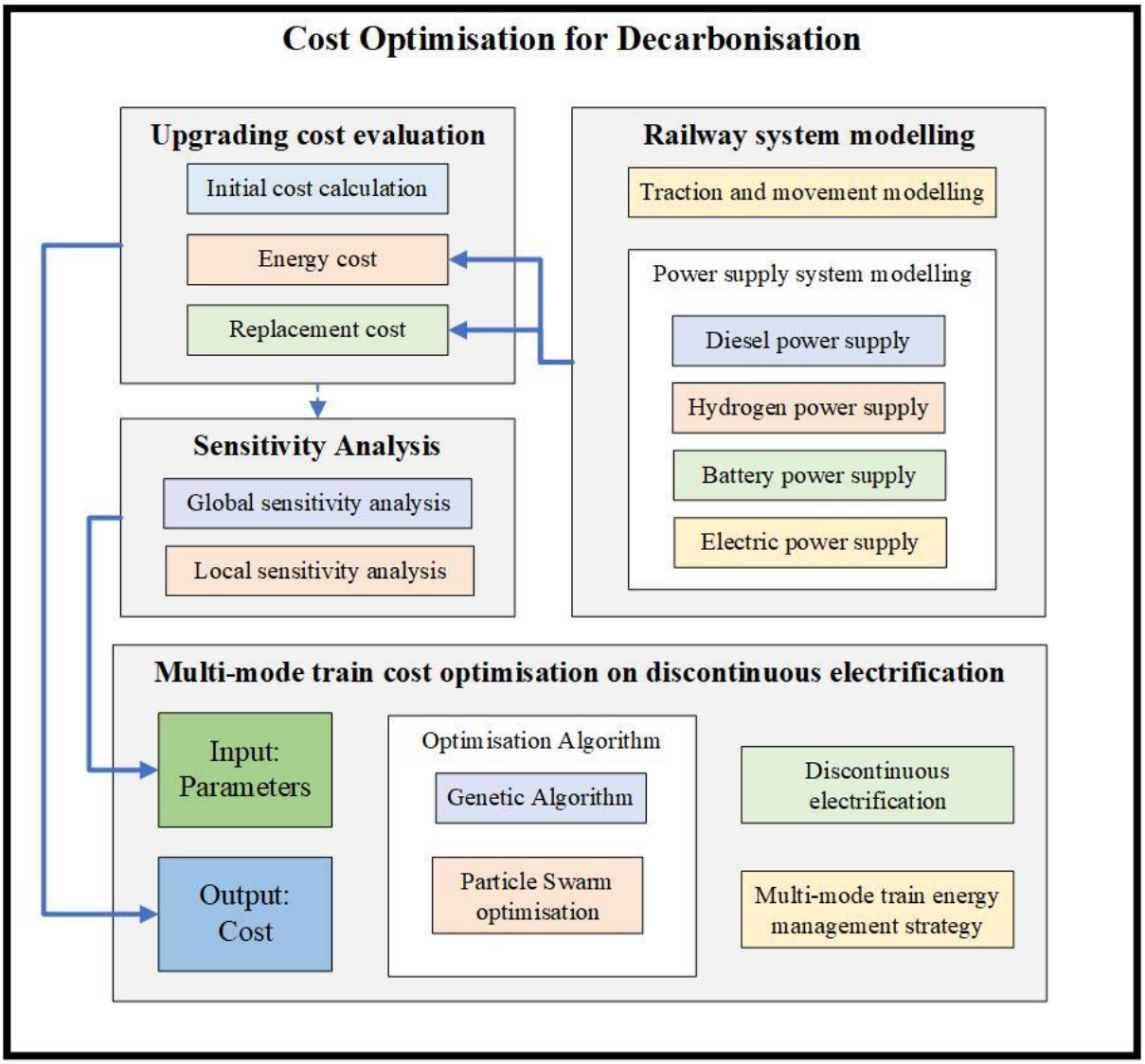

Figure 11 The research on cost optimisation

As the Figure 11 shows, the fundamental research is made up of four parts: railway system modelling, upgrading cost evaluation, sensitivity analysis, and multi-mode train cost optimisation on a discontinuously electrified route.

The railway system modelling part is primarily about building the integrated railway system simulator. It has two relevant simulations. The traction and movement simulation presents the train's moving performance during the whole journey. The power supply system also affects

the train's performance in power-relative parameters. And the energy usage information is calculated by the power supply system simulation.

The upgrading cost evaluation part receives the train performance and energy consumption information from the railway system simulation. The energy consumption is converted to the energy cost. Besides that, the train components are aged depending on the train's performance, so the cost evaluation considers the cost of replacing train components. Additionally, as a railway upgrading plan, the changes from the original system to the new system require train conversion and route reconstruction. Both costs are subsumed into the initial cost. All those costs are summed as overall cost, and it is the standard output of evaluation.

Railway upgrading is varied, and different upgrading plans have additional contributions to sensitivity. Local sensitivity analysis and global sensitivity analysis are employed to analyse the contribution of various parameters to the evaluation results. Some of the sensitive parameters are then used as the variables for the optimisation.

Discontinuous electrification and the multi-mode train energy management strategy are introduced into the variable optimisation in the cost optimisation parts. The parameters from the sensitivity analysis results become the optimising objects and are the input of evaluation. The output corresponding to them is the overall cost. Both inputs and outputs are sent to the optimisation algorithms (Genetic Algorithm and Particle Swarm Optimisation) to minimise the overall upgrading cost.

2.5 Conclusion

This chapter reviews the current different potential upgrading methods for decarbonisation. It contains the basic principles of different power upgrading methods and the latest research about each method. Partly electrified routes have been studied by other researchers. Some of them

tried to find a replacement for the current diesel train on discontinuously electrified routes and others want to electrify the route to meet decarbonisation aims.

3 Power system and traction system modelling

3.1 Introduction

As the hot topic of the digital twin has become more popular in recent years, more researchers have tended to replace physical prototypes with digital twins. To build a reliable digital twin system, the important aspect is the creation of model-based solid system simulators. In 1978, the first transportation simulator was constructed [60]. In the following decades, researchers focused on increasing the accuracy of simulator performance by perfecting railway modelling. Moreover, some tried to add more components into the model to simulate complex modern trains. The Single-Train Simulator (STS) was developed by Dr Stuart Hillmansen at BCRRE [61]. This thesis develops a Train Performance Simulator (TPS) with energy management system to figure out train traction and movement as Section 3.4 shown. The movement part is based on the principle of the STS but dynamic power and energy calculation.

This chapter serves as the thesis's fundamental chapter. It will show modelling of two distinct systems, namely the power supply system and the train movement system, and the integrated simulator will be used throughout the thesis. Section 3.2 discusses the modelling of several types of onboard power systems, diesel engines, hydrogen fuel cells, and battery packs. Section 3.3 illustrates the modelling of the overhead line electrification power supply system. This model depicts the system in its entirety, from the substation to the train. This modelling includes estimations of substation internal resistance, transmission losses, and transmission line resistance. Section 3.4 discusses train traction and movement modelling based on STS and the link between train operating performance and energy cost.

3.2 Modelling of self-powered traction systems

Except for an electric train's overhead line power supply system, all other power systems, such as diesel engines, hydrogen fuel cells, and battery packs, are placed on board. It costs money

to create energy and transfer it to a power bus using fuel stored in a tank or other chemical materials within a battery pack.

3.2.1 Diesel engine systems

Diesel fuel is sent to an internal combustion engine and transferred to mechanical energy. The efficiency of converting chemical energy to mechanical energy is $\eta_{Diesel\ engine}$. Then the engine drives the alternator to generate AC electricity by the efficiency of $\eta_{Alternator}$. The electricity from a utility grid cannot be used directly. All electrical devices on the trains have their specific input requirement. After convertors adjust their frequency, amplitude, and phase by the efficiency of $\eta_{Convertor}$, they send electricity to the final electric motor or other auxiliary devices. The energy transmission for the diesel-electric train is as follows:

$$E_{Diesel\ system\ output} = \eta_{Diesel\ engine} \times \eta_{Alternator} \times \eta_{Convertor} \times E_{Diesel\ fuel} \qquad (1)$$

3.2.2 Hydrogen fuel cell systems

3.2.2.1 Hydrogen fuel cell train modelling

The critical part of a hydrogen fuel cell system is the fuel cell. High-pressure hydrogen from the tank is injected into the fuel cell, reacting with oxygen to produce water. The circuit current appears with the electrons flowing from cathode to anode. The efficiency of fuel cell electricity production is $\eta_{hydrogen\ FC}$. But hydrogen fuel cell efficiency is not permanently fixed: it varies depending on the fuel cell's output power. At first the output power increases, the efficiency increasing simultaneously at the beginning since the output power increases and steadily decreases if the output power continuously increases. Before being sent to the power bus, the electricity needs to be progressed by convertors, and the converter efficiency is $\eta_{FC\ convertor}$.

$$E_{FC\ system\ output} = \eta_{hydrogen\ FC} \times \eta_{FC\ convertor} \times E_{High-pressure\ hydrogen} \qquad (2)$$

where $E_{FC\ system\ output}$ is the hydrogen fuel cell power system output energy to the power bus , $\eta_{FC\ convertor}$ is the converter efficiency between hydrogen fuel cell and DC link, and $E_{High-pressure\ hydrogen}$ is high-pressure energy consumption.

3.2.2.2 Energy losses in a hydrogen fuel cell train

Figure 12 shows the energy losses during operation of a hydrogen fuel cell train. Some of the energy is lost in the reaction of hydrogen and oxygen by producing heat. In this study, the fuel cell's energy output is partially allocated to the auxiliary system, while the majority propels the train forward. Consequently, except for the energy expended to overcome resistance to motion, all traction energy is converted into kinetic and potential energy. Notably, electrical braking is not considered for the hydrogen fuel cell train but battery train in Section 3.2.3; hence, all traction energy is ultimately dissipated through mechanical braking without energy regeneration.

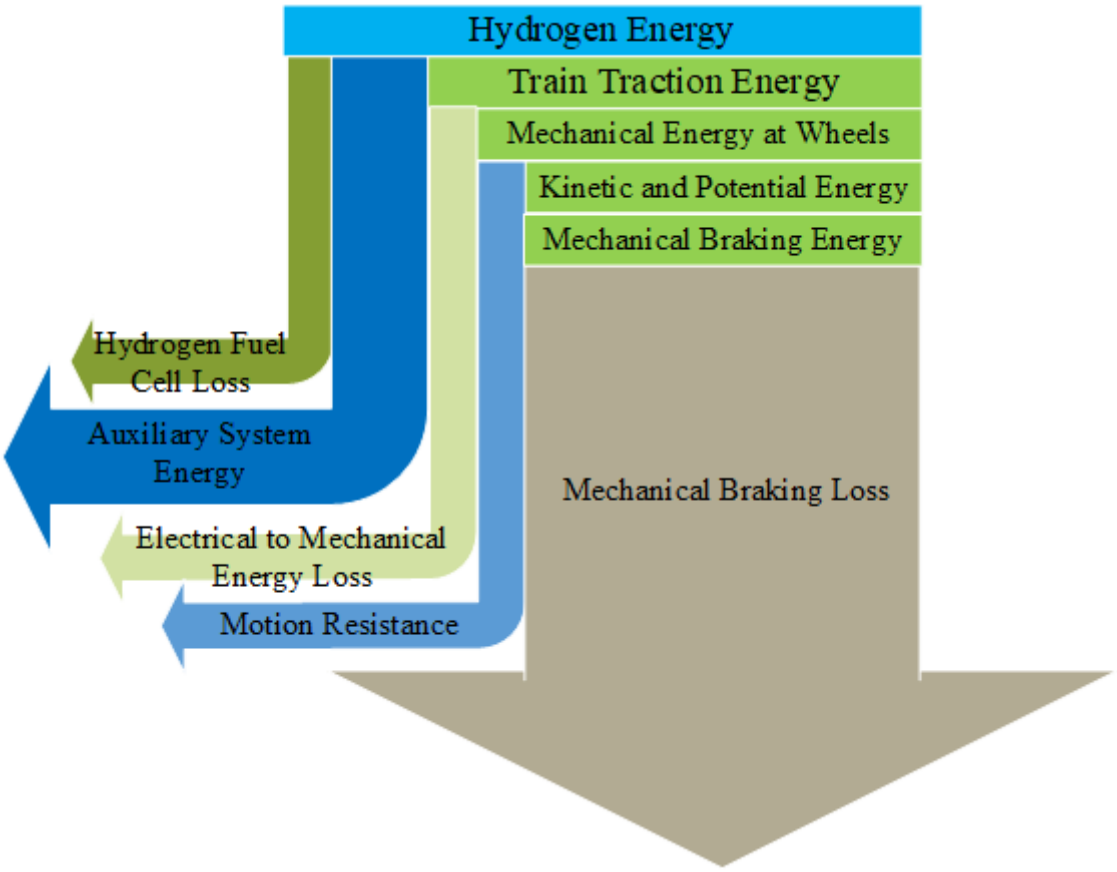

Figure 12 Energy losses in a hydrogen fuel cell train

3.2.3 Battery pack systems

In contrast to diesel and hydrogen systems, battery pack systems may be charged and discharged while the train is running with the efficiency of $\eta_{BP\ charging}$ and $\eta_{BP\ discharging}$, respectivelyIn practical scenarios, it is generally observed that the efficiency of battery discharging is slightly higher than that of charging, mainly due to the internal generation of heat [62]. Nevertheless, for the purposes of simplification in this thesis, it is assumed that the efficiencies of both charging and discharging are equivalent, facilitating easier computation. When the battery pack is charging, energy from the power bus ($E_{To\ charge\ BP}$) is sent via convertors to the battery with the efficiency of $\eta_{BP\ convertor}$. two main battery charging ways are the overhead line and regeneration. The battery pack gets the following energy:

$$E_{Charging} = \eta_{BP\ charging} \times \eta_{BP\ convertor} \times E_{To\ charge\ BP} \quad (3)$$

If the battery pack is discharged, the stored energy is consumed. The discharging process is quite similar to that of hydrogen fuel cells. After processing the convertors, the inner material reaction creates energy and delivers it to the power bank.

$$E_{Discharging} = \eta_{BP\ discharging} \times \eta_{BP\ convertor} \times E_{To\ consumed} \quad (4)$$

3.2.3.1 Battery model and strategy

This thesis's battery model's most significant distinguishing characteristic is its dynamic status monitoring. Unlike other battery models, this battery type checks the battery state prior to operation. The battery's working charge $SOC_{working}$ is between the range of SOC_{low} to SOC_{high} as follows:

$$SOC_{low} \leq SOC_{working} \leq SOC_{high} \quad (5)$$

where SOC_{low} is the lower limit of the state of charge and SOC_{high} is the higher limit. Also, during the charging stage, the power for charging changes. This happens because of different reasons like getting older, temperature, and how much charge is there. In this thesis, the power used for charging only depends on the remaining energy level, and the battery getting older is considered when thinking about replacing batteries. For now, we don't include temperature parameters because this needs a big thermodynamic model for the train system. So, the power used to charge the battery pack is decided only by how much charge it currently has. The battery pack receives increased charging power while the battery's capacity is depleted. Once the state of charge is over SOC_{CC}, the charging mode switches to constant voltage charging mode, and a much lower charging power is applied. $P_{BP(CC\ charging)}$ and $P_{BP(CV\ charging)}$ are the charging power in these two different stages.

$$P_{BP(charging)} = \begin{cases} P_{BP(CC\ charging)}, & SOC < SOC_{CC}, \\ P_{BP(CV\ charging)}, & SOC \geq SOC_{CC}, \end{cases} \quad (6)$$

3.2.3.2 Energy losses in a battery pack train

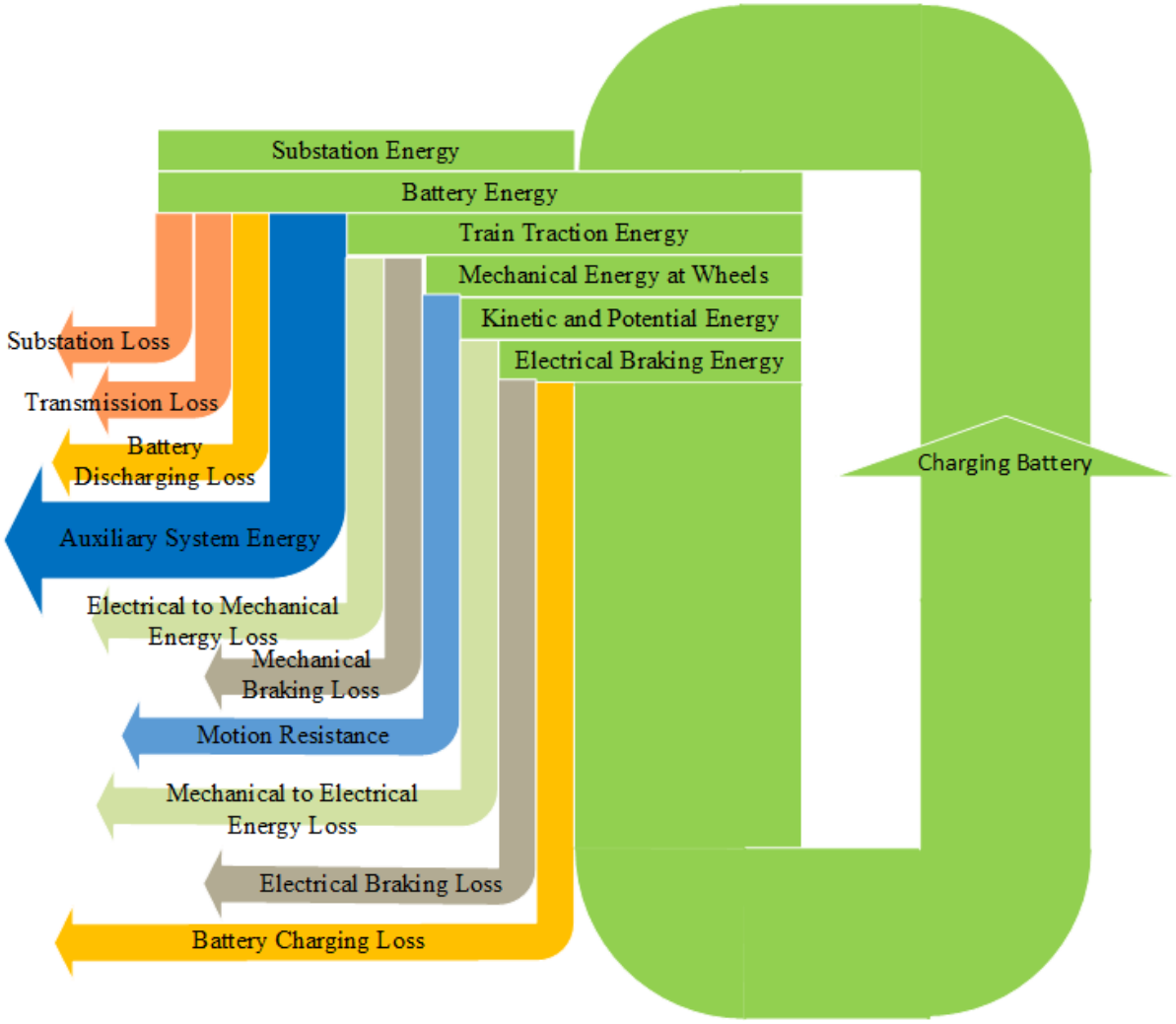

Figure 13 Energy losses in a battery train

Compared with a hydrogen fuel cell train, a battery train has much higher energy efficiency. Even though the energy in the battery is usually charged by pantograph, which means there are more paths to lose energy, the overall battery power system energy losses are still low.

3.3 Modelling of overhead line power systems

In the UK, the railway network encompasses approximately 15,800 route kilometres and includes over 30,000 structures such as bridges, tunnels, and viaducts, in addition to myriad auxiliary components like signals and level crossings. The network boasts around 2,500 stations and facilitates more than 1.7 billion passenger journeys and over 16 billion net tonne-kilometres of freight transportation annually [63, 64]. In terms of traction power, the UK's railway system is categorised into four primary segments [17]:

• diesel-powered unelectrified lines;

• lines electrified with 25,000 V AC overhead equipment;

• lines with 1500 V DC overhead equipment;

• lines electrified with a 650 V/750 V DC third rail.

Presently, over 6,000 route kilometres of the railway are electrified, constituting 42% of the UK’s total railway infrastructure [65]. The electric train network utilises a distinctive overhead line power system, wherein substations feed electricity to the trains, with transformers at these substations stepping down the voltage from the utility grid before it is transmitted to the overhead lines.

3.3.1 AC overhead line impedance

Calculating the impedance of an AC overhead line or rail is far more complexed than calculating the resistance of a DC line or rail. There is not only resistance but also reactance for AC transmission wire [66]. An electromagnetic field is formed and impacts the neighbouring conductor as a result of the high-voltage charging current flowing in the inductive transmission line [67]. Additionally, the electromagnetic field has an effect on the skin effect’s internal current: the majority of current flows through the conductor’s surface due to counter-electromotive force. When the current density is substantially higher near the surface, the

conductor's impedance increases significantly, and it will continue to increase as the current frequency increases [66, 68]. The following figure shows the equivalent radius R_{eq}:

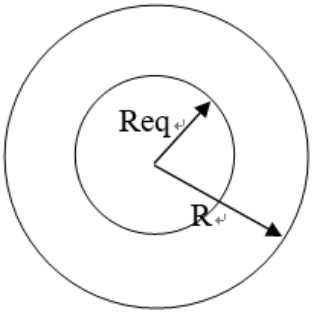

Figure 14 Cross section of an electrical conductor [66]

The self-inductance is:

$$L_{ii} = \frac{\mu_0}{2\pi} ln \frac{2H}{R_{eq}} \quad (7)$$

These two inductances are equivalent:

$$R_{eq} = R \times e^{-\frac{1}{4}\mu} \quad (8)$$

where μ is the conductor magnetic permeability, μ_0 is the magnetic permeability constant, μ_r is the relative magnetic permeability, and H is the average height of conductor. Because overhead lines and rails are not entirely isolated from the earth, an underground circuit includes a fourth wire (earth wire) in addition to the catenary wire, rail, and feeder wire. The following image depicts an underground earth wire:

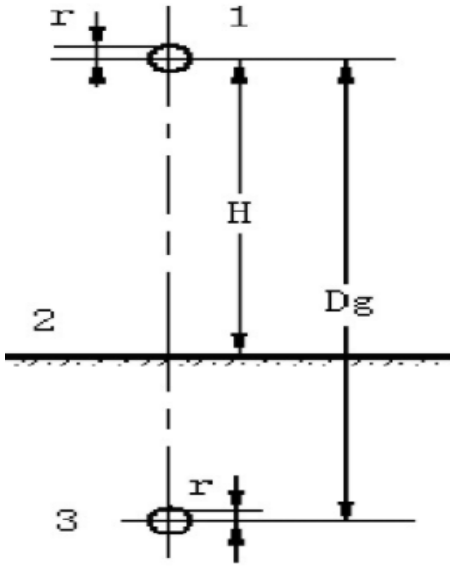

Figure 15 Carson's equivalent model [69]

Conductor 1 is an infinite-length wire at height *H* over than ground. Surface 2 is flat ground. Conductor 3 is the image earth wire. Depending on Carson's equation, the earth wire equivalent depth can be calculated as:

$$D_g = \frac{2.085 \times 10^{-3}}{\sqrt{f\delta 10^{-9}}}\ m = 655\sqrt{\rho/f}\ \text{m} \qquad (9)$$

where D_g is the equivalent depth, f is the frequency in Hz, δ is the earth conductivity in 1/(Ohm metres), and ρ is the earth resistivity in Ohm metres. Depending on the Carson equation for earth equivalent impedance:

$$r_e = \pi^2 f \times 10^{-4}\ (\frac{\Omega}{km}) \qquad (10)$$

For f = 50 Hz, it is equal to $r_e = 0.05(\frac{\Omega}{km})$. Considering Carson's equation and electromagnetic field theory [69, 70], the self-inductance for the overhead line and image earth wire can be:

$$L_1 = \frac{\mu_0 \mu_r}{8\pi} + \frac{\mu_0}{2\pi} ln \frac{2l}{R_1} = \frac{\mu_0}{2\pi} ln \frac{2l}{R_{eq1}} \quad (11)$$

so earth wire self-inductance L_2 is given by:

$$L_2 = \frac{\mu_0}{2\pi} ln \frac{2l}{R_{eq2}} \quad (12)$$

and the mutual inductance M_{12} between two conductors is given by:

$$M_{12} = \frac{\mu_0}{2\pi} ln \frac{2l}{d} \quad (13)$$

while in the overhead line-earth circuit [70]:

$$\begin{cases} Z_1 = r_1 + j\omega L_1 \\ Z_2 = r_2 + j\omega L_2 \\ Z_{12} = j\omega M_{12} \end{cases} \quad (14)$$

total impedance *Z*:

$$\begin{aligned} \mathrm{Z} &= Z_1 - 2Z_{12} + Z_2 \\ &= (r_1 + r_2) \\ &\quad + j\omega \frac{\mu_0}{2\pi} (ln \frac{d^2}{R_{eq1} R_{eq2}}) \end{aligned} \quad (15)$$

and

$$D_g = \frac{d^2}{R_{eq2}} \quad (16)$$

hence

$$\mathrm{Z} = (r_1 + r_2) + j\omega \frac{\mu_0}{2\pi} (ln \frac{D_g}{R_{eq1}}) \quad (17)$$

where r_1 is the conductor resistance in $\frac{\Omega}{km}$, and r_2 is the earth equivalent resistance $r_2 = 0.05\ \left(\frac{\Omega}{km}\right) when\ 50Hz.$

3.3.2 Rail impedance

Overhead line cross sections are always round or nearly circular in shape [71]. This form makes it simple to compute the total impedance. Even though AC flow at the conductor of an overhead line can alter the impedance slightly, the overhead line AC resistance can be roughly equated to DC resistance, which equals resistivity divided by the equivalent radius. However, rail design is more intricate, and the AC significantly affects the resistance value.

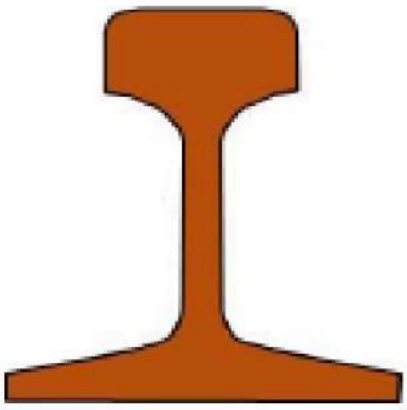

Figure 16 Cross section of a rail [71]

Nevertheless, the rail model can be simplified as a rectangle:

$$\text{Thickness } t = \frac{\left[\frac{p}{2} - \left(\left(\frac{p}{2}\right)^2 - 4A\right)\right]}{2} \qquad (18)$$

$$\text{width } w = \frac{p}{2} - t \qquad (19)$$

where p is the perimeter of the conductor. For European standard rail UIC 60, w = 317 mm and t = 24 mm [71]. As in the description above, the rail also has a skin effect, while the skin depth is:

$$\delta = [\frac{\rho}{\pi f \mu_0 \mu_r}]^{0.5} \quad (20)$$

where $\mu_0 = 4\pi 10^{-7}$ H/m, μ_r is the relative magnetic permeability of the steel rail, f is the frequency in Hz, and ρ is the resistivity of the steel rail in Ohm metres. The rectangular conductor also needs to be concerned about the edge and corner current; a coefficient K_C multiplied by R is used to correct the error of the rectangular conductor. Finally, the rail impedance R_{ac} is roughly equal to:

$$R_{ac} = \frac{R_{dc} K_C}{1 - e^{-x}} \, \Omega \quad (21)$$

where

$$K_C = 1 + F(f)[\frac{1.2}{e^{\frac{2.1t}{w}}} + \frac{1.2}{e^{\frac{2.1w}{t}}}] \quad (22)$$

$$\mathrm{F(f)} = (1 - e^{-0.026P}) \quad (23)$$

$$\mathrm{P} = A^{0.5}/(1.26\delta) \quad (24)$$

$$\mathrm{x} = 2\left(1 + \frac{\mathrm{t}}{\mathrm{w}}\right)\delta/\mathrm{t} \quad (25)$$

$$R_{dc} = [\frac{\rho 2l}{wt}] \quad (26)$$

where ρ is the rail resistivity in Ohm metres, l is the track length, and A is the cross-sectional area of the conductor.

3.3.3 DC railway resistance

DC railway system impedance does not consider the inductance of the transmission wire or rail, hence the conductor impedance is also equal to the conductor resistance. A two-substation model in DC railway is shown as follows [72]:

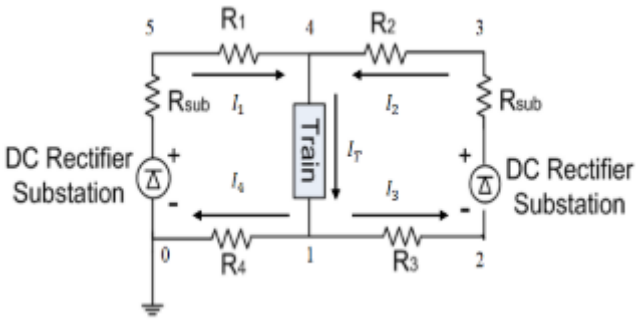

Figure 17 DC resistances in a two-substation model [72]

In Figure 17, R_{sub} is an inner resistor of a substation due to the power electronics devices. R_1 and R_2 are the transmission line resistances and R_3, R_4 are the track resistances. All resistance values are based on the transmission line resistivity and rail resistivity, and they are positively correlated with the length of the conductor.

3.3.4 Power flow solver and test results

3.3.4.1 Power flow modelling

Unlike a DC system, an AC AT system needs only one side of a single substation to power a train. Each substation has two sides, and at the end of each side is a neutral point. This is because every neighbouring side gets power from a different phase of a three-phase source. Due to this isolated point, each side can be looked at separately, which helps to avoid problems from a three-phase imbalance caused by a one-phase network. In this part, all the diagrams of railway circuits are made using Tina-Ti, and the pictures showing results are from MATLAB scripts.

The current loop analysis in Figure 18 is for an AT feeding system with four ATs and one 55 kV voltage source divided into two 27.5 kV voltage sources for examination. The purpose of employing 55 kV rather than 50 kV is to boost the voltage by 10% for further transmission. Z_1 and Z_2 represent the voltage source's internal impedance, whereas the remaining impedances (Z_3–Z_{16}) represent the transmission line impedance.

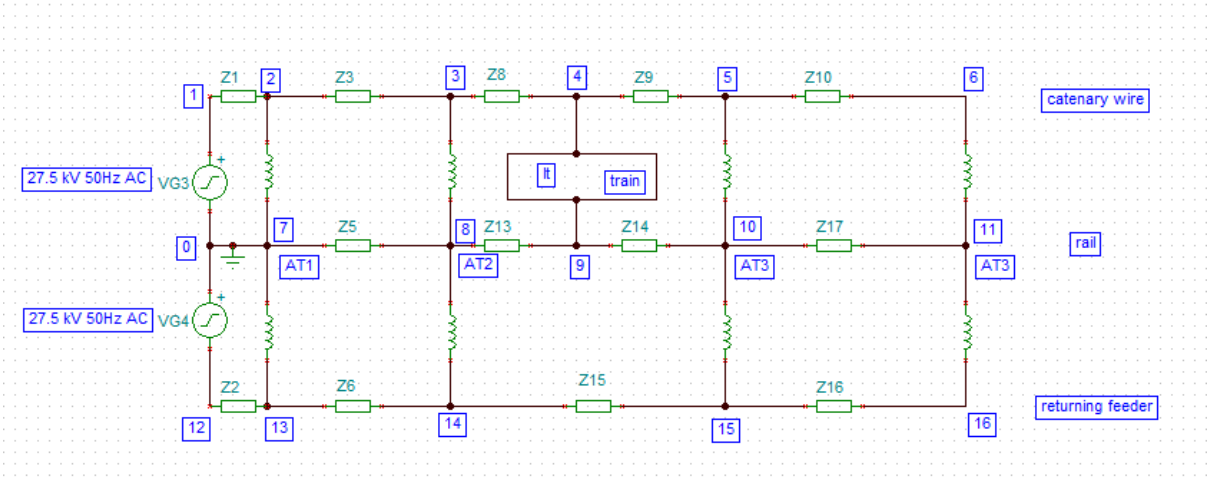

Figure 18 AT feeding system with four-AT structure

Loop current analysis may be used to determine the system's power flow regardless of the train's location. For instance, imagine the train travels between AT_2 and AT_3. The impedance of the catenary wire and the rails separates into two sections behind and ahead of the train.

Due to the AT's symmetrical arrangement, all current from rail to feeder wire is added to equal half the train current (I_t), resulting in a current via the voltage source of $I_t/2$ as I_1. To determine the current value across each AT, the train's loops 2-4-9-7, 3-4-9-8 (clockwise loop) and 4-5-10-9, 4-6-11-9 (anti-clockwise loops) should be considered for AT_1, AT_2, AT_3, and AT_4, respectively. Assume the currents in the loop above are $I_{2,1}$, $I_{2,2}$, $I_{2,3}$, and $I_{2,4}$, all of which pass through the train.

$$I_1 + I_{2,1} + I_{2,2} + I_{2,3} + I_{2,4} = I_t \qquad (27)$$

and for substation current:

$$I_1 = I_t/2 \qquad (28)$$

so, the sum of loop current is:

$$I_{2,1} + I_{2,2} + I_{2,3} + I_{2,4} = I_t/2 \qquad (29)$$

The loop current arrangement depends on the sum of each loop transmission impedance:

$$R_{loop\ ATi} = R_{rail_{ATi\ to\ train}} + R_{catenary\ wire_{ATi\ to\ train}} \qquad (30)$$

The admittance of each loop:

$$[Y_{loop\ ATi}] = [R_{loop\ ATi}]^{-1} \qquad (31)$$

so the current through each loop can be calculated as:

$$I_{2,\mathrm{i}} = \frac{[Y_{loop\ ATi}]}{\sum[Y_{loop\ ATi}]} \qquad (32)$$

After determining the current flow through each loop, the voltage distribution in overhead lines and rails and train voltage (the voltage difference between catenary wire and rail at train $V_4 - V_9$) can be easily calculated. It depends on the self-impedance and mutual impedance of the catenary, rail, and feeder wire, the current through the wire as well.

3.3.4.2 Newton–Raphson iteration

Typically, the voltage and current of the train cannot calculated by the circuit equations directly. These equations are unnecessarily complicated and nonlinear. As a result, most AT system studies employ the iteration approach to resolve this issue. The Newton–Raphson iteration method will be employed in this study [73, 74]. Figure 19 shows the Newton-Raphson iteration

for current and voltage calculation. Firstly, the train current is assumed as 400 A as the high-speed train current is between 300A to 400A [75]. Then, the algorithm corrects the train current by comparing the instantaneous constant power to the calculated power after calculating the approximate voltage value based on the current assumption. Instantaneously, the train may be seen as a continuous power load. The new train current sort out according to the train load power and its new voltage value.

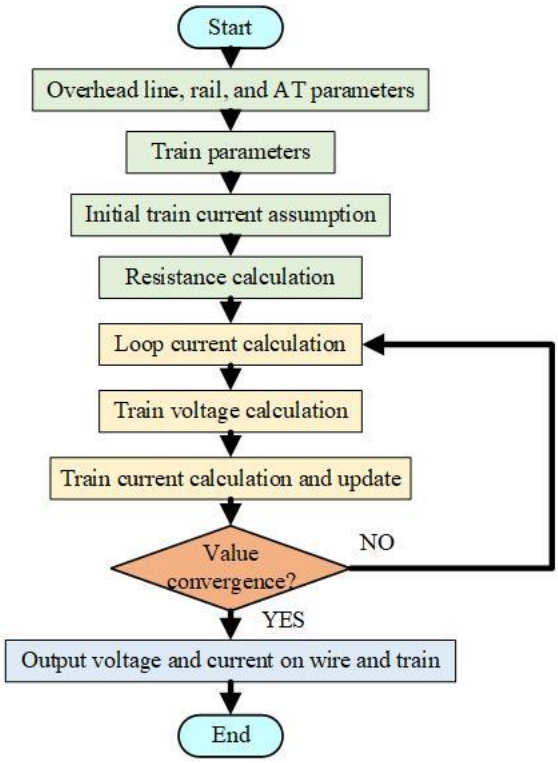

Figure 19 The Newton-Raphson iteration method for current and voltage

Here is the example of Newton–Raphson iteration. It is assumed that the train is located between AT1 and AT2 like Figure 18. The point 4 is where train connecting with overhead line. According to the equations in Section 3.3.4.1. The voltage difference between overhead line Point 2 to Point 3 is:

$$V_{2,4} = V_{2,3} + V_{3,4} \tag{33}$$

The voltage difference between overhead line Point 2 to Point 3, and between Point 3 to Point 4 are:

$$V_{2,3} = \left(I_1 + I_{2,1}\right) \times Z_c \times D_{2,3} - 2I_{2,1} \times Z_{cr} \times D_{2,3} - \left(I_1 - I_{2,1}\right) \times Z_{cf} \times D_{2,3} \quad (34)$$

$$V_{3,4} = \left(I_1 + I_{2,1} + I_{2,2}\right) \times Z_c \times (D_t - D_{2,3}) - 2(I_{2,1} + I_{2,2}) \times Z_{cr} \times (D_t - D_{2,3}) - \left(I_1 - I_{2,1} - I_{2,2}\right) \times Z_{cf} \times (D_t - D_{2,3}) \quad (35)$$

Similarly, the voltage difference between Point 7 to Point 9 is:

$$V_{7,9} = V_{7,8} + V_{8,9} \quad (36)$$

and separately, the voltage difference between rail Point 7 to Point 8, and between Point 8 to Point 9 are:

$$V_{7,8} = 2I_{2,1} \times Z_r \times D_{2,3} - \left(I_1 + I_{2,1}\right) \times Z_{cr} \times D_{2,3} + \left(I_1 - I_{2,1}\right) \times Z_{rf} \times D_{2,3} \quad (37)$$

$$V_{8,9} = 2\left(I_{2,1} + I_{2,2}\right) \times Z_r \times \left(D_t - D_{2,3}\right) - \left(I_1 + I_{2,1} + I_{2,2}\right) \times Z_{cr} \times \left(D_t - D_{2,3}\right) + \left(I_1 - I_{2,1} - I_{2,2}\right) \times Z_{rf} \times (D_t - D_{2,3}) \quad (38)$$

Hence, the voltage difference between overhead line and rail at train location is V_t:

$$V_t = V_{4,9} = 27.5 - (Z_1 + Z_2) \times I_1 - V_{2,4} + V_{7,9} \quad (39)$$

where $(Z_1 + Z_2)$ is the system impedance, Z_c, Z_r are the self-impedance of overhead line and rail. Z_{cf}, Z_{rf}, Z_{cr} are the mutual impedance between overhead line and feeder wire, rail and feeder wire, overhead line and rail. $D_{2,3}$ is the distance between substation to the first autotransformer, D_t is the distance between substation to the train.

Suppose

$$f\left(I_t^i\right) = \Delta P = P_t - I_t^i (V_t^i)^* \tag{40}$$

According to Newton–Raphson iteration, the next iteration of train current :

$$I_t^{i+1} = I_t^i - \frac{f\left(I_t^i\right)}{f'\left(I_t^i\right)} \tag{41}$$

where

$$f'\left(I_t^i\right) = -(V_t^i)^* - I_t^i (\frac{V_t^i}{I_t^i})^* \tag{42}$$

Combine Equations in Section 3.3.4.1 and this section, a new iteration I_t^{i+1} of train current can get. If the new current value meet the convergence condition,

$$\begin{aligned} |Re\left(I_t^i - I_t^{i+1}\right)| < \varepsilon \\ |Im\left(I_t^i - I_t^{i+1}\right)| < \varepsilon \end{aligned} \tag{43}$$

The iteration can stop and output current value. Or starting a new iteration.

3.3.4.3 Single-train power system simulator

The simulator for a single-train, single-track power system computes the distribution of network voltage. The dual rails are modelled in a simplified manner based on track bonding. Within this simulator, a train commences operation from the substation and travels to an extended distance. During the journey, parameters such as voltage, current, and the equivalent system impedance of the train are continuously monitored and recorded.

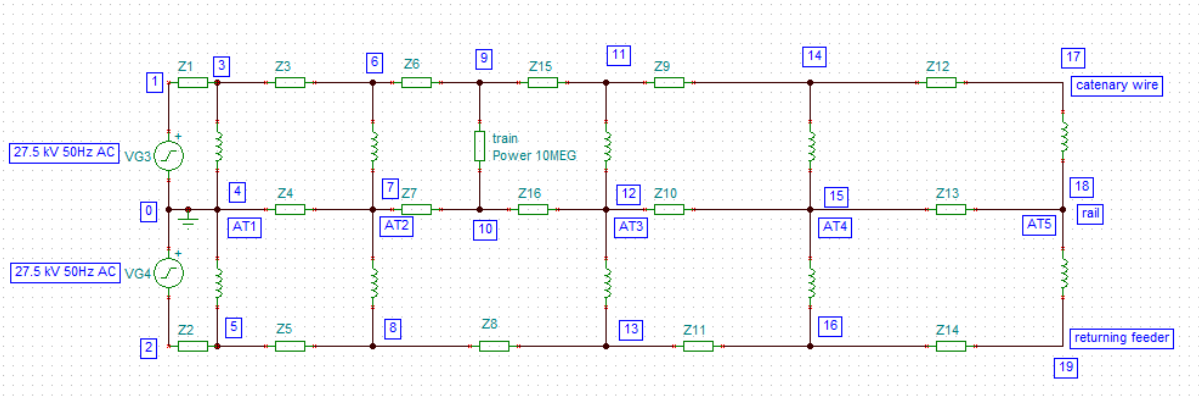

Figure 20 Train operating between AT_2 and AT_3

Figure 20 depicts the simulator model circuit operating as the train travels between AT_2 and AT_3. MATLAB code may calculate the train's path from the first to the fifth AT. In this case, it is supposed that the train is a continuous power load of 10 MW (400 A and 25 kV), with a power factor (PF) of 1 [75]. Five kilometres separates nearby ATs.

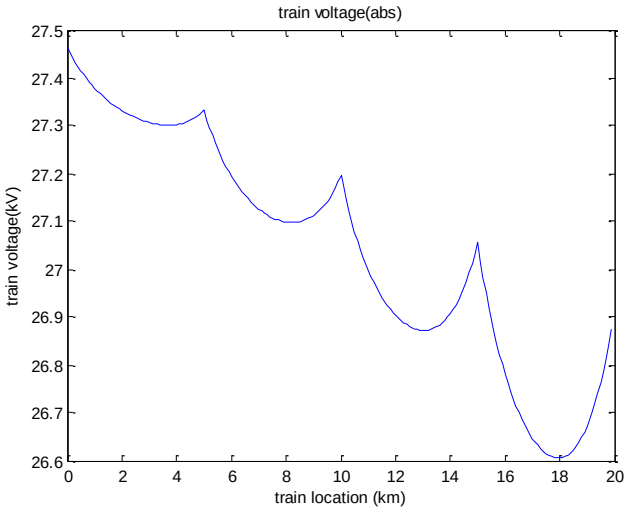

Figure 21 Train voltage changes against location

Figure 21 demonstrates how the voltage of the train varies while it is moving from the first transformer to the last one. This curve indicates that the train gets a higher voltage at the point of the autotransformer. Due to the characteristics of the autotransformer power supply, the

current conducted to the rail through the train will mostly be equally transmitted back to the contact line and feeder wire by the autotransformer. This additional current flow causes the autotransformer's contact line to be at a higher voltage state. This is the reason why modern railway systems use autotransformers to make the power supply length longer for each arm. However, due to the increase in energy transmission losses over distance, even at the location of the autotransformer, it becomes challenging to maintain high voltage values as the distance increases. This extension has its limits because the voltage still decreases significantly over long distances.

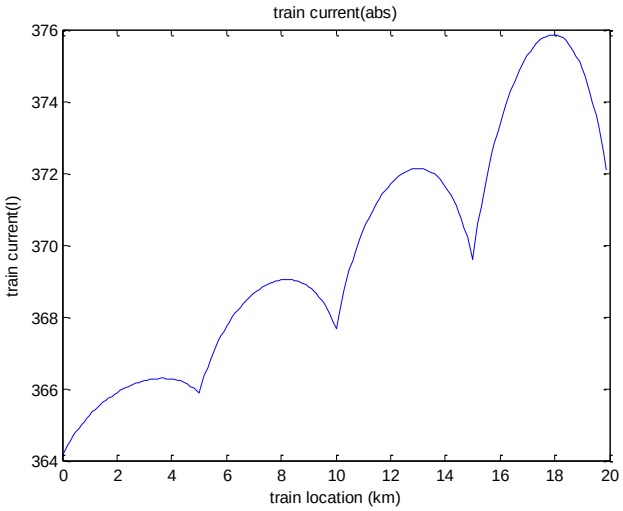

Figure 22 Train current changes against location

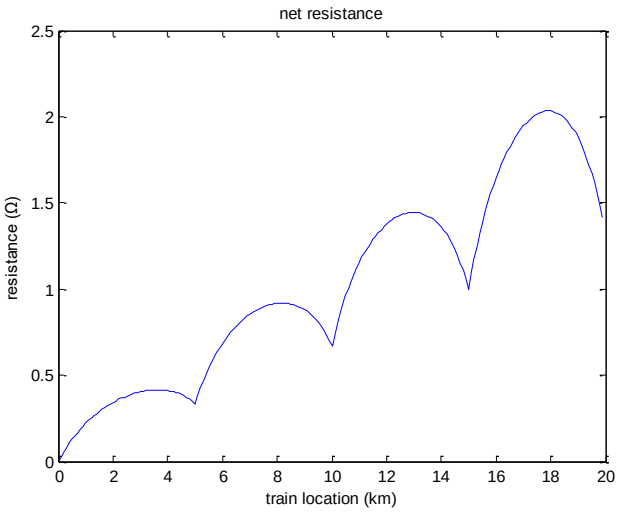

Figure 23 Net resistance in any location

As the train's voltage decreases as it approaches the substation, its current should increase to maintain the load's constant power like Figure 22. Moreover, Figure 23 shows the overall impedance of system is increasing. The total network current likewise grows in this condition, and the power losses along the transmission line increase. Combined with Equation (28), the transmission wire active power losses show as Equation (44):

$$P = 2UI_{train}\cos(PF) = 4R_{wire}{I_{train}}^2\cos(PF) \qquad (44)$$

Figure 24 shows the power factor on feeding wire. When the train travels a greater distance, a more inductive conductor (overhead line and feeder wire) is added to the circuit, and the whole load, including the train and transmission line, becomes inductive. Increased reactive power generation is occurring, and power quality is deteriorating.

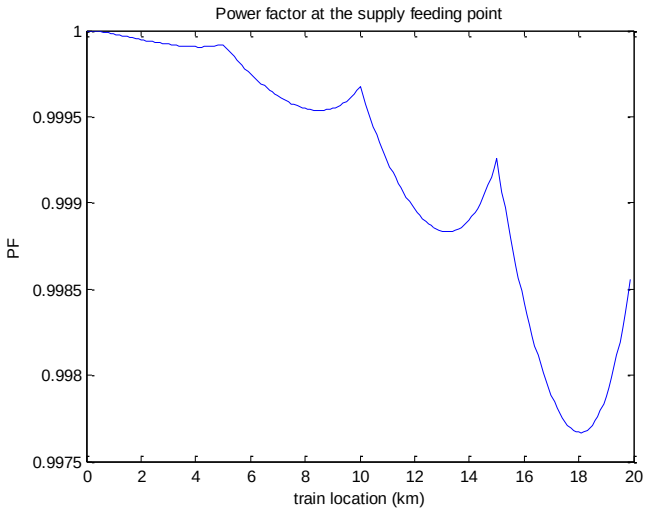

Figure 24 Power factor changes at feeding wire

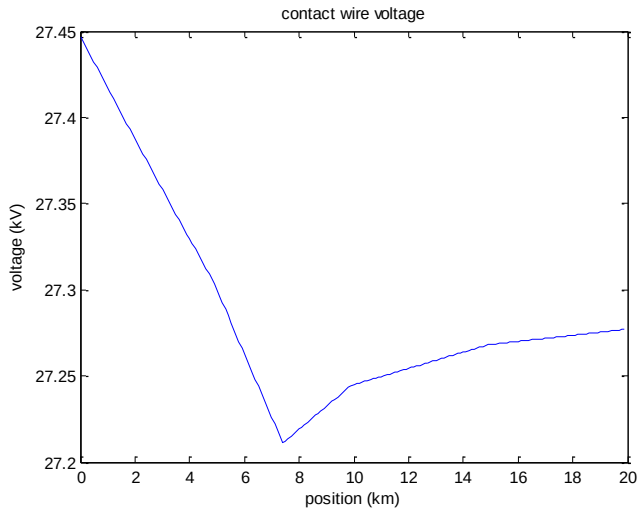

Figure 25 Contact wire voltage when train is at 7 km

Another profile for calculating network voltages may display the voltage distribution at any location on the network, regardless of where the train is located. Assume the train is at 7 kilometres, as shown above. Because the catenary wire at the train's point has the lowest voltage, every other point must send current to the lowest voltage point in order for the train to continue travelling.

3.3.4.4 Multi-train single-track power system simulator

In contrast to a single-train power system simulator, a multi-train single-track power system simulator should examine all trains in the same arm and aggregate their current flows for analysis. After determining the current loop for each train, the voltage distribution is calculated and the inaccuracy is corrected.

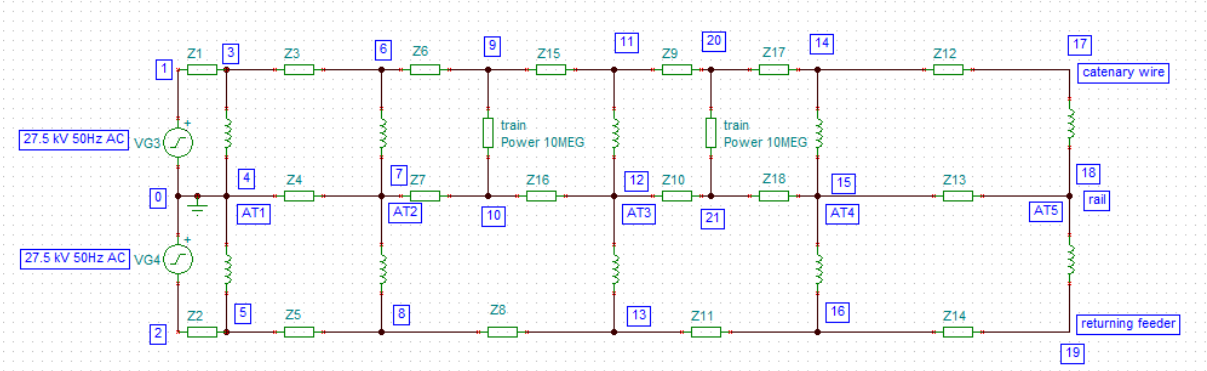

Figure 26 Multi-train single-track power system structure

When computing the loop current, these two trains may be seen as two separate trains in order to calculate the loop current individually.

The alternative method of calculating voltage distribution is to first calculate network voltage by dividing the route into small segments, accumulating the voltage difference between each segment based on transmission impedance and current flow calculations, and then determining which train voltages through the network voltage distribution correct the error. Compared to the approach used to simulate a single-train power system, this method may take longer to gather network voltage. Nonetheless, this system is much easier to grasp and modify when other features or profiles are introduced.

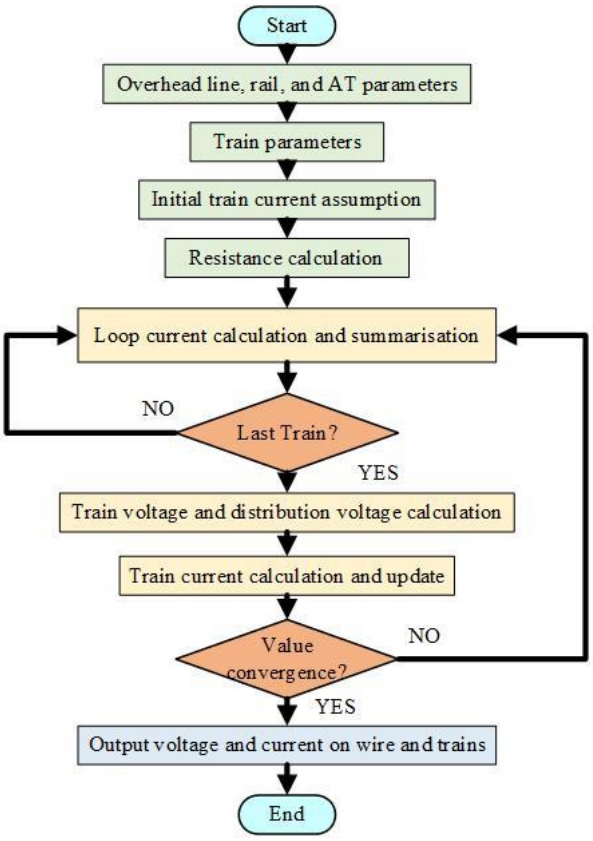

Figure 27 Multi-train electric power system

This simulator can determine the net voltage distribution and power flow regardless of the number and location of the trains. Similarly, imagine two trains run in the same arm of a substation; for the sake of comparison, assume one train is positioned at 7 kilometres, identical to the location of the train in the single-train power system simulator. At the same time, the other is located at 11 kilometres.

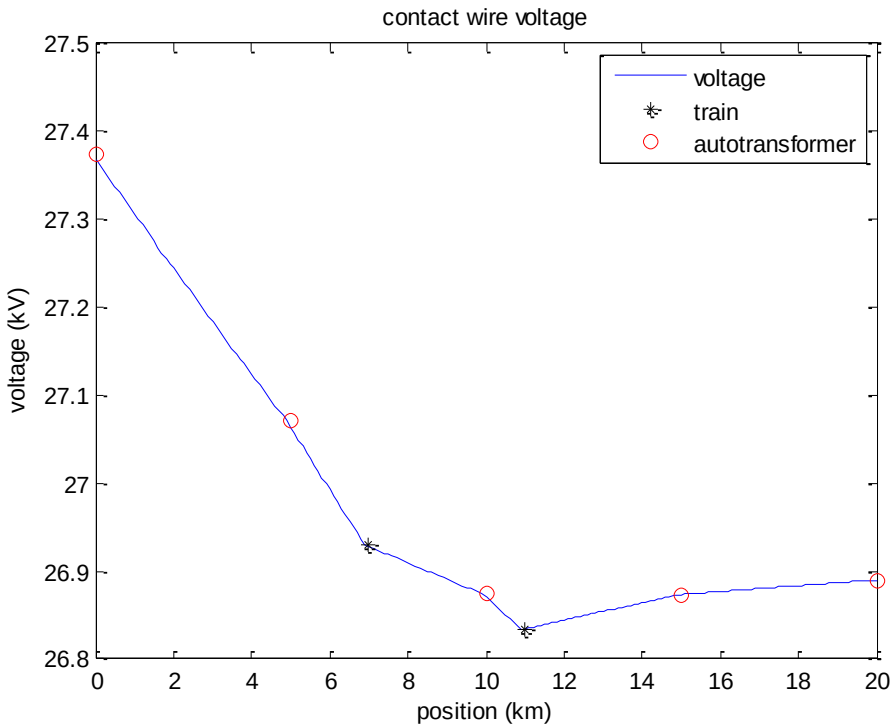

Figure 28 Contact wire voltage with two trains

In comparison to Figure 25, the voltage loss across the catenary wire rises while another train runs in the same arm. At the point of first train, the voltage drops from the substation to the train is 0.24 kV for one train system whereas the difference for two train system is 0.48 kV, double the voltage drops compared with single train system. Two-train systems waste almost twice as much energy as a single-train system at the start point as nearly double the current on the transmission wire, where the first AT is placed. These two trains are reasonably close together and share a continuous power demand, resulting in identical current flows.

3.4 Traction system simulation

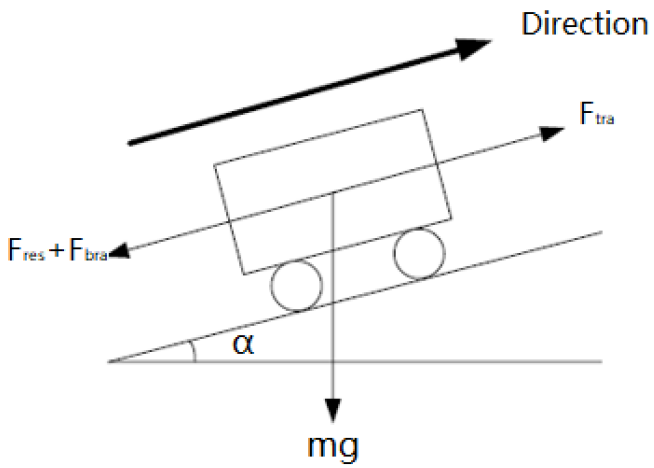

Figure 29 Forces on a traction vehicle

As Figure 29 shows, train movement modelling includes forces of external effect shown as gradient forces and resistance forces, including headwinds, friction, and other associated resistance. Train traction movement depends on Newtonian motion equations as in Equation(45).

$$m(1+\lambda)a = \mathrm{F_{tra}} - F_{bra} - mgsin(\alpha) - \mathrm{F_{res}} \quad (45)$$

$$F_{res} = (A + Bv + Cv^2) \quad (46)$$

$$\mathrm{F_{tra}} = \eta_{train} \times (P_{demand}/v) \quad (47)$$

where m is the mass of the train and a is the train acceleration/deceleration rate. The inertial effect, also called the rotary allowance, $\lambda = 8\%$, and α is the angle of the slope. The resultant force consists of the traction force F_{tra}, braking force F_{bra}, gravity force mg in the direction of movement, and resistance according to the Davis equation [56], Equation (46), where A, B, and C are the Davis equation constant coefficients. A is a constant parameter, B is the parameter

proportional to the operation velocity, and C is proportional to the square of operation velocity; v is the operation velocity. The braking force F_{bra} combines the force of both electrical braking and mechanical braking. Traction power is supplied by the motor powered by a multi-mode power system, and the effort is inversely proportional to velocity. η_{train} is the efficiency of the train, typically set as 85%.

Traction simulation simulates the movement of trains by traction and the power system over the whole route. In the first two steps of Figure 30, train and route reconstructions are sent to the simulator to represent upgrading the original train and route. Train reconstruction considers converting a diesel train to a multi-mode train using hydrogen fuel cell power and battery power, and route reconstruction considers extending the electrified track length. In this part of simulation, it is assumed that the power supply system is a box with a combination of energy supply method including diesel engine, hydrogen fuel cell, battery, overhead line, and motors. For the loop to calculate train traction, this simulator is computed based on the distance domain (discretisation distance space ΔD). At the beginning of each space, the power system status is the same as that at the end of the previous area. As Equation (48) shows, train velocity at the end of the discretisation space $V(i)$ is calculated according to the acceleration/deceleration rate in Equation (48) and the end velocity of the previous space $V(i-1)$. Time consumed $\Delta T(i)$ in any space is calculated by the average velocity in each step i:

$$V(i) = \sqrt{V(i-1)^2 + 2 \times a \times \Delta D} \tag{48}$$

$$\Delta T(i) = \frac{2 \times \Delta D}{V(i-1) + V(i)} \tag{49}$$

$$\mathrm{P}(i) = \frac{V(i) - V(i-1)}{\Delta T(i)} \times m(1+\lambda) \times \frac{V(i) + V(i-1)}{2} \tag{50}$$

$$\mathrm{E}(i) = \mathrm{P}(i) \times \Delta T(i) \qquad (51)$$

Then, as it shown in Equation (50), the actually power required can be computed by the Speed profile $V(i)$ and Time $\Delta T(i)$. Besides, the energy required depends on the power required and the time consumed in this space. The status at the end of step is determined and set as the start status of the next step $i + 1$. Once that has been completed for all spaces (whole journey), the completed performance of the train operation can be shown. This traction simulator is based on the Single-train simulator at BCRRE.

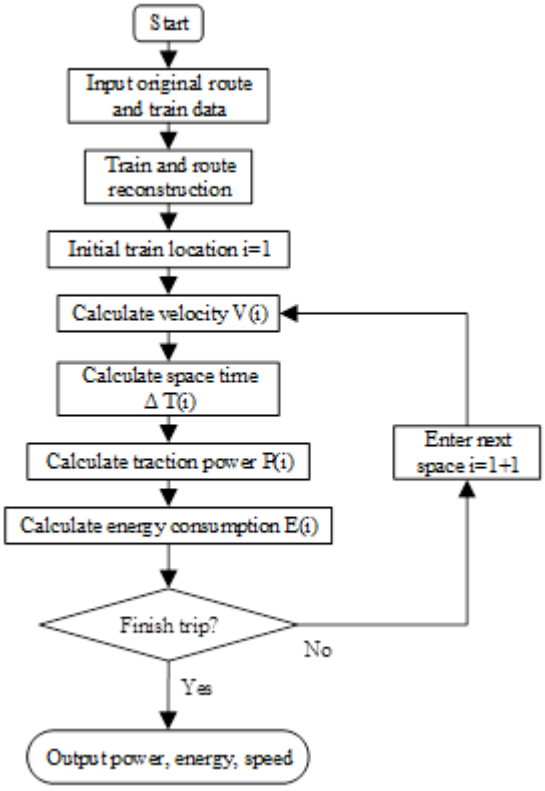

Figure 30 Traction simulator flow chart

3.5 Integration of power supply and traction systems

The power supply and traction system are the two independent systems in a railway system. To combine these two system models as an integrated model, an integrated simulator needs to be developed. It is necessary to find a connection point between these two models. The primary

parameters for the power supply system are regrading to the power and energy. At the same time, although the traction system considers the mass, speed, acceleration rate, and force, as shown in Equation (45), the power demand used to maintain the force is the parameter based on power. Hence, the integrated simulator is presented in Figure 31:

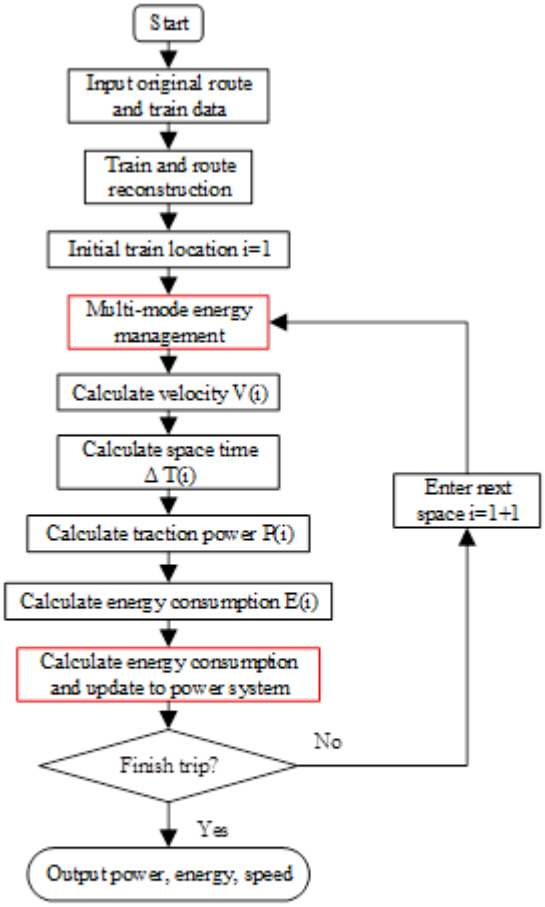

Figure 31 Integrated simulator

This integrated simulator has two more power supply system related blocks compared with the traction simulator in Figure 30 Traction simulator flow chart. Figure 30. These two block have been inserted to the beginning and end of traction computation loop. The one insert to the beginning of the loop is Multi-mode energy management, which includes a energy

management system and power supply availability check system. Figure 32 shows before starting the distributing energy, the simulator would check the availability of each power supply system first, and send the status to energy management system to arrange the power supply system usage.

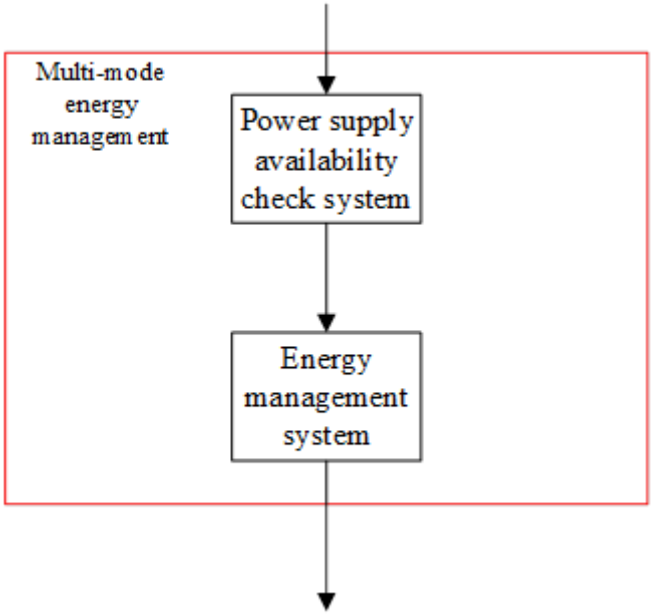

Figure 32 Multi-mode energy management

The function of another block is to update the real power and energy requirements to each of power supply system. Those information will be defined by specific power management strategy and the overall power and energy requirement. For single powered system, the strategy will be defaulting set as all energy from one power supply. For multi-mode train, the strategy will be explained and shows how the train allocated energy requirement. Power supply systems usage will be recorded, and the updated status will be sent to the next step to achieve dynamic power management.

3.6 Conclusion

This chapter is focused on developing the Train Performance Simulator (TPS), an essential tool for modelling diverse railway power systems. It elaborates on the TPS's ability to accurately represent various systems, such as diesel engines and hydrogen fuel cells. The simulator's detailed modelling of real-world railway scenarios makes it a valuable asset for analysing and enhancing railway efficiency, particularly in the context of reducing carbon emissions in railway transportation. The integrated simulator with two energy supply related blocks solves the problem of allocating multi-mode energy supply and dynamic updating energy supply system. this simulator has been used for the journal paper “Development of a smart hybrid drive system with advanced logistics for railway applications” published *in International Journal of Hydrogen Energy* [76].

4 Evaluation of diesel train power pack replacement and operation cost

4.1 Introduction

In the UK, the railway sector is instrumental in achieving zero carbon emissions. Facing a key juncture, the sector must update its infrastructure to significantly reduce CO2 emissions. This involves a critical choice between replacing diesel trains with hydrogen-powered ones or investing in new electric lines. This chapter undertakes a full study in this regard, set against the backdrop of global environmental concerns and the increasing demand for sustainable energy in transportation. This section examines the shift from diesel to more environmentally friendly train power systems, conducting a thorough comparison of their operational costs and environmental impacts. The analysis extends beyond mere cost comparisons, incorporating financial aspects of substituting diesel with alternative energy sources for trains. This inquiry is indispensable for the railway industry as it seeks to navigate the complexities of adopting greener technologies. The chapter further explores the broader implications of this transition, addressing some potential opportunities that come with railway decarbonisation. Highlighting the necessity of strategic planning and investment in green technologies, this chapter makes a significant contribution to the discourse on sustainable transportation. It provides critical insights and data, aiding in the evolution of more efficient, cost-effective, and environmental-friendly rail systems. This extensive analysis plays a key role in directing the future of railway transportation, ensuring its alignment with worldwide sustainability targets.

Section 4.1 of this chapter summarises the current railway economic analysis and explains why it is not used in this thesis. Section 4.2 breaks down the total cost of railway modernisation into many smaller components. Section 4.3 examines a case study of the Midland Main Line from

London to Sheffield. The assessment findings were analysed to demonstrate the likely reasons for the disparate performance of these various schemes.

4.2 Overall cost calculation

Modernising the railway system to reduce carbon emissions will require significant initial funding and ongoing costs for new trains and their upkeep. Below are the key costs evaluated in this study:

• Initial infrastructure costs – These include a variety of capital and renewal expenses over time, which account for the cost of installing overhead electric lines.

• Fuel costs for trains – These vary depending on how much fuel different types of trains use and the distance they travel according to the passenger timetable.

• Replacement costs – There are higher costs for maintaining overhead line infrastructure and different costs for maintaining trains, depending on how far each type of train travels according to the passenger timetable.

As detailed in section 4.1, there are three main types of total costs: those for infrastructure, energy use, and replacement. As the initial cost shown in Section 4.2.1. The costs for converting trains also differ based on the method (changing a diesel train to a battery train, an overhead electric line train, or a hydrogen fuel cell train). Like Section 4.2.2 represented, the energy cost could be any type of energy source, so there is a description containing different energy consumptions and their final cost. Moreover, the equipment needed for different upgrade methods has a limited life and will need ongoing maintenance or replacement when it is no longer in good condition. The cost of such repairs or replacements must also be considered. Section 4.2.3 shows different equipment replacement calculation and their specific information details should be with case study in following chapters.

In summary, the total cost C_{total} can be separated into three different parts: initial cost C_{ini}, energy cost C_e, and replacement cost C_{rep} as shown in Equation (52).

$$C_{total} = C_{ini} + C_e + C_{rep} \quad (52)$$

4.2.1 Initial cost

The initial cost is the total cost of the train before operation. All railway upgrade plans must include replacing older vehicles with new ones. As a result, the original cost of all three kinds of trains consists of the cost of train conversion. Purely battery or purely hydrogen trains do not require the overhead line infrastructure in the route rebuilding cost because there is no electrification considered. On the other hand, an electric train requires electrification infrastructure to deliver power through the overhead line. Thus, the electric train's initial cost includes not only train conversion cost C_{conv} but also route rebuilding cost $C_{route\,reb}$. The initial costs associated with each of the three upgrade methods are calculated as given in Equation (53):

$$C_{ini} = \begin{cases} C_{conv} & Battery\ train \\ C_{conv} & Hydrogen\ trian \\ C_{conv} + C_{route\,reb} & Electrical\ train \end{cases} \quad (53)$$

4.2.1.1 Train conversion cost

C_{conv} as shown in Equation (54) includes the essential fixed rebuilding cost C_{fixed} which includes the cost of the motor, circuit, converter, and other components, and the cost of the battery pack and its associated components C_{BP}, as well as fuel cell cost C_{FC} and hydrogen tank cost C_{Hy_t}. The number of converted trains is counted as N_{trains}.

$$C_{conv} = N_{trains} \times (C_{fixed} + C_{BP} + C_{FC} + C_{Hy\_t}) \quad (54)$$

4.2.1.2 Route rebuilding cost

The cost of route rebuilding was assessed in this evaluation by classifying the unelectrified rail network into two groups, each with its cost rate for electrifying a single-track kilometre (STK). The route's complexity was determined using the following criteria: the route's length and civil engineering complexity (i.e. considering the number and nature of bridges and tunnels on the route). At this time, normal route electrification costs have been projected, ranging from £1 million to £2.5 million per STK [7]. Equation (55) illustrates two aspects of $C_{route\ reb}$. Except for tunnels, the normal route cost C_{normal} comprises electrification infrastructure and the cost of renovating the route from the ends of the electrified portion to the terminal station. Tunnel electrification costs are calculated individually as C_{tunnel} since they are much greater than for ordinary routes owing to the challenges associated with upgrading tunnels or bridges [7].

$$C_{route\ reb} = C_{normal} + C_{tunnel} \qquad (55)$$

4.2.2 Energy costs

The energy costs of diesel and multi-mode trains are evaluated independently in Equations (56) and (57). For diesel trains, the energy cost $C_{e_{diesel}}$ only includes diesel consumption multiplied by the diesel fuel price Pr_D , the engine P_{Engine}, and the engine efficiency η_{Engine}, whereas for multi-mode trains, the cost includes both hydrogen $E_{\mathrm{Hy\_C}}$ and electricity $E_{\mathrm{Ele\_C}}$ energy consumption multiplied by their respective prices $\mathrm{Pr_H}$ and $\mathrm{Pr_E}$. In this study, the power demand is determined by the movement status like 3.4 showed. Assuming that the energy price Pr changes yearly and that the price change slope a is the same as it has been in prior decades [77-81], the fuel price in the j-th year is represented by Equation (58). The original price of energy β is defined as $Pr_\beta(0)$. If all trains operate as planned and use N_{annu} fuel each year,

the total cost C_β of energy β (diesel, hydrogen, or electricity) for the next 40 years is provided by Equation (59) [82].

$$C_{e_{diesel}} = Pr_D \times \frac{\int P_{Engine} dt}{\eta_{Engine}} \tag{56}$$

$$C_{e_{multi-mode}} = \mathrm{Pr_H} \times E_{\mathrm{Hy\_C}} + \mathrm{Pr_E} \times E_{\mathrm{Ele\_C}} \tag{57}$$

$$Pr_\beta(j) = Pr_\beta(0) \times (1 + j \times a) \tag{58}$$

$$\mathrm{C}_\beta = N_{annu} \times \sum_{j=1}^{40} Pr_\beta(j) \tag{59}$$

4.2.3 Replacement cost

Usually, all equipment has an estimated life cycle. On reaching the end of its lifespan, it should be replaced. In this thesis, the battery pack $C_{BP\,rep}$, fuel cell system $C_{FC\,rep}$, and traction system equipment $C_{motor\,rep}$ are considered, and their costs are summed as C_{rep} in Equation (60). The battery pack needs to be replaced due to its degradation. Every time it charges or discharges, the degradation effect of the materials reduces the battery capacity [83]. If the maximum capacity decreases to approximately 75%, it would be considered degraded and replacing by another battery [84]. In this thesis, the standard for degrading of battery is the depth of discharge. The sum of all state of charge changes due to energy discharging is counted as the total depth of discharge [85]. The replacement of the battery pack is determined according to the times of its lifespan, depth of discharge $DOD_{lifespan}$, and total depth of discharge as in Equation (61). However, the replacement period for the fuel cell and the motor is assumed as a fixed period of years, $year_{FC\,period}$ and $year_{motor\,period}$ in Equations (62) and (63), respectively. They would be replaced when reaching their own lifespan limit. Except for the

replacement cost, the first-time system installation cost is included in year 1, and all equipment has an estimated life cycle. On reaching the end of its lifespan, it should be replaced. In this thesis, the battery pack $C_{BP\,rep}$, fuel cell system $C_{FC\,rep}$, and overhead line equipment $C_{OLE\,rep}$ are considered and their costs are summed as C_{rep} in Equation (60). The replacement period of the battery pack is determined according to the times of its operating depth of discharge because it directly affects the number of charge-discharge cycles a battery can undergo before its capacity significantly degrades, and the cost is shown as in Equation (61) [85]. However, the replacement period for the fuel cell, overhead line equipment, and motor is assumed as a fixed long time in Equations (62) and (63). The first-time system installation cost is included in C_{conv}.

$$C_{rep} = C_{BP\,rep} + C_{FC\,rep} + C_{motor\,rep} \quad (60)$$

$$C_{BP\,rep} = C_{BP} \times \left(\frac{DOD_{total}}{DOD_{lifespan}} - 1\right) \quad (61)$$

$$C_{FC\,rep} = C_{FC} \times \left(\frac{year_{total}}{year_{FC\,period}} - 1\right) \quad (62)$$

$$C_{motor\,rep} = C_{fixed} \times \left(\frac{year_{total}}{year_{motor\,period}} - 1\right) \quad (63)$$

4.3 Cost evaluation and analysis case study

4.3.1 Modelling data

4.3.1.1 Route selection

This cost–benefit study examines the route connecting London and Sheffield through Derby. This route is served by the Midland Main Line, a major railway line in the UK. The plan includes 16 significant stops and pauses totalling 256 kilometres [86, 87]. On the Midland Main Line, there are currently some electrification projects in progress [88], but only about 31% of

the tracks from London St. Pancras to Bedford are completely electrified; additionally, electrification of the route from Bedford to Kettering, which accounts for approximately 13.5% of the entire route, began in December 2018.

Table 3 Locations of Midland Main Line stations [86]

Station	**Location [km]**
London St. Pancras	0.00
Luton Airport Parkway	46.78
Luton	48.38
Bedford	79.46
Wellingborough	104.22
Kettering	115.22
Market Harborough	132.68
Leicester	158.54
Loughborough	178.58
East Midlands Parkway	189.20
Long Eaton	192.56
Derby	205.00
Belper	217.10
Chesterfield	233.60
Dronfield	241.60
Sheffield	256.00

Table 4 Location and length of tunnels [86]

Tunnel	**Location [km]**	**Length [m]**
Bromham Viaducts (River Ouse)	81.44	140
Clapham Viaducts (River Ouse)	83.16	120
Oakley Viaducts	85.38	120
Milton Ernest Viaducts	86.74	160
Radwell Viaducts	87.93	130
Sharnbrook Viaducts	89.92	180
Sharnbrook Tunnel (slow line only)	94.40	1701
Irchester Viaducts (River Nene)	102.00	140
Wellingborough Viaducts (River Ise)	103.42	120
Knighton Viaduct	155.8	80
Knighton Tunnel	156.84	95
Hermitage Brook Flood Openings	178.36	60
Flood openings	180.36	40
Redhill Tunnels	190.12	160
Trent Viaduct	190.34	220
River Derwent Viaduct	204.86	60
Nottingham Road Viaduct	205.60	60
Burley Viaduct (River Derwent)	210.68	80
Milford Tunnel	214.14	782
Swainsley Viaduct	215.54	80
Broadholme Viaducts	217.82	140
Toadmoor Tunnel	220.94	118
Wingfield Tunnel	223.34	239
Clay Cross Tunnel	234.02	1631
Alfreton Tunnel	216.22	770
Unstone Viaduct	239.78	120
Bradway Tunnel	244.18	1853
East Bank Tunnel	252.82	73

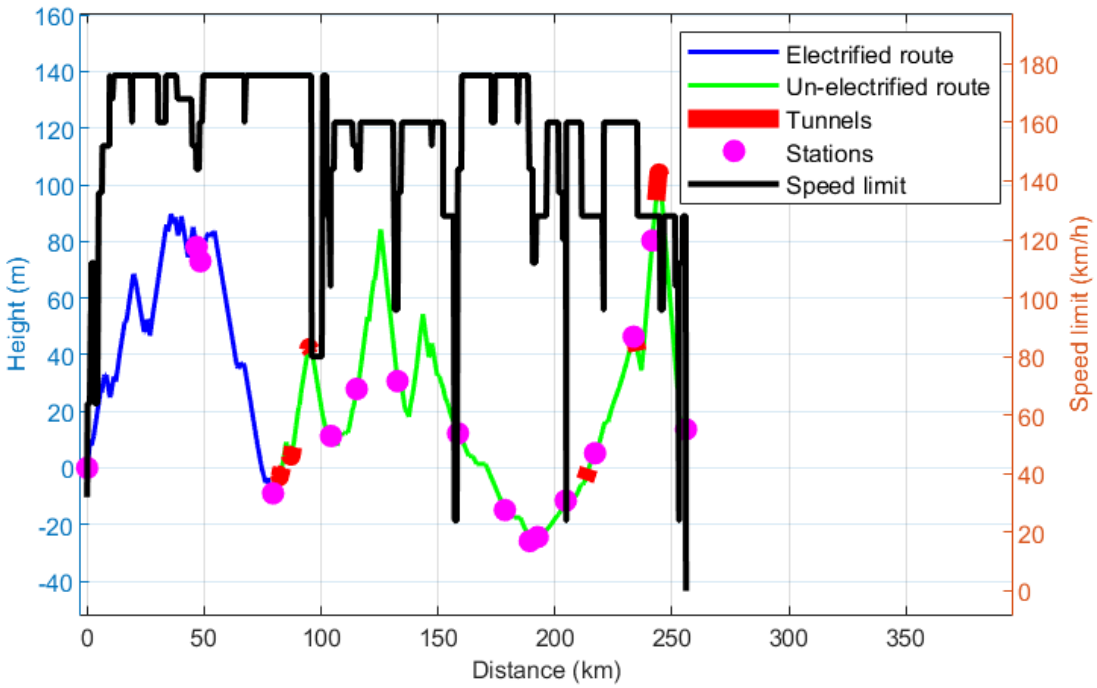

Figure 33 Line altitude, stations, and speed limit from St. Pancras to Sheffield

4.3.1.2 Vehicle model

Table 5 Class 222 (four cars) parameters

Parameter	**Value**	**Reference**
Traction power	560 kW/car	[89]
Weight	214 tonnes	Assumed
Train efficiency	85%	[90]
Engine weight	1.9 tonnes/car	[91]
Diesel tank (empty)	0.1 tonnes/car	[91]
Diesel	1500 litres/car	[91]
Auxiliary equipment	3 tonnes	Assumed

The Class 222, a diesel multiple-unit high-speed train, serves as the benchmark model for this research. Table 5 shows some parameters of a four-car Class 222. Each vehicle on this train is equipped with a 560 kW engine (2240 kW in total for four cars) [89]. Assume the Class 222

train weighs is similar as the other Class 220 family trains, which weigh 214 t. The train's efficiency is 85% when all components and gear energy losses are included [90]. Each Class 222 vehicle is equipped with a QSK19 diesel engine weighing 1.9 t, a 1500 litre diesel tank weighing 1.26 t, and auxiliary items totalling around 3 t [91]. It can travel roughly 2170 kilometres after refuelling [92]. Based on the simulation results for the initial diesel Class 222, the journey from London St. Pancras to Sheffield, spanning a distance of 256 km, necessitates approximately 2243.5 kWh of traction energy. This energy requirement is equivalent to 7478.2 kWh of fuel when considering the efficiency of the diesel engine. Moreover, for a similar operation performance, the traction energy consumption for 2170 km operation is approximately $\frac{2170}{256} \times 2243.5\ kWh = 19017.2\ kWh$. Considering the efficiency of the diesel engine and the energy density of diesel fuel, it can be calculated that 6000 litres of fuel, containing 60 MWh of energy, can be converted into 18 MWh of traction energy [93]. That is highly similar to the calculation results. Because all new conversion trains will be electric, diesel engines and tanks should be removed. Electrical motors should be equipped with a pantograph for operation on the electrified route. Furthermore, when contemplating the adoption of a self-powered traction system, such as hydrogen fuel cells or battery packs, it becomes necessary to account for the relative weight changes of various components including the hydrogen fuel cell, hydrogen tank, battery pack, and other related elements.

4.3.1.3 Battery characteristics

Table 6 Simulation battery pack characteristics

Parameter	**Value**	
Working SOC range	**lowest**	0.1
	highest	1
Discharging rate	5C	

Charging rate	**CC**	2 C
	CV	0.1 C

The battery utilised in this thesis is a $LiFeO_4$ battery; as Table 6 shows, the battery operates within its specified state of charge (SOC) range from 0.1 to 1. The SOC range mean that the energy remain in the battery should only between 10% to 100% of its capacity. The discharge rate in the table is the maximum discharging power, and its capacity is proportional to that power. When the SOC is less than 0.93, the constant current (CC) charging mode is activated throughout the charging process. When the SOC exceeds the threshold, the charging mode is changed to constant voltage (CV) charging which is slower [94, 95].

4.3.1.4 Train conversion design

Table 7 Train conversion characteristics

Parameter	**Value**	**Reference**
Overhead line energy efficiency	87%	[13]
Hydrogen fuel cell efficiency	Varied	[96]
Diesel engine efficiency	30%	[93]
Battery charging/discharging efficiency	94%	[97]
Diesel engine system	6.78 tonnes/car	[91]
Electrical motor system	4 tonnes/train	Assumed
Battery pack system	20 kg/kW	[98]
Fuel cell system	2.5 kg/kW	HydroFlex
Hydrogen tank (350 Pa)	0.66 kg/kWh	[40]

The simulated period is based on the typical train lifetime of 40 years; 12 Class 222 diesel trains are estimated to have been converted, with each train consisting of four cars. The overhead line is the most efficient supply system (87%), while diesel engines are the least

efficient at 30%. To simplify the modelling computing, most of the efficiency are set as fixed. However, the hydrogen fuel cell has a really high range of efficiency during operating. Simultaneously, it is assumed that the efficiency of hydrogen fuel cells is not set at its most extreme level. The efficiency of hydrogen conversion to electricity varies according to the output power of the hydrogen generator. According to the hydrogen fuel cell efficiency study, the efficiency continues to improve, reaching roughly 52% at 20 kW output power [96]. Furthermore, it decreases roughly linearly as output power increases, reaching 45% at 100 kW [96]. Figure 34 illustrates the efficiency curve in crude form.

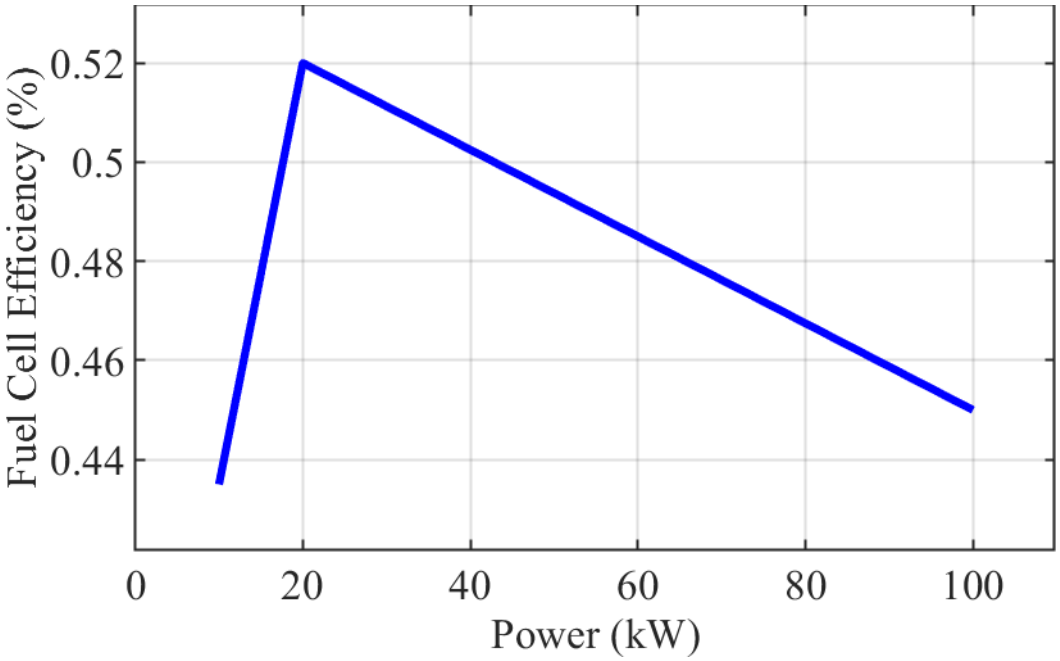

Figure 34 Hydrogen fuel cell efficiency vs fuel cell output power [96]

When discussing train conversion design, it is believed that the train's weight will vary. When comparing diesel trains to electric trains, the weight difference is constant, but the weight of the power system varies according to its planned capacity or power [25, 36]. The data on system power–weight ratios come from the University of Birmingham's HydroFLEX 1.1 study. Each

battery pack employed in HydroFLEX contains 84 kWh of energy, and it can supply 125 kW of power. HydroFLEX is the UK's first hydrogen-fuelled train, tested on the mainline in 2019.

4.3.1.5 Data for cost calculation

Table 8 Price of different parameters

Parameter	Price	Reference
Fixed cost	£40k/car	[23]
Battery system	£217/kWh	[99]
Fuel cell system	£1200/kW	[23]
Hydrogen tank	£8/kWh	[23]
Normal route electrification	£1.8 M/ptk	[7]
Tunnel electrification	£7.5 M/ptk	[7]
Diesel fuel	£0.13/kWh	[78, 100]
Hydrogen fuel	£0.3/kWh	[101, 102]
Electricity	£0.1/kWh	[77, 100]

Table 8 details the costs of train conversion, route reconstruction, and fuel. As with train weight, the cost of train conversion varies based on the design of the power system. The route's repair cost is included in its length, and each line has two tracks [7]. The replacement period varies according to the type of equipment. The battery pack has a life of 3000 full-depth charges [85]. The lifespan of hydrogen fuel cells for railway applications is expected to be long, typically designed to match the operational lifecycle of the train as 40 years. Besides, it is assumed that the hydrogen fuel tank as same frequency as hydrogen fuel cell.

4.3.2 Cost evaluation results

In this case study, three prospective enhancement methods are explored: electrification, hydrogen fuel cells, and battery packs. As per the energy capacity analysis detailed in Section 4.3.1.2, it is deduced that the train must carry a minimum of 19 MWh of energy onboard to

maintain its performance post-conversion from diesel. Consequently, equipping the entire train solely with battery power, as outlined in Table 6 and Table 7, would necessitate the installation of battery packs weighing approximately 1900 tonnes for a four-carriage train. This weight substantially exceeds the total mass of a standard four-carriage train, which is around 220 tonnes. Typically, each coach of the train is supported by four axles, with an axle load capacity of approximately 25 tonnes. This implies that the axles of the train can sustain a maximum load of 400 tonnes, far less than the required battery weight.

In this case, the pure battery train is not an acceptable upgrading choice as the hydrogen train and electric train can be designed without too much change in weight. These two upgrading methods will be evaluated and analysed in this case study. Only pure hydrogen fuel cell train and pure electric train are analysed in this case study.

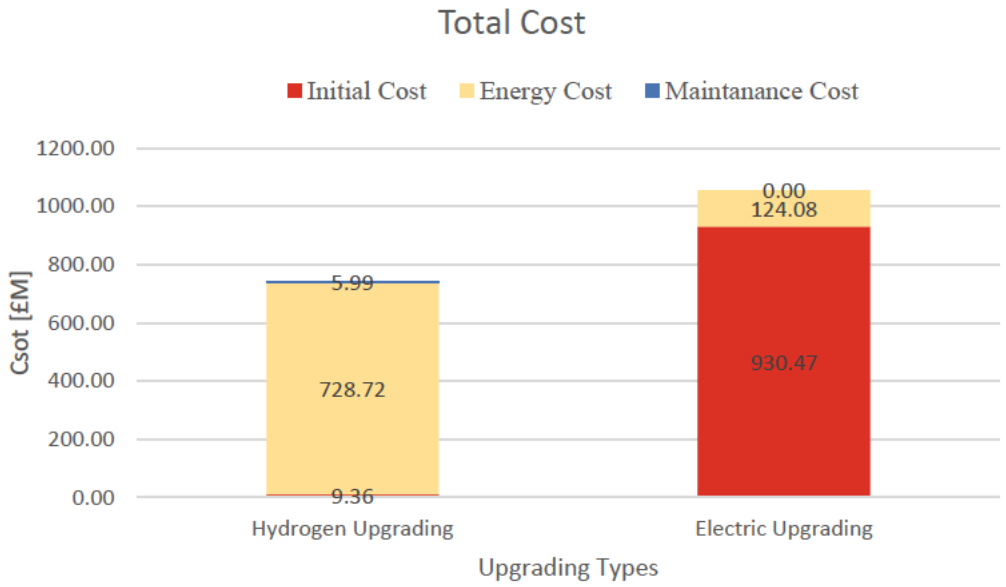

Figure 35 Total upgrading cost

The cost of both hydrogen and electric upgrades is depicted in Figure 35. Clearly, the cost of electrification is far higher than the cost of hydrogen trains. The cost of converting a railway

to hydrogen energy is minimal since it only considers the train conversion, including removing diesel engines and installing a new electrical motor powered by a hydrogen fuel cell energy system. However, converting an electric train does not just include the cost of the train conversion; it also provides for the cost of route reconstruction. Already, the starting cost is higher than the entire cost of a hydrogen train. Additionally, electrified trains do use energy. Although the energy cost is far less than the cost of hydrogen fuel cell trains, it still accounts for a fraction of the entire cost. The electric upgrading does not contain any hydrogen fuel cell and hydrogen tank replacement cost in this situation, so the replacement cost is 0.00 in this figure.

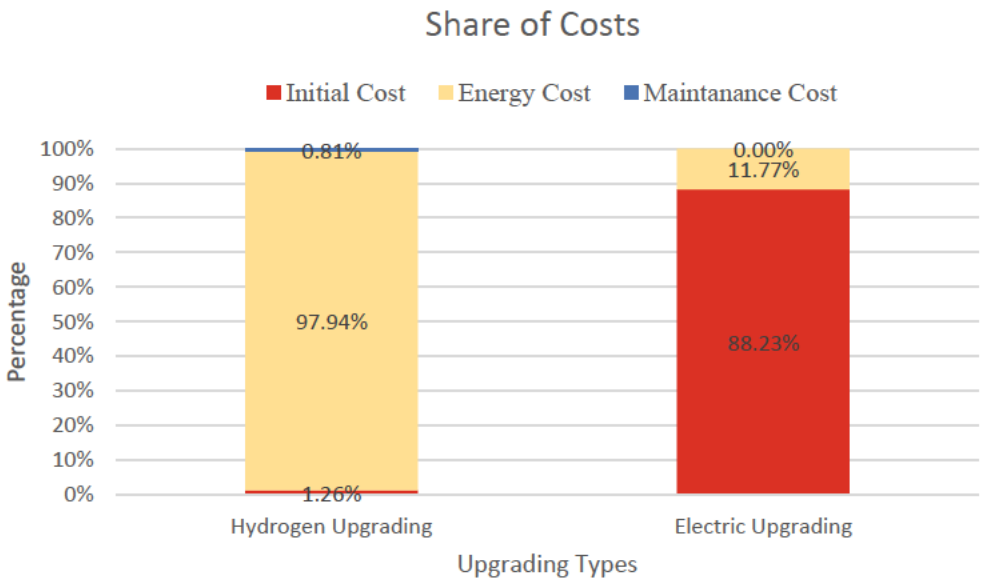

Figure 36 Share of upgrading cost

The cost distributions for both upgrading strategies are shown in Figure 36. Both hydrogen fuel cell trains and electric trains have exceptionally cheap replacement costs that may be disregarded. A significant portion of the cost is utilised as the starting cost for electric trains. The length of the electrification project and the STK unit pricing are critical factors in

determining the cost of upgrading electric trains since they significantly impact the cost evaluation of electric trains. In contrast to the original cost, which accounts for 88.23% of the total cost of an electric train, the energy cost accounts for just 11.77%. However, the cost-sharing for hydrogen trains is quite different. Almost all the expense of a hydrogen fuel cell is in the energy component. Energy costs are high due to both energy use and energy prices. The hydrogen replacement cost is quite low compared to the energy cost. The absence of a specified replacement cost implies that the proportion of replacement cost in electric upgrading is also zero.

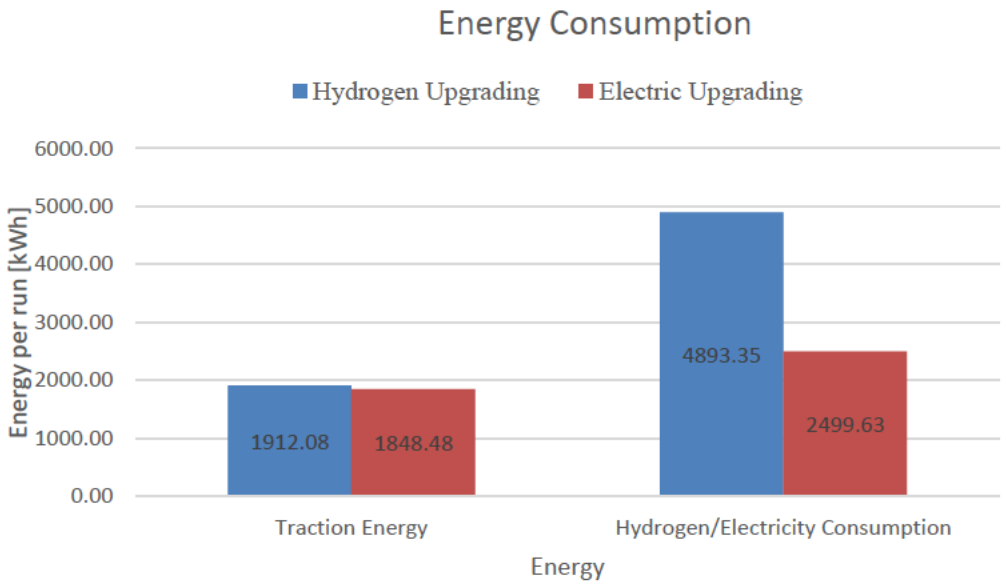

Figure 37 Energy consumption

The energy consumption of specific parts of trains is seen in Figure 37. The left bar indicates the amount of energy used by the traction system. It represents the mechanical energy required to pull the train along the route. Traction energy consumption is approximately the same for both upgrade techniques. The difference between these two strategies is merely 3.5%. However,

hydrogen fuel consumption is about double that of electricity. This figure is directly proportional to the cost of energy.

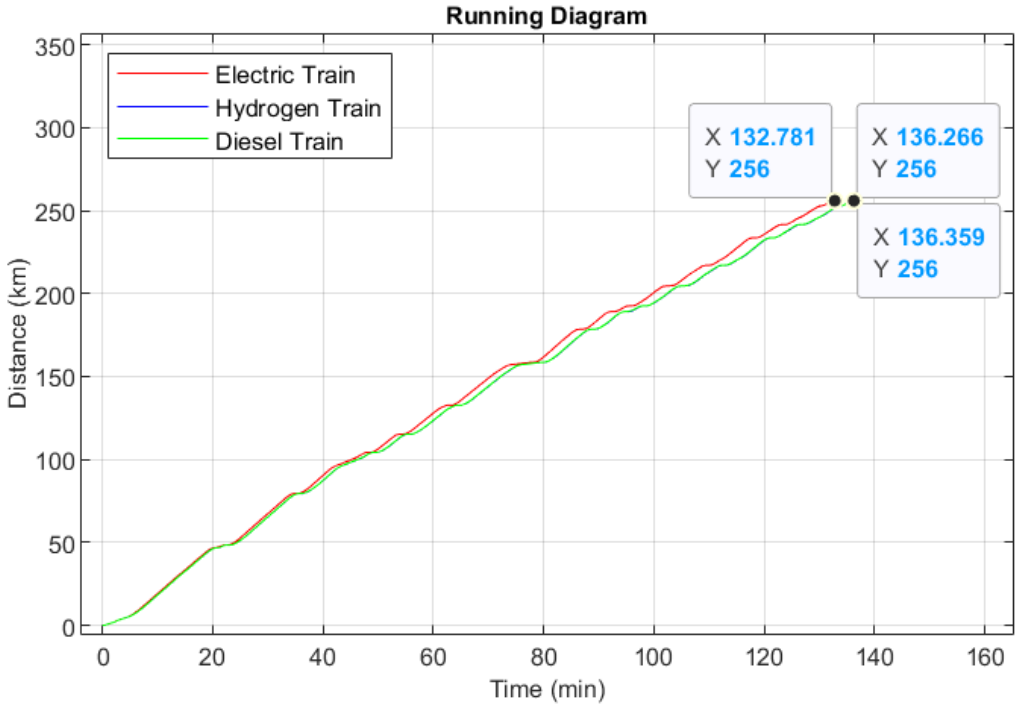

Figure 38 Three-train running diagram

Figure 38 illustrates the different trains' running diagrams. Electric trains are the quickest, taking 132 minutes and 47 seconds to complete the route. The hydrogen train performs comparably to the benchmark train. Both trains take about 136 minutes and 30 second, with the hydrogen train taking 6 seconds longer.

4.4 Conclusion

This chapter discusses a method for determining the cost–benefit ratio of railroad power system modifications. It is determined by the cost of a single new improvement to the railway system. The total cost comprises the initial investment, the cost of electricity, and the cost of railway component maintenance. The initial cost is made up of train conversion and route rehabilitation costs. Thus, when considering an electric train, one must bear in mind that the initial cost would

be relatively high due to the high cost of route reconstruction. Energy costs are decided mainly by the quantity of energy utilised during the period of the project's 40-year operation. Different applications of energy sources would result in significant cost disparities.

Moreover, railway maintenance is mainly concerned with the battery pack, hydrogen fuel cell, and associated tank maintenance and replacement. The Midland Main Line upgrade is analysed in this case study. For this 256-kilometre rail line, only the first 80 kilometres have been electrified; the remaining 176 kilometres require extensive electrification owing to its length and interconnection with tunnels and bridges. The cost of route reconstruction is more than the entire lifespan cost of a hydrogen fuel cell train. Although 31% of the route has been electrified in this case study, it is evident that upgrading to hydrogen fuel cell trains is a better fit for the electric train. However, after analysing the cost-sharing, it is shown that nearly all of the hydrogen cost is spent on energy consumption. Thus, if future energy prices shift significantly, the appraisal of the proposal to upgrade to hydrogen fuel cell trains would be significantly altered. Chapter 5 will apply a sensitivity analysis to determine the parameters' relevance in the railway cost evaluation function. In Chapter 6, a multi-mode train is developed, and its design is optimised using optimisation techniques that take energy price variations into account.

5 Determination of Railway System Parameter Importance Based on Sensitivity Analysis

5.1 Introduction

The modern railway system in the UK enables a significant transformation of the electricity grid. The previous diesel traction technique is highly environmentally unfriendly, while the government has advocated many alternatives for improving the railway power system. Bi-mode diesel-electric trains, hydrogen fuel cells, and electrification are the most feasible options for decarbonisation. The selection between such strategies is made in a variety of ways. Numerous variables are uncertain due to industrial, installation, and operating concerns, among others. These risks add to the level of uncertainty around the ultimate cost.

Consequently, it is advised that when evaluating the total cost of railway decarbonisation improvements, the statistical characteristics of the overall cost with uncertain parameters are considered. In general, various uncertain factors affect the overall cost of upgrading and running a railway differently. That is the focus of the research, which also includes a cost sensitivity analysis. This thesis includes a sensitivity analysis utilising both local and global sensitivity analytic methods. Sensitivity analyses assess the effect of input factors on a model's output using a range of different definitions and methodologies. Local sensitivity analysis is used to determine the effect of each parameter's nominal value on the model's output at the local level. The direct derivative or finite difference method is often utilised to determine parameter indices. Global sensitivity analysis examines the impact of changing the model's input parameters on the model's output and dependents.

This chapter compares two methods of upgrading: hydrogen fuel cell upgrades and train electrification upgrades, using the cost evaluation method demonstrated in Chapter 4. The parameter influences vary according to the upgrading situation. Sensitivity analysis is used to

determine the impact of other uncertain parameters. In this study, local sensitivity analysis looks at twelve factors: Station distance, Service frequency, Train efficiency, Regeneration efficiency, Weight, Davis A, Davis B, Davis C, Maximum power, Maximum speed, Energy price, and Electrification price. It's obvious that trains travelling longer distances and heavier trains need more energy, but the rate of this increase might be different. Some reports have said that hydrogen trains might be better than electric trains for services that don't run very often [15]. Sensitivity analysis is important for understanding how important these things are. The efficiency of the train and the Davis coefficients are about how much energy is lost, while how well energy is regenerated is about getting back traction energy. The impact of the train's maximum power and speed is always a key thing for how well a train performs. The prices of energy and electrification directly affect the cost of running and the initial cost. Since these prices change a lot, looking at them can help people making decisions know which way to go for upgrading, even if prices keep. The five parameters examined by global sensitivity analysis are chosen from above 12 parameters by their results. It is intended to train the conversion cost model by determining which parameters respond more precisely to significant changes in the output cost.

Unlike optimisation studies, this study focuses on finding more essential parameters that can be optimised and figures out the relations between those parameters. The highlights of this chapter are:

- A wide range of local sensitivity analyses to determine the importance of 12 parameters in the railway upgrading total cost model.
- Analysis of which parameter changes influence the competitiveness of both upgrading methods.

- The high-order Sobol global sensitivity index represents the five parameters' cross effect for the final cost.

In this chapter, Section 5.1 illustrates the changes in railway energy supply methods and the reason for employing sensitivity analysis. Section 5.2 explains two different practical upgrading methods, and some relative parameters which would be used to check the sensitivity are picked out. Section 5.3 reviews different railway system types that can influence the design of upgrading methods. Those specifications which change the upgrading cost are pointed out. Section 5.4 deeply discusses the two different sensitivity analyses and their principle. The method follows necessary mathematic proof in sensitivity analysis, and the Monte Carlo method is used for computing integration. Section 5.5 presents a case study for sensitivity analysis of upgrading parameters based on the Midland Main Line, and also analysis the Edinburgh Trams to present a comparison. The comparison results may show the difference and similarity of different upgrading method in different scenarios. Finally, Section **Error! Reference source not found.** shows the findings, which establish a reference point for further investigating the relationship between overall cost uncertainty and the optimisation variables chosen for railway system modernisation.

5.2 Different types of railway traction

5.2.1 Electrification

Electrification is optimal for upgrading old railway lines in an intensively used railway. Compared with a diesel engine, an electrical motor has fewer carbon emissions which means it is better for the environment. Moreover, changing the traction method from diesel engine to electrical motor significantly increases energy efficiency and makes operation quieter. After removing the diesel tanks and engines from the vehicle, an electric train is lighter even once

the motor is installed, which decreases train body inertia so that train speed can be accelerated fast. All the above can markedly reduce energy consumption. Therefore, there are many energy cost savings from long-term financial considerations. However, the cost of building electrification infrastructure is extremely high. Furthermore, according to the RSSB analysis, electric traction power is the only low-carbon non-diesel alternative available that can offer services at speeds greater than 100 mph [17].

5.2.2 Hydrogen fuel cells

If it is not possible to rebuild a particular line to electrify it due to unaffordable initial infrastructure costs, another choice is to obtain a new self-power traction method powered by greener fuel to take the place of a diesel engine. Hydrogen fuel cells consume hydrogen from the hydrogen tank and produce electricity for electrical motors to move vehicles forward. Like electric trains powered by overhead lines, hydrogen fuel cell trains also make less noise and are more efficient than diesel trains. However, the current hydrogen storage technique limits the application of hydrogen fuel cell trains. Even in the more recently introduced 700-bar hydrogen tank, the hydrogen energy density is still low. If only the widely used 350-bar tank were applied, the amount of hydrogen stored could not support hydrogen train operation for a long trip with high power output. Once more hydrogen is needed in a single journey, more space should be made for the hydrogen tank, and fewer passengers can be carried. To balance the capacity of hydrogen tanks and passengers, a hydrogen fuel cell train applies a motor with less power. Its low power means the train cannot accelerate to a high speed. The speed of the UK’s first hydrogen fuel cell train, HydroFLEX, cannot be over 150 km/h.

5.3 Tram and mainline train specifications

5.3.1 Mainline rail systems

As the very basic train, the mainline train is the most common train on railways. It is mainly used on the main railway between two cities. It is a heavy vehicle with high traction power demand. For example, the British Rail Class 43 (HST), 500 ton 8-car train usually needs 2600 kW traction power demand. Mainline railways typically have at least a double track for the capacity requirement in most countries. When considering railway upgrading by electrification, multiple tracks mean multiple times the cost of infrastructure building. However, for hydrogen fuel cell upgrading, the amount of parallel track does not impact the railway cost. A typical mainline rail system's maximum operating speed is not as high as 200 km/h for most mainline railways.

5.3.2 Tram systems

A tram system, also called light rail, is a form of public urban street transportation. A tram is usually lighter and shorter than a mainline vehicle, so that the resistance of the tram is relatively low and the power demand is lower than that of a mainline vehicle. Nowadays, there are some trams powered by electrified systems. However, the existing tram power supply system's vary, some being powered by gas or liquid fuel like diesel or petrol. Compared with other urban vehicles, a tram has more efficient energy usage.

5.4 Sensitivity analysis

In this study, sensitivity analysis emerges as a important tool for identifying key factors influencing output variability, pinpointing parameters that can be altered or eliminated, and understanding the interactions between parameters. This method significantly aids in the simplification of complex models, preserving essential system dynamics and interactions while enabling more rapid generation of results. Key applications include a study on the critical speed

of railway bogies [103], and an analysis of the principal risks associated with Belt and Road railway projects [104]. Local sensitivity analysis was utilised to assess the energy consumption of electric locomotives, although these studies lacked physical constraints in their modelling [105, 106]. Research into traction and pantograph catenary systems also revealed that local sensitivity analysis might not fully capture the overall sensitivity and interplay among parameters [107]. Moreover, a global sensitivity analysis of energy loss in stationary energy storage systems identified several sensitive factors amenable to optimisation [108]. Thus, conducting sensitivity analysis on the parameters of railway upgrading cost models is imperative for the accurate prediction and optimisation of railway costs.

5.4.1 Local sensitivity analysis

The most widely used local sensitivity analysis is the so-called OAT (one factor at a time) which is mainly used in financial problem-solving and prediction [109]. This method examines the output response by changing one of the parameters in a specific range. The approach of local sensitivity analysis saves time. It primarily uses the derivative method to do its research. The absolute and difference methods are both included in the derivative calculation. They are widely used because they are highly accurate. However, obtaining the derivative function might be difficult if the original procedure is too complicated. Regardless of the function specifics, the difference method is determined based on output and input changes. As a result, it can save time by eliminating the calculation of partially differential functions. Increasing or decreasing a parameter will considerably change the objective function if a parameter is sensitive. Where applicable, insensitive parameters and subsystems are adjusted or eliminated, and more clearly understandable formulations are substituted.

5.4.1.1 Absolute method

The absolute sensitivity function of y related to x_i is as follows:

$$S_{x_i}^{y} = \frac{\partial y}{\partial x_i}\Big|_{x_0} \tag{64}$$

where x_0 stands for the 'local point', which means all variables set as 0 or predefined at typical operating values. The partial differential of the function should apply to y only concerning x_i. The resulting unit of the absolute method is the function unit divided by the variable unit. For different variable sensitivity analysis comparisons, if the unite of variables are different, they cannot simply be ranked by their sensitivity values.

5.4.1.2 Relative method

Analysing the contributions of the input parameters to the output response in the same framework is challenging since distinct parameters often have different dimensions and scales. As a result, relative local sensitivity is defined as the change in the output response due to a difference in the input parameters. The relative method is more valuable for comparing the effects of the parameters. The close function is defined as follows:

$$S_{x_i}^{y} = \frac{\partial y}{\partial x_i}\Big|_{x_0} \times \frac{x_0}{y_0} \tag{65}$$

The relative method is more appropriate than the absolute method for analysing the sensitivity of parameters with different units. Compared with the absolute method, the unit of sensitivity becomes 1 (per unit) after being multiplied by x_0 over y_0.

5.4.1.3 Difference equations

Local sensitivity analysis can also be represented by using difference equations. The sensitivity of a quantity x_i concerning quantity y using difference is defined by:

$$S_{x_i}^{y} = \frac{y_1 - y_2}{y_1} \times 100\% \qquad (66)$$

where y_1 is the value of *y* at specific parameters x_0; y_2 is the value of *y* on changing x_i by 1% (either increase or decrease) and keeping the other parameters the same. However, the sensitivity value should compare parameters in the same direction because parameters are sometimes more sensitive in one direction. A difference equation is a simple method for sensitivity analysis compared with the relative method. It does not involve any derivative. Moreover, it can effectively solve complex functions for which it is challenging to obtain the derivative. This thesis uses a different method for the local sensitivity analysis due to its complex cost function.

5.4.2 Global sensitivity analysis

Global sensitivity analysis focuses on the variance of model output *Y* and, more precisely, on how the input variability influences the output variance and gives a quantitative overview of the influence. Sobol sensitivity analysis is a variance-based method of sensitivity analysis [110]. A simple variable change is required if the input variables are not defined in this interval. Suppose the cost function in Chapter 4 is given by Equation (67). In the considered framework, it is thus possible to show that φ can be decomposed into elementary functions, which can also be called ANOVA representation in Equation (68) [111, 112]. For further analysis, the global sensitivity analysis is conducted with the distribution type and regions of all known parameters.

$$Y = f(x) \tag{67}$$

$$Y = F_0 + \sum_{i=1}^{D} f_i(x_i) + \sum_{1 \le i < j \le D} f_{ij}(x_i, x_j) + \cdots + f_{i \ldots p}(x_1, \ldots, x_D) \tag{68}$$

$$x = (x_1, x_2, \ldots, x_D) \tag{69}$$

where $f(x)$ is the integrable cost function, x is a *D*-dimensional variable which is given by (69), F_0 is a constant which is the overall average function value, and $f_{1,\ldots,s}$ should satisfy the following condition:

$$\int (f_{l_1 \ldots l_v}(x_{l_1}, x_{l_2}, \ldots, x_{l_v}))dx_{l_x} = 0 \tag{70}$$

5.4.2.1 Total sensitivity index

The total sensitivity index means the entire output response by one parameter x_i. It includes the effect of the parameter itself responding (S_i), and all other mixed effects which combine with different parameters.

$$S_{x_i}^{total} = S_{x_i} + \sum_{l_1 \neq x_i} S_{x_i l_1} + \sum_{l_1, l_2 \neq x_i, l_1 < l_2} S_{i l_1 l_2} + \cdots + S_{x_i l_1 \ldots l_{d-1}} \tag{71}$$

where $S_{x_i}^{total}$ is total sensitivity index, S_{x_i} is the first-order sensitivity index or primary effect of x_i, and $S_{i l_1 \ldots l_{j-1}}$ means the $j-th$ order sensitivity index.

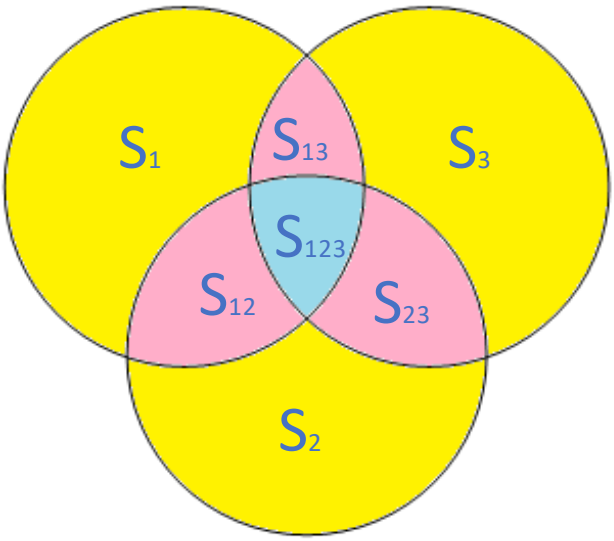

Figure 39 Total sensitivity index distribution for a three-variable function

For example, assuming there is a function with three different uncertain parameters and those three parameters influence the output when changed. The distribution of the sensitivity indices of the three variables is shown in Figure 39. It includes all first-order (S_1, S_2, S_3), second-order (S_{12}, S_{13}, S_{23}), and third-order sensitivity indices (S_{123}). All sensitivity indices are summed as shown in Equation (72). Moreover, in Equation (73), those higher-order sensitivity indices, which include any parameter, belong to that parameter's total sensitivity index.

$$S_1 + S_2 + S_3 + S_{12} + S_{13} + S_{23} + S_{123} = 1 \quad (72)$$

$$S_{x_1}^{total} = S_1 + S_{12} + S_{13} + S_{123}$$

$$S_{x_2}^{total} = S_2 + S_{12} + S_{23} + S_{123} \quad (73)$$

$$S_{x_3}^{total} = S_3 + S_{13} + S_{23} + S_{123}$$

Before the calculation, there are two definitions of the average value and variance value of function *Y*. Assuming $x \sim p(x)$ where $p(x)$ is the joint distribution of *x* with $\int p(x)dx = 1$, then the overall average value of the cost function can be defined as:

$$E(Y) = \int (f(x) \times p(x))dx \qquad (74)$$

Hence, its unconditional variance value is given by:

$$\begin{aligned} Var(Y) &= \int \left(\left(f(x) - E(Y)\right)^2 \times p(x) \right) dx \\ &= \int \left((f^2(x) \times p(x) \right) dx + E^2(Y) \\ &-2 \int ((E(Y) \times f(x) \times p(x))dx \\ &= E(Y^2) + E^2(Y) - 2E^2(Y) \\ &= E(Y^2) - E^2(Y) \end{aligned} \qquad (75)$$

This means the unconditional variance can be simplified as an average value calculation. Furthermore, there is a law of total variance [112]:

$$Var(Y) = E_{x_i}\left(Var_{x_{\sim i}}(Y|x_i)\right) + Var_{x_i}\left(E_{x_{\sim i}}(Y|x_i)\right) \qquad (76)$$

where $Var(Y)$ is called unconditional variance, while $Var_{x_{\sim i}}(Y|x_i)$ is called the conditional variance of x_i, which is the variance of *Y* under the condition of $x_i = x_i^*$. $E_{x_i}\left(Var_{x_{\sim i}}(Y|x_i)\right)$ is called the residual and the term ($Var_{x_i}\left(E_{x_{\sim i}}(Y|x_i)\right)$) is known as the first-order effect of x_i on function *Y*. The sensitivity index of parameter x is given by:

$$S_x = \frac{Var\big(E(Y|x = x_i)\big)}{Var(Y)} \tag{77}$$

To compute the total sensitivity index, a formula is defined as:

$$\begin{aligned} S_{x_i}^{total} &= 1 - \frac{Var_{\sim x_i}\left(E_{x_i}(Y|x_{\sim i})\right)}{Var(Y)} \\ &= 1 - \frac{Var_{\sim x_i}\left(E_{x_i}(Y|x_1, x_2, \dots, x_{i-1}, x_{i+1}, \dots, x_d)\right)}{Var(Y)} \end{aligned} \tag{78}$$

where $Var_{\sim x_i}\left(E_{x_i}(Y|x_1, x_2, \dots, x_{i-1}, x_{i+1}, \dots, x_d)\right)$ is the variance of the average value of Y under the condition of all other variables ($x_{1,2,\dots i-1,i+1,\dots,d}$) fixed except x_i. According to the law of total variance, Equations (76) and (78) can be altered to:

$$S_{x_i}^{total} = \frac{E_{\sim x_i}\left(Var_{x_i}(Y|x_1, x_2, \dots, x_{i-1}, x_{i+1}, \dots, x_d)\right)}{Var(Y)} \tag{79}$$

5.4.2.2 First-order sensitivity index

The first-order sensitivity index represents the main effect of the parameter without any interaction with other parameters. It is also called the importance measure, sensitivity index, or correlation ratio. It can be shown as:

$$S_i = \frac{Var_{x_i}\left(E_{x_{\sim i}}(Y|x_i)\right)}{Var(Y)} \tag{80}$$

A smaller conditional variance value of x_i means a more significant influence of parameter x_i. However, a single conditional variance value highly depends on the position of ${x_i}^*$. Choosing a different ${x_i}^*$ would significantly affect the importance of x_i. To avoid randomness, the average value of the overall ${x_i}^*$ conditional variance is used to present the sensitivity. The

average of x_i conditional variance is written as $E_{x_i}(Var_{x_{\sim i}}(Y|x_i))$ and this value is always smaller or equal to unconditional variance $Var(Y)$. The molecular Equation (80) can be simplified according to the law of total variance in Equation (76). Hence, the first-order sensitivity index can also be written as:

$$S_i = \frac{Var(Y) - E_{x_i}\left(Var_{x_{\sim i}}(Y|x_i)\right)}{Var(Y)} \qquad (81)$$

5.4.2.3 Higher-order sensitivity index

Higher-order sensitivity terms describe the interaction effects of the input parameters on the output variance. Assume a set of *m* variables $y = \left(x_{k_1}, \ldots x_{k_m}\right), 1 \le k_1 < \cdots < k_m \le D$, and z to be the set of remaining $D - m$ variables, then $x = (y, z)$. Computation of the higher-order sensitivity index is based on the following representation:

$$S_y = \frac{Var_y\left(E_z(Y|y)\right)}{Var(Y)} \qquad (82)$$

where $Var_y\left(E_z(Y|y)\right)$ can be calculated by:

$$Var_y = \int \left(f(x) \times f(y, z')\right) dx dz' - F_0^2 \qquad (83)$$

5.4.2.4 Monte Carlo method

It is impossible to figure out all possible points in global sensitivity analysis and get the sensitivity indices for a complex function. The Monte Carlo method, also called the Monte Carlo algorithm, is a way to estimate function results. It detects a set of *M* samples to assess the overall sensitivity instead of calculating it depending on all possible points. The accurate rate is relevant to the sample size *M*. Once the number M of samples is high enough, the results

calculated according to those samples can be estimated as the overall sensitivity indices. To reduce the impact of randomness and get higher accurate result, the range of each variable has been separated into 5 same-length part. Hence, there would be 5^i pools for all the samples. Then all the samples are divided equally among each pool. Each pool can get $\frac{M}{5^i}$ samples. By using the Monte Carlo method and comparison with the Sobol sensitivity analysis calculation, the overall average value of function Y is given by Equation (84):

$$E(Y) = \frac{1}{M}\sum_{i=1}^{M} Y_i \qquad (84)$$

From Equation (75), the overall unconditional variance of function Y is:

$$Var(Y) = \frac{1}{M}\sum_{i=1}^{M} Y_i^2 - (\frac{1}{M}\sum_{i=1}^{M} Y_i)^2 \qquad (85)$$

The first-order conditional variance computing formula can also be converted as shown in Equation (86).

$$Var_{x_i}\left(E_{x_{\sim i}}(Y|x_i)\right) = \frac{1}{M}\sum_{j=1}^{M}\left(f(x_i) \times f(x_i, x'_{\sim i})\right) - F_0^2 \qquad (86)$$

Similar to the first-order sensitivity index and according to Equation (83), the higher-order conditional variance of parameter set $y = \left(x_{k_1}, \ldots x_{k_m}\right)$, is:

$$Var_y = \frac{1}{M}\sum_{j=1}^{M}\left(f\left(x_j\right) \times f\left(y_j, z'_j\right)\right) - F_0^2 \qquad (87)$$

Combining Equations (77), (86), and (87), the first-order and higher-order global sensitivity index can be figured out. Furthermore, the total sensitivity index of parameter set y is:

$$S_y{}^{tot} = \frac{Var_y{}^{tot}}{Var} \quad (88)$$

where the total conditional variance of y is:

$$Var_y{}^{tot} = Var - (\frac{1}{M}\sum_{j=1}^{M}\left(f(x_j) \times f(y_j', z_j)\right) - F_0^2) \quad (89)$$

It is extremely hard to compute a large set of parameters by global sensitivity analysis simultaneously because of the time complexity. The Monte Carlo sample calculation time is:

$$N_{total} = N(n_p{}^{ho} + n_p{}^{ho-1} + \cdots + n_p{}^{1} + 1 + \mathrm{n_p}) \quad (90)$$

where N_{total} is the overall computing time, N is the number of samples, n_p is the number of parameters, and ho is the highest order of the sensitivity index. Typically, ho is the same as n_p. However, the higher the sensitivity index order, the less all those parameters affect the final cost. It is not necessary to compute all orders of indices.

5.5 Case study

5.5.1 Train model and line data

5.5.1.1 Tram data

The benchmark tram line in this thesis is based on the Edinburgh Trams line. As this line was built as an electrified route, for the railway upgrading cost research, assuming that it is a diesel tram operating on the line before and analyses the tram upgrading by two methods. This train's body mass is 56.85 tonnes, and its A, B, and C Davis resistances are 1.085, 0.003, and 0.011, respectively. Its maximum traction power is 904 kW. There are 13 intermediate stations located on the Edinburgh Tram Line on this 13.8 km route. On average, the distance between two stations is 1 km. The maximum train operation speed is limited to 70 km/h on this line, which

means the distance between stations is short. This speed limit is below the maximum speed of a hydrogen train, so hydrogen fuel cell trains are also well-fitted for the tram route [48]. Generally, the tram does not have much cruising time because it will enter the braking stage before the train reaches maximum speed. The daily tram operation is approximately 10 minutes between two functions which are around 105 daily cycles as shown in Table 9.

Table 9 Nominal values of tram system parameters

Parameter	**Quantity**	**Units**
Station distance	1	km
Service frequency	105	Per day
Train efficiency	0.85	
Regeneration efficiency	0.15	
Weight	56.85	tonnes
Davis (A)	1.085	N
Davis (B)	0.003	$N * \frac{s}{m}$
Davis (C)	0.011	$N * (\frac{s}{m})^2$
Maximum power	904	kW
Maximum speed	70	km/h

5.5.1.2 Mainline train data

The benchmark diesel mainline train on the Midland Main Line is a Class 222 diesel multiple-unit high-speed train. The train has a high traction power output of 2.24 MW. This powerful engine propels the 214-tonne heavy train forward at a fast rate of speed. The Midland Main Line connects London St. Pancras to Sheffield. There are 16 major stations and stops throughout the route's 265 kilometres [86, 87]. The tested route distance between two adjacent stations is 20 km, approximately the same as on the Midland Main Line. The maximum speed

in the mainline system is always higher than the tram line on Midland Main Line, which is assuming as 176 km/h. This speed limit is about 10% above the hydrogen fuel cell train's current maximum speed. Therefore, the default line speed limit is 150 km/h. The operation time gap of the mainline railway is longer than that of the tram: about four operations per hour which is not so intensive. In total, it is assumed that there are 68 operations each day, as shown in Table 10.

Table 10 Nominal values of mainline system parameters

Parameter	**Quantity**	**Units**
Station distance	20	km
Service frequency	68	Per day
Train efficiency	0.85	
Regeneration efficiency	0.15	
Weight	214	tonnes
Davis (A)	3.454	N
Davis (B)	0.077	$N * \frac{s}{m}$
Davis (C)	0.004	$N * (\frac{s}{m})^2$
Maximum power	2.24	MW
Maximum speed	176	km/h

5.5.1.3 Energy price and route rebuilding price

Regarding the energy price and route rebuilding price, all the financial data used for sensitivity analysis are the same as described in Chapter 4.3.

5.5.2 Local sensitivity analysis

The OAT method is applied to generate all local sensitivity analysis results for the tram system and mainline railway which is shown in Section 5.5.2.1 and Section 5.5.2.2 respectively. Thus,

parameters with different units in any railway system are also valid. In this analysis, the results show the sensitivity of 12 parameters:

- Station distance
- Service frequency
- Train efficiency
- Regeneration efficiency
- Weight
- Davis (A)
- Davis (B)
- Davis (C)
- Maximum power
- Maximum speed
- Energy price
- Electrification price

To better compare the sensitivity level between different parameters, all sensitivity indices shown in the figure are absolute values. In contrast, the positives and negatives will be pointed out in the discussion. Based on the evaluation model in Chapter 4, the equations in Section 5.4.1 has been applied to show the following statistical results.

5.5.2.1 Tram system sensitivity analysis

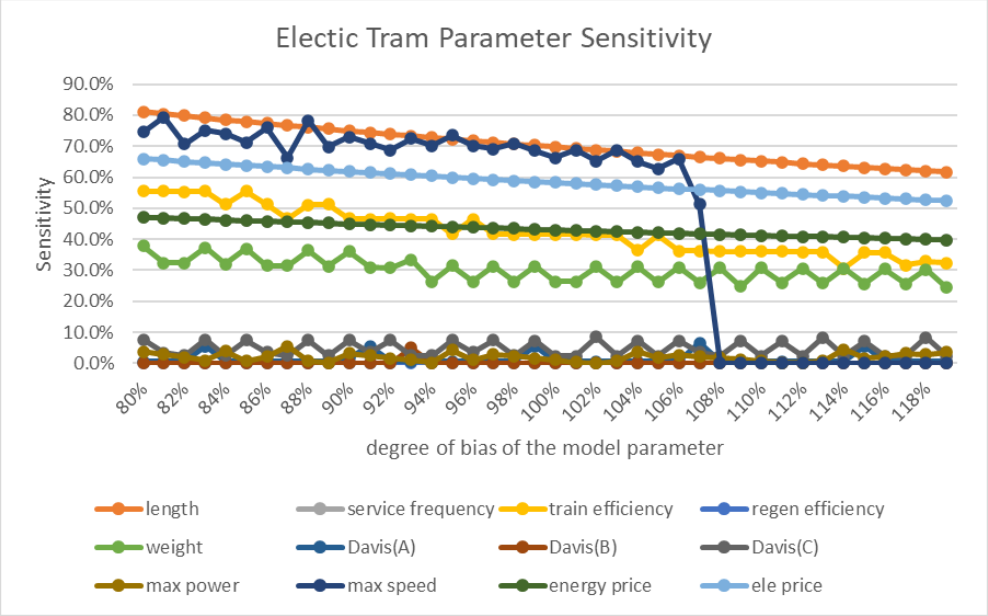

Figure 40 Local sensitivity of electric tram parameters

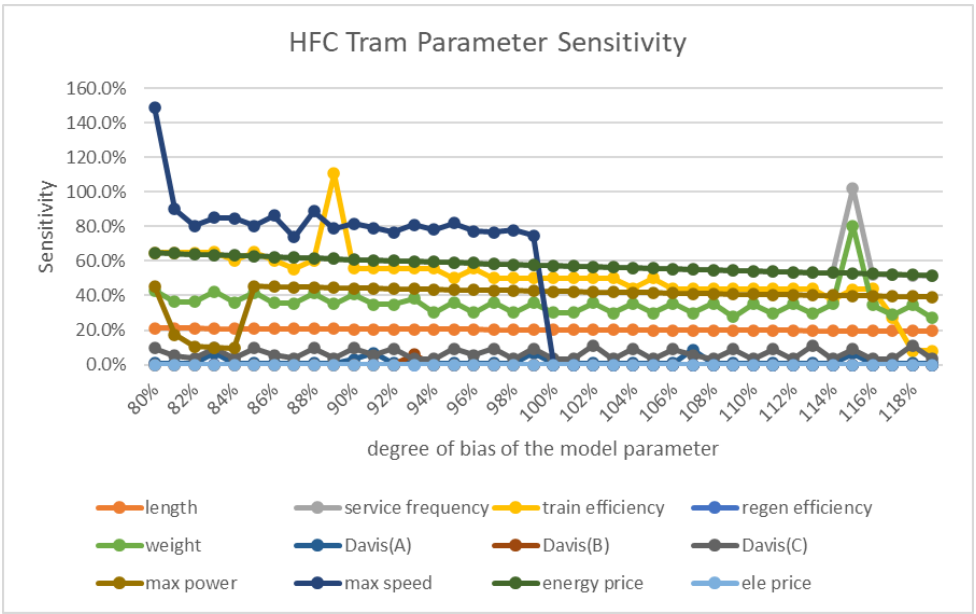

Figure 41 Local sensitivity of hydrogen fuel cell tram parameters

The results of the local sensitivity analysis of tram parameters are shown in Figure 40 and Figure 41. Almost all the sensitivities tend to reduce from 80% to 120% in the parameter range.

In the electric tram figure, ignoring those parameters that show a sharp change in sensitivity, the two extremely sensitive parameters are the line length and electrification price, with average sensitivity of 70% and 60%, respectively. Both parameters are positively correlated with the final cost. If either of these two parameters increase by 1%, the final cost would rise by 6.5% as well. There are three parameters with sensitivity located around 40%: train efficiency, energy price, and tram weight. This level of sensitivity is classified as very sensitive. When those very sensitive parameters change, it only has two-thirds of the impact on the final cost for 40 years of operation compared with changing the extremely sensitive parameters. None of the parameters are classified as sensitive (sensitivity around 20%) for the electric tram, and the rest of the parameters are not sensitive. All of them can have a very limited influence on the final cost.

The top-level sensitivity of the hydrogen fuel cell tram is quite different from that of the electric tram. The importance of line length is much lower, showing only 20% sensitivity. Due to no route rebuilding being required, electrification price (the second most important parameter for the electric tram) shows 0% sensitivity. The very sensitive parameters are the same as for an electric tram but with an extra parameter of train maximum power. Except for the above parameters and top speed, the other parameters, including Davis coefficients and regeneration efficiency, are still not sensitive.

The most interesting sensitivity curve above is the maximum speed curve. Before a threshold speed, 108% for an electric tram and 100% for a hydrogen fuel cell tram, the sensitivity of top speed stays at the highly sensitive level. Once the speed exceeds that threshold, the sensitivity suddenly drops to 0%. The tram moving curve at threshold speed is shown in Figure 42.

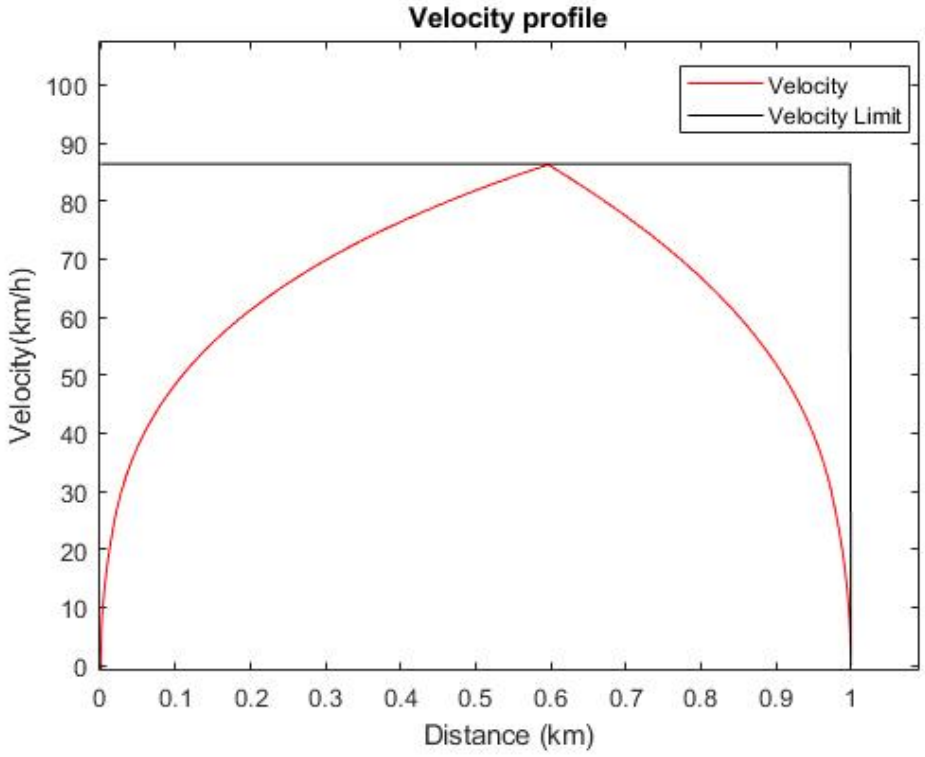

Figure 42 Hydrogen fuel cell tram operation curve at a threshold speed

Figure 42 is the hydrogen fuel cell tram operation curve. This curve is generated by the MATLAB simulation developed in Chapter 3. The tram is almost at its maximum speed in the line. According to the train resistance figure in Figure 43, the theoretical maximum speed is around 150 km/h. However, considering the braking distance, the tram cannot accelerate to the theoretical maximum speed before braking. After that, even the operation maximum speed can be set higher than the maximum threshold speed. The moving curve would no longer change and have no influence on the final cost. Once the length of upgraded line is longer and the train can increase to a higher speed, the maximum speed can continuously influence the final price.

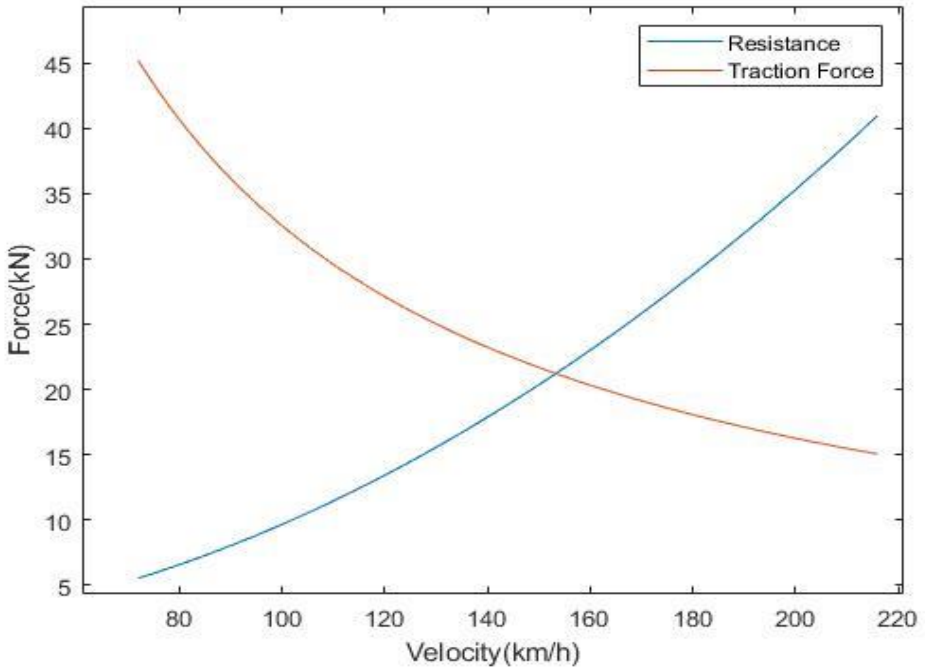

Figure 43 Theoretical maximum speed of the hydrogen fuel cell train

Many studies have mentioned that regeneration can reduce the overall energy consumption with a driving strategy. However, the sensitivity of both tram upgrading methods shows that changes in regeneration efficiency have almost no effect (less than 0.1%) on the final cost. From the power point of view, the limit of current onboard regeneration is not the regeneration efficiency. The regenerator output power is much higher than the battery charging power. Hence, increasing regeneration efficiency cannot help the onboard energy storage system store more energy. After doing extra sensitivity analysis for battery charging power, it has 1.3% sensitivity, higher than that of regeneration efficiency.

Table 11 Tram average local sensitivity index ratios

Parameter	**Electric tram**	**Hydrogen tram**	**Ratio**
Line length	70.47%	20.23%	3.484

Service frequency	43.25%	58.99%	0.733
Tran efficiency	42.65%	50.50%	0.844
Regeneration efficiency	0.00%	0.04%	0.000
Weight	30.11%	35.50%	0.848
Davis A	1.29%	1.69%	0.766
Davis B	0.16%	0.19%	0.818
Davis C	4.78%	6.31%	0.757
Maximum power	2.02%	39.20%	0.052
Maximum speed	48.91%	42.05%	1.163
Energy price	43.25%	57.79%	0.748
Electrification price	58.69%	0.00%	N/A

In the default parameter setting, the simulation evaluated that total cost over lifespan for the electric tram and hydrogen fuel cell tram is calculated at £6.2 million and £9.2 million, respectively. Looking at the average local sensitivity, if the sensitivity ratio of a parameter in the two upgrading methods is more than 1, then the electric tram becomes less sensitive. From Table 11, it's clear that the Line length has the highest sensitivity ratio when comparing the electric tram to the hydrogen tram. The sensitivity index for the electric tram is about 3.5 times that of the hydrogen tram. This is mainly because, for electric upgrades on the tram route, both the initial cost and energy cost are important. Extending the line length increases both the electrification cost and the energy cost simultaneously. However, for hydrogen upgrades, the additional part of the extended route has a low acceleration rate. This means it needs less energy to speed up the tram, so the increase in energy cost is not as noticeable as with electric upgrading. In a similar way, the difference in the sensitivity index of maximum power is due to the different rates of energy cost change. Increasing the maximum power allows the hydrogen tram to have a longer high-speed acceleration stage, but this doesn't affect the electric

tram as much because most of its acceleration is already at a high rate. Extra maximum power doesn't significantly alter the operation curve.

5.5.2.2 Mainline railway

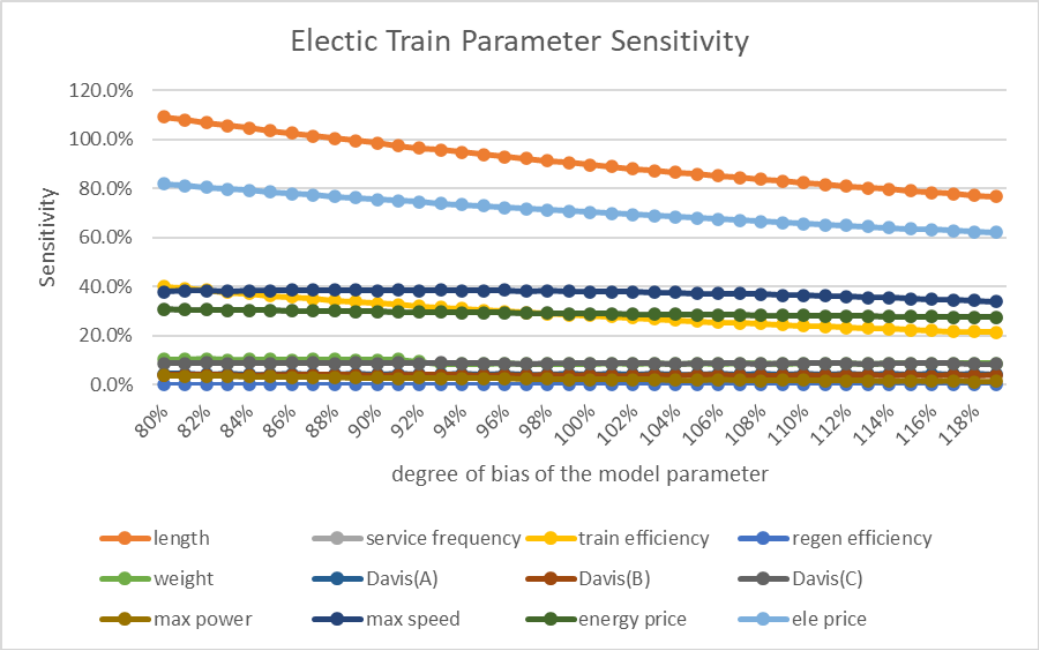

Figure 44 Sensitivity indices of electric mainline train parameters

According to Figure 44, the two parameters most impacting the electric mainline train are line length and electrification price, which are similar to what is observed for the electric tram in Table 11. However, in comparison to the electric tram, the significance of these two parameters is greater for the electric mainline train: the impact of line length is 15% higher, and the impact of electrification price is 10% higher. This difference indicates that, unlike other railway types and upgrading methods, the effect of line length on the electric mainline train is nearly equivalent to its overall cost. In the second tier, parameters like maximum speed, train efficiency, energy price, and service frequency are less sensitive, yet they still fall into the very sensitive category.

Moreover, train efficiency gets less important if it rises to a high degree and touches the sensitive parameter class line. The influence of train weight also decreases, becoming an insensitive parameter with the Davis coefficient. However, the sensitivity index of Davis C coefficient increases to around 9%. The mainline has a higher operation speed, increasing the importance of the Davis C coefficient.

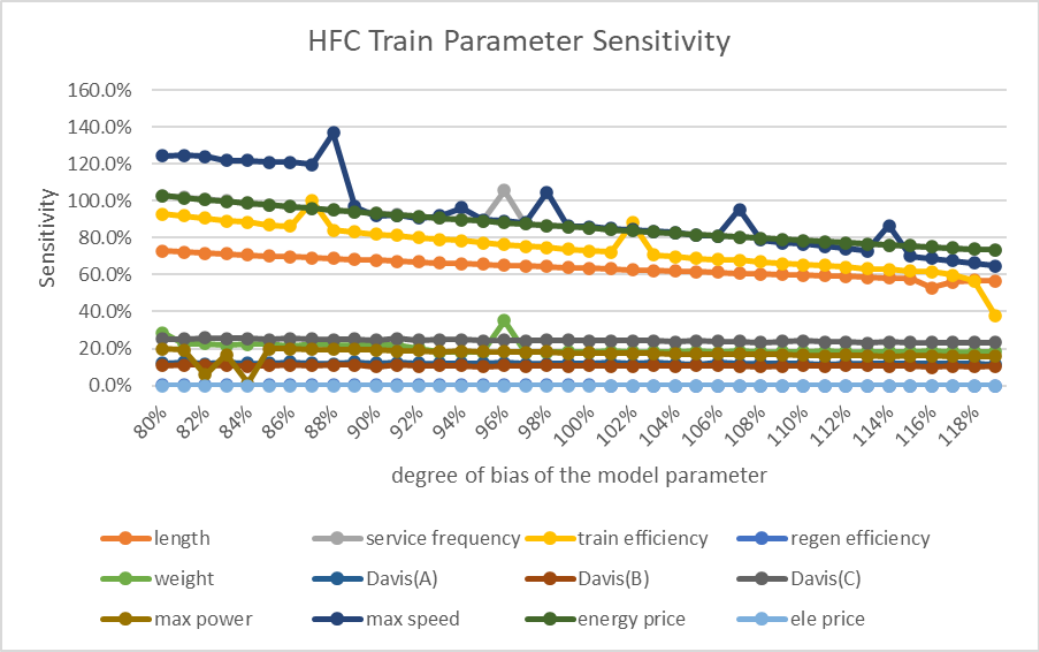

Figure 45 Sensitivity indices of hydrogen fuel cell mainline train parameters

For the hydrogen fuel cell mainline train, compared with the hydrogen fuel cell tram, it is obvious that all sensitivity indices are more or less increased except for weight and regeneration efficiency. As analysed in the tram part, the regeneration efficiency is almost in front of that needed, and extra efficiency cannot provide more benefit. The energy proportion used to overcome the train's inertia is reduced, and more energy needed for maintaining the speed might be why the importance of the weight parameter decreases.

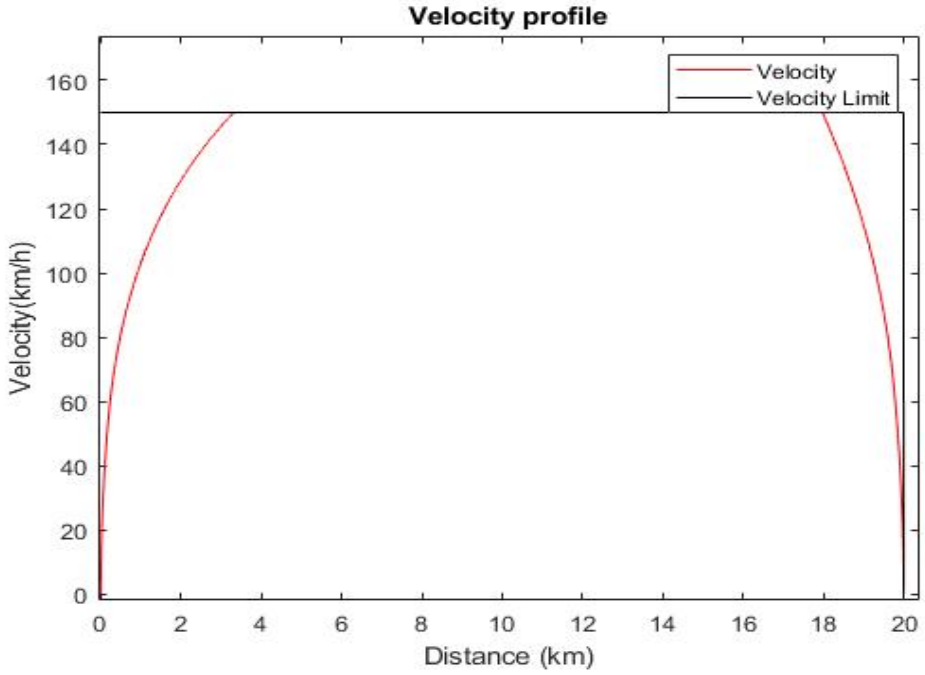

Figure 46 Hydrogen fuel cell mainline train operation curve at a speed limit of 150 km/h

Furthermore, the impact of maximum speed on the mainline train differs from its effect on the tram. The sensitivity gradually decreases from 40% to 33.7%, but it never drops to 0%. As shown in Figure 46, there is additional capacity for acceleration and braking, which means that any increase in maximum speed can continuously influence the final cost. In the context of local sensitivity analysis for mainline trains, the default cost for electrification upgrading is estimated at £103 million, compared to £75.4 million for hydrogen fuel cell upgrading. In Table 12, the average local sensitivity index ratios for the mainline train show a marked contrast to those for the tram. The most significant ratio is still line length, but it has decreased from 3.484 to 1.423 compared with the tram line length sensitivity index ratio in Table 11. This implies that the importance of line length is more closely aligned between the electric and hydrogen fuel cell mainline trains. From a sensitivity perspective, the electric mainline train shows a 20% higher sensitivity compared to the hydrogen fuel cell mainline train. In mainline railway, the

distance between station to station would be really long. The huge price of electrification shares most of the price. Compared with electric mainline train, the hydrogen mainline train is not that sensitive on Line length. It would increase the energy consumption but most of the extra length is for cruising which require less energy than acceleration. Service frequency is similar to train efficiency and energy price, because these three are the most direct way to increase the energy consumption. And of hydrogen mainline train cost share is the energy cost. Maximum speed is a super highly sensitive parameter for mainline hydrogen train. The reason is still about energy. During high-speed operation, the resistance increase rate is v^2, hence the energy cost would shapely increase.

Table 12 Mainline train average local sensitivity index ratios

Parameter	**Electric mainline train**	**Hydrogen mainline train**	**Ratio**
Line length	90.98%	63.93%	1.423
Service frequency	28.95%	86.95%	0.333
Trian efficiency	29.01%	74.55%	0.389
Regeneration efficiency	0.00%	0.06%	0.000
Weight	9.03%	20.09%	0.449
Davis A	4.29%	12.02%	0.357
Davis B	3.79%	10.67%	0.355
Davis C	8.61%	24.33%	0.354
Maximum power	2.23%	16.94%	0.132
Maximum speed	37.26%	92.29%	0.404
Energy price	28.95%	86.44%	0.335
Electrification price	70.95%	0.00%	N/A

5.5.3 Global sensitivity analysis

For this global sensitivity analysis on the tram and mainline trains to be analysed, five parameters are chosen: line length, train efficiency, Davis C, weight, and energy price. Furthermore, the highest order is two due to the significant computation. In this study, to get a more accurate global sensitivity index, the sample quantity for each parameter is 100 k. Hence 500 k samples are analysed in total [13].

5.5.3.1 Total sensitivity index

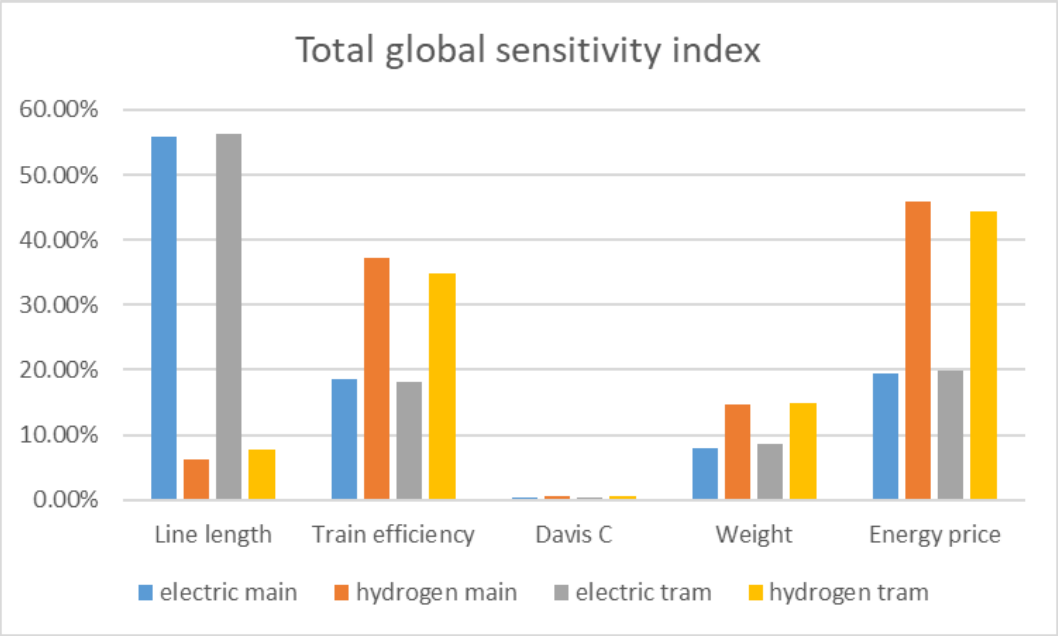

Figure 47 Total global sensitivity index of both trains

As shown in Figure 47, the interesting content is that even though the railway lines are different, the global sensitivity index is similar when using the same upgrading method. This means that the sensitivity level of the parameter mainly depends on the upgrading method, not the railway type. Also, from a parameter point of view, tram line length is less important than mainline route length. As shown in Figure 47, for different types of railway performance, once the route length of these two types of railway increases at the same time with the same rate, the tram

performs more acceleration operations while the mainline train is cruising on the extra route. Acceleration consumes more energy than cruising for the same operating distance. Hence, the importance of tram line length is more sensitive than for the mainline train. The sensitivity of train efficiency and energy price hold almost the same proportions, and the energy price sensitivity is slightly higher. Both parameters are related to the operating energy cost, and the energy price factor relationship is more straightforward than train efficiency.

Moreover, the other two parameters are not sensitive among the five analysed parameters, especially the Davis C coefficient. The Davis C coefficient is a resistance parameter, and it makes no apparent contribution to the final overall cost compared with other parameters due to its dependents. The global sensitivity index can be almost ignored. Hence, compared to other parameters that directly affect the results, Davis C coefficient is not an efficient parameter influencing the final cost.

5.5.3.2 First-order and higher-order sensitivity indices

Table 13 First-order global sensitivity indices

Parameter	**Electric**	**Hydrogen**	**Electric**	**Hydrogen**
	Tram		**Mainline**	
Line length	53.92%	6.32%	52.65%	5.94%
Tran efficiency	16.24%	32.57%	15.36%	29.88%
Davis C	0.91%	0.34%	0.74%	0.26%
Weight	6.35%	12.42%	7.01%	13.11%
Energy price	17.87%	43.07%	19.65%	41.20%

The first-order global sensitivity indices in Table 13 show the parameters' independent effects. The first-order global and total sensitivity indices have similar results except for Davis C

coefficient. Therefore, in railway system cost modelling, those four parameters got higher independent influence for the final output. However, the higher-order sensitivity indices in Table 14 list the dependents between two parameters. The dependents of any two-parameter group are relatively low in value. However, after summarising and comparing the higher-order and first-order sensitivity analysis results, it can be seen that the Davis C parameter's higher-order sensitivity index is more significant than its first-order sensitivity index. This also proves that Davis C coefficient depends more on the cross effect with other parameters.

Table 14 Second-order global sensitivity indices

Parameters		**Electric**	**Hydrogen**	**Electric**	**Hydrogen**
		Tram		**Mainline train**	
Line length	**Train efficiency**	1.48%	1.32%	2.23%	1.39%
Line length	**Davis C**	1.15%	3.67%	2.03%	0.97%
Line length	**Weight**	1.58%	4.57%	1.99%	1.21%
Line length	**Energy price**	1.53%	2.92%	3.02%	1.10%
Tran efficiency	**Davis C**	1.25%	3.32%	1.98%	1.04%
Tran efficiency	**Weight**	1.28%	3.59%	1.25%	1.99%
Tran efficiency	**Energy price**	1.23%	3.64%	2.89%	1.47%
Davis C	**Weight**	1.13%	3.39%	2.18%	0.94%
Davis C	**Energy price**	1.16%	3.42%	2.41%	0.87%
Weight	**Energy price**	1.58%	3.62%	2.66%	1.34%

Most mainline train parameters have a higher cross effect with others compared with tram parameters, especially for the electric mainline train. Except for the cross effect of line length and train efficiency, all other second-order global sensitivity indices are near or above 3%. More parameters need to be optimised simultaneously to get better optimal results when considering hydrogen tram optimisation.

5.6 Conclusion

This thesis looks at how much it costs to modernise railways using two different methods. It sets up a cost model for 40 years and checks the sensitivity of costs using both local and global analysis. The study explains the basic ideas and rules of these two types of sensitivity analysis, which helps to understand how different inputs affect the final results. Many graphs and tables are used to show the differences in sensitivity.

In the local sensitivity analysis, a method called the difference equation, part of the OAT approaches, is used. This method is quick and gives a clear local sensitivity index. The results show that the cost of electric trams is more affected by things like the length of the tram line, its maximum speed, and how much it costs to make it electric. On the other hand, hydrogen trams are more affected by their maximum speed, how efficient they are, and the cost of energy. Electric mainline trains are similarly affected by their length and electrification cost, but not as much by speed. However, hydrogen fuel cell trains have similar sensitivities to hydrogen trams. There's an interesting pattern in the local sensitivity of trams. After a certain point, the effect of speed quickly goes down. This study finds that the length of the line limits how fast the train can go, which might explain why this isn't seen in mainline trains.

The global sensitivity analysis, conducted using the Monte Carlo method, is a important part of the thesis. This analysis reveals how significantly the Davis C coefficient and other factors influence the costs in railway modernisation projects. These insights are important for understanding the complex interactions of different elements in railway systems. This detailed analysis provides essential guidance for future research and strategies aimed at improving railway efficiency and sustainability, marking a significant contribution to the field of railway decarbonisation. Many of the factors looked at in this chapter will be used to improve things even more in the following chapter.

6 Cost optimisation of multi-mode train on discontinuously electrified route

6.1 Introduction

The energy price for both diesel and electrified railways has been increasing annually [113]. Railways generate a large amount of greenhouse gas due to their high energy consumption. The UK government has claimed that all diesel-only trains will be removed by 2040 [15, 114]. Electrification is a way to decrease energy consumption. Seventy per cent of the European railway network is electrified, and about 80% of trains run on an electrified route [113]. However, although only 42% of railway routes are electrified in the UK [115], a number of electrification projects have been cancelled, such as the Cardiff to Swansea route, the Oxenholme to Windermere branch, and the Kettering to Nottingham and Sheffield route as part of the Midland Main Line due to financial problems [6]. While hybridisation and the employment of multiple-mode trains are not the ideal long-term answer, they provide an excellent chance to cut emissions and progressively achieve the advantages of electrification. They should be explored in conjunction with the electrification project, even if they are not the most cost-effective long-term answer. As current multi-mode vehicles demonstrate, the optimal design allows for the phase-out or total replacement of diesel generator sets or engines. Operational cost savings can be realised by discontinuous or discrete electrification. As discussed in Section **Error! Reference source not found.**, the problems inherent in delivering such a solution are context-specific and must be integrated into the business case for each project following the completion of more thorough development work. The highlights of this chapter are as follows:

- A multi-mode train powered by pantograph, hydrogen, and battery simulator is developed.
- Its state and train performance control the dynamic battery pack model.

- A specific energy management strategy optimises multi-energy usage.
- The cost model includes initial financial costs and further operation costs.
- Adaptive particle swarm optimisation is used to find the optimal cost solution.

The structure of this chapter is organised as follows: Section 6.1 explains the current situation of changes to railway energy supply methods. Section 6.2 reviews the train's variable supply system. Section 6.3 describes the definition of different railway electrification types. Section 6.4 describes the advantages of multi-mode trains. Section 6.5 shows the multi-mode train energy management strategy employed and demonstrates how it works in different scenarios. Section 6.6 allocates the optimisation algorithms used in this chapter and shows how they differ from the original algorithm. Section 6.7 presents a case study of the rebuilding plan for the route from London St. Pancras to Leicester and train conversion. An existing diesel train is compared with converted trains in different electrification scenarios. Estimated energy price changes are considered to forecast the effect of rising energy prices on the simulation results.

This chapter is an expanded version of the studies that resulted in a journal paper, 'Cost optimization of multi-mode train conversion for discontinuously electrified routes' published in the *International Journal of Electrical Power & Energy* [116]. The author of this thesis is the first author of the journal paper and made a major contribution to the paper. This chapter is reproduced by permission of Elsevier.

6.2 Trains with various power supplies

6.2.1 Bi-mode trains

Bi-mode trains may run on either an electrified or non-electrified network, utilising either a diesel engine or a battery to provide traction power. They use a variety of various energy sources, such as operating 'under the wire' or diesel, but not both simultaneously.

6.2.2 Hybrid trains

Hybrid trains are self-sufficient and do not require grid electricity. They power the trainset with a combination of stored and rechargeable energy sources, which provide benefits that neither source can provide alone. They may employ a single or a mix of energy sources. Although a hybrid train can use energy storage devices, including capacitors, flywheels, hydraulic accumulators, hydrogen, or LPG, the most common hybrid design is diesel-electric.

6.2.3 Tri-mode or multi-mode trains

The advantages of bi-mode and hybrid trains are combined in a tri-mode/multi-mode trainset. However, like with bi-mode and hybrid trains, the additional components increase technical difficulties and increase the train's weight. These factors will also affect the train's performance [117].

6.3 Discontinuously electrified routes

Continuous electrification refers to those segments of a line where the electrified network is continuous. Electric trains may operate, stop, and restart along their path using just electric power. A railway segment is electrified using an overhead line or third rail equipment in a discontinuously electrified route. Simultaneously, an entirely unelectrified route is entirely devoid of any power source. This thesis refers explicitly to the electrified segment as the route's overhead line equipment was installed. According to the study Long Term Passenger Rolling Stock Strategy for the Rail Industry, the electrification rate of the UK railways is 42% , or 8106 STM out of 19,291 STM (12,969 STK out of 30,865 STK). Additionally, electrified trains account for 80% of rides per kilometre [118].

As an electric train on an electrified line, the train may obtain energy from the contact wire to power the traction system. Once the train operates on a route without an overhead wire, no current can be delivered to the motor from the electrification system. On an unelectrified route,

another traction system that can utilise the train's stored energy is necessary. A self-powered traction system is a name for this type of traction system. This category includes classic steam trains, fossil-fuel-powered diesel trains, and contemporary trains powered by batteries or fuel cells.

As a result of the electrification gap, a self-powered traction system is required in situations of discontinuous electricity. The fleets usually are just self-powered trains if the operation route involves discontinuous electricity. In this case, the trains solely utilise stored energy on electrified and non-electrified lines without overhead line equipment. At the same time, some electric trains are running between stations along the electrified track.

6.4 Advantages of multi-mode train structure

A multi-mode train is a typical case of how electrification may be used. It contains at least two power supply systems that work in parallel. One is the fundamental electrical train, which uses the overhead line power supply system. Diesel engines, fuel cells, and battery systems are among the others. These systems can work with the pantograph system on an electrified route, and on an unelectrified route they can be the primary power source.

Most rail lines are partly electrified in the UK. On discontinuously electrified routes, the power supply is divided into two parts: overhead line power to the motor as the main or only supply system on the electrified part, and a self-powered traction system such as hydrogen fuel cells and battery pack, to supply power to the motor together, on the non-electrified part. Making the best use of electrification is an effective way to save energy costs, and a self-powered traction system is also necessary when no overhead line is accessible. A train traction system powered by a multi-mode power system is applied in this situation. A hydrogen fuel cell (HFC) train can operate on the track regardless of the discontinuous electrification. Similar to diesel trains, HFC trains consume fuel to propel them. The onboard HFC can produce electricity by

consuming hydrogen. The electricity can be sent to the motor and converted to kinetic energy. Traction power is supplied by the motor powered by a multi-mode power system in Equation (92), and the effort is inversely proportional to velocity in Equation (93).

$$\mathrm{F_{tra}} = \eta_{train} \times (P_{demand}/v) \qquad (91)$$

$$P_{demand} = P_{Pan} + P_{FC} + P_{BP\_disch} \qquad (92)$$

$$\mathrm{F_{bra}} = P_{bra}/v \qquad (93)$$

where η_{train} is the efficiency of the train set (typically 85%), and P_{Pan}, P_{FC}, and P_{BP_disch} are the output power of the pantograph, HFC, and battery pack, respectively. The sum of the power supply system is equal to the power demand of the traction motor P_{demand}. The braking force F_{bra} depends on the braking power and the operating speed.

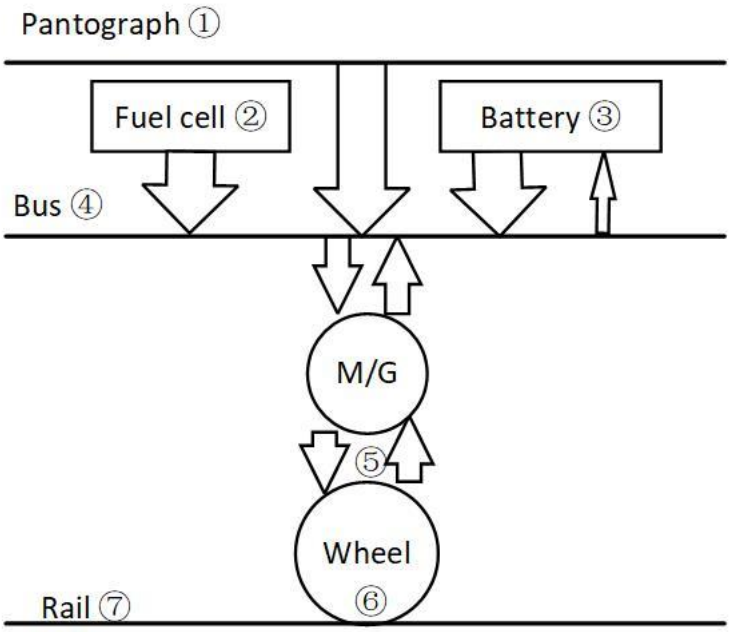

Figure 48 Energy flow

Seven kinds of energy flow inside the trains are shown in Figure 48. Energy from the pantograph ①, fuel cell ②, and battery pack ③ connect to the power bus ④. Electrical energy in the power bus ④ is converted into mechanical energy ⑤ by the motor and sent to the wheels through the gearbox to push the train forward. When the train is braking, kinetic energy ⑥ and potential energy ⑦ are regenerated to electricity and sent back to the power bus ④. Any electricity in the power bus which is not consumed can charge the battery pack ③.

In Equation (94) and (95), the energy consumption from each source integrates the power supplied by different systems. In this thesis, the battery pack energy consumption ΔE_{BP} will be charged through a transmission line. When considering the use of battery pack energy, the difference in the energy remaining in the battery pack in kWh is given by Equation (96).

$$E_{\text{Ele\_C}} = \frac{\int P_{Pan} dt + \Delta E_{BP}/\eta_{BP}}{\eta_{\text{Pan}}} \tag{94}$$

$$E_{\text{Hy\_C}} = \frac{\int P_{FC} dt}{\eta_{FC}} \tag{95}$$

$$\Delta E_{BP} = \left(SOC_{fin} - SOC_{ini}\right) \times Capa_{BP} \tag{96}$$

where $E_{\text{Hy\_C}}$ and $E_{\text{Ele\_C}}$ represent hydrogen and electrical energy consumption, respectively; η_{FC} and η_{Pan} are the energy efficiency of the HFC and pantograph, respectively, before injection to trains; η_{BP} is the battery pack efficiency; and $Capa_{BP}$ is the battery pack capacity. SOC_{fin} and SOC_{ini} are the battery's state of charge when the train arrives at the terminal station and departs from the start station, respectively. The energy losses diagram is shown in Figure 49. All losses described in Chapter 3 are summarised in this diagram. After considering the

losses and auxiliary system usage, the rest of the kinetic and potential energy can be returned to the battery pack by regeneration as the battery train performs.

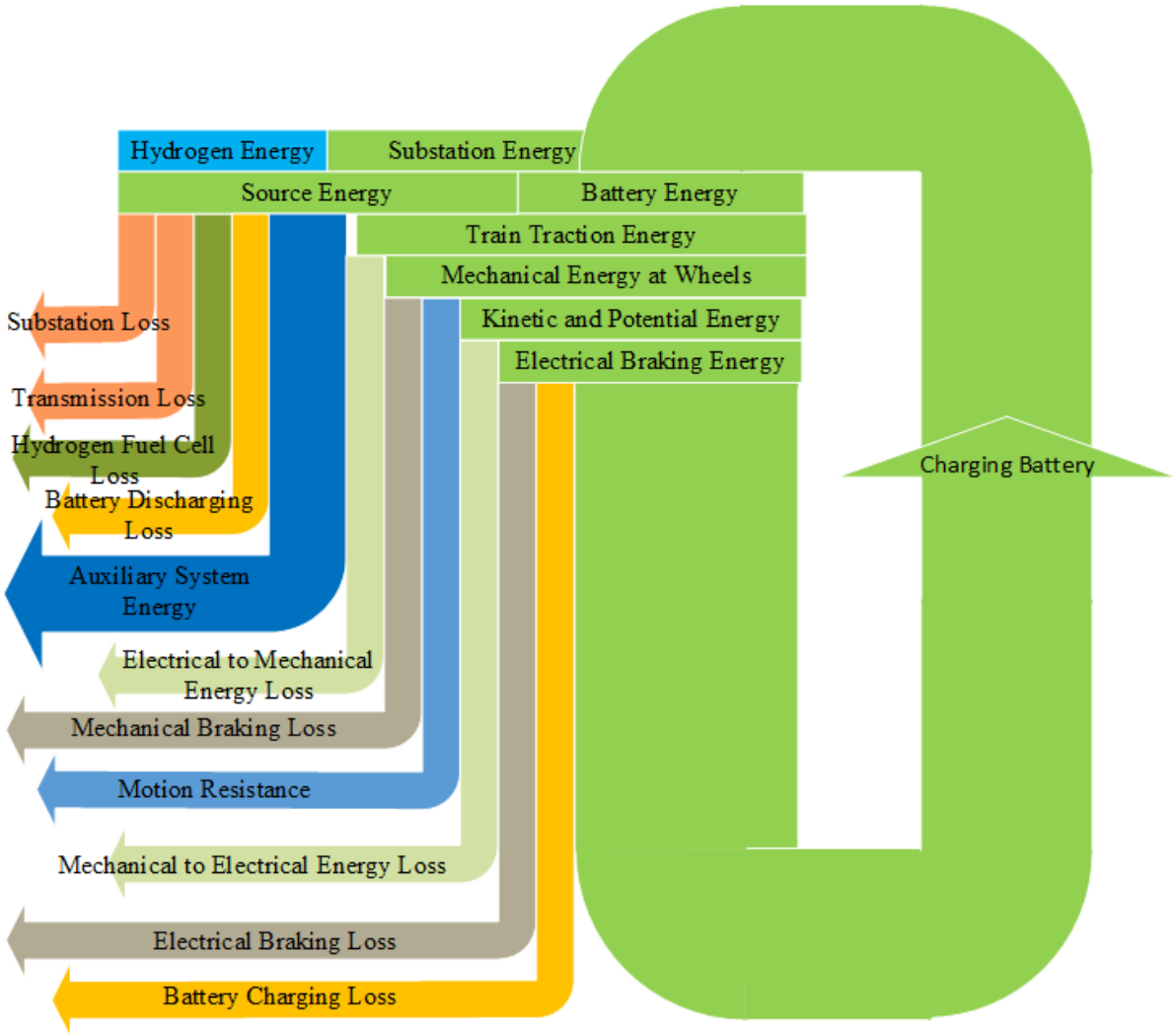

Figure 49 Multi-mode train energy losses

6.5 Multi-mode train power supply strategy

The energy management system controls the use of the multi-mode energy source. This thesis identifies four driving scenarios according to differences in train operation and route electrification. A default management strategy is set to cover these driving scenarios, as shown in Figure 50.

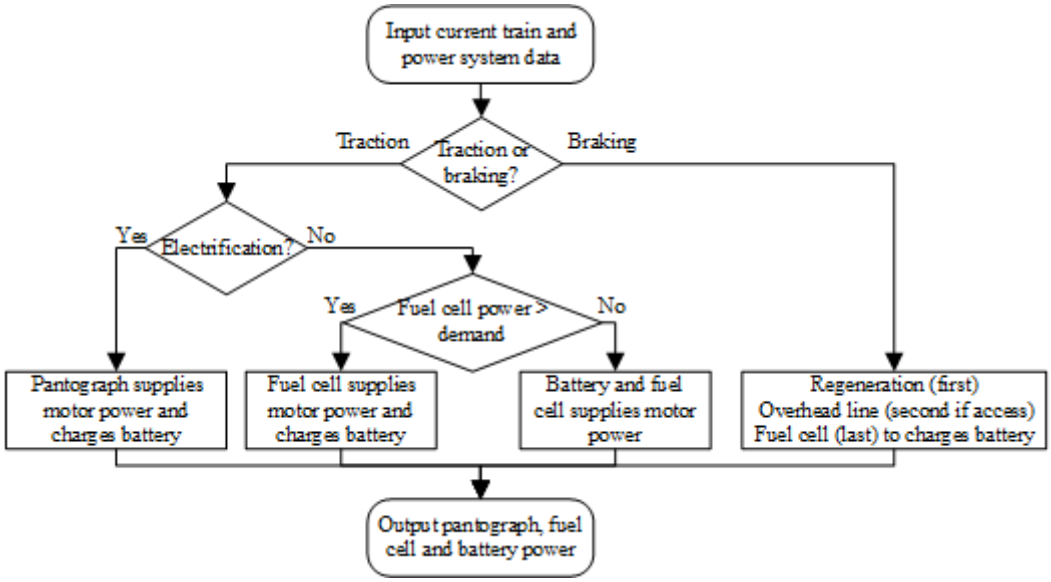

Figure 50 Flow chart for the energy management system

6.5.1 Traction on an electrified route

On an electrified route, the overhead line can supply all the power needed by the motor and battery pack. Because of the extremely high-power supply, the battery pack is always charged at its maximum charging power on electrified routes.

6.5.2 Traction on a non-electrified route with low power demand

Less traction power is demanded if the train operates in a low-speed acceleration stage or a low traction-force stage like cruising or going downhill. The fuel cell can charge the battery pack if motor power demand P_{demand} is below the fuel cell maximum power $P_{FC\ MAX}$ as shown in Equation (97).

$$P_{BP\_ch} = P_{FC\ MAX} - P_{demand} \qquad (97)$$

where P_{BP_ch} is the charging power of the battery pack.

6.5.3 Traction on a non-electrified route with high power demand

When the train operates in high power demand situations such as high speed or high traction force, if the installed fuel cell does not have such a high output power, it no longer meets the

power demand. The maximum power $P_{FC\ MAX}$ is sent to the power bus, and the battery pack is discharged to compensate for the power demand as given by Equation (98). The battery pack stops discharging when the SOC is below the low operation limit. ΔE_{BP} in Equation (96) is the change in battery pack energy. It should also be equal to the sum of the battery pack discharging power P_{BP_disch} minus the sum of battery pack charging power P_{BP_ch} after considering the battery pack efficiency.

$$P_{BP\_disch} = P_{demand} - P_{FC\ MAX} \tag{98}$$

$$\Delta E_{BP} = \frac{\int P_{BP\_disch}\, dt}{\eta_{BP}} - \eta_{BP} \times \int P_{BP\_ch}\, dt \tag{99}$$

Overall, on a non-electrified route, the HFC is the primary power supply system, whereas the battery pack only compensates for peak power demand.

6.5.4 Braking stage

At the braking stage, regenerative braking and non-regenerative braking work simultaneously. When the train operates electrical braking, the generator regenerates high power to charge the battery through the power bus. The rest of the power that cannot be transferred to the power saving in the battery pack is consumed by non-regenerative braking, such as disc braking. Regenerative power from the generator has the highest charging priority. If the regenerative power is not as high as the battery's maximum charging power, the overhead line electricity charges the battery to compensate for the charging power. However, if the train brakes in the non-electrified part, the fuel cell charges the battery by taking the overhead line. In this thesis, it is assumed that the combination braking power P_{bra} is always set as its maximum value, as Equation (100) shows. Uncertain braking power may result in different movement curve, train usually gets better movement performance with maximum braking power [119]. For each kind

of train, the braking power, braking force, and deceleration have their cap value (maximum value), respectively.

$$P_{bra} = P_{regen} + P_{non-regen} \tag{100}$$

$$P_{bra} \leq P_{bra_{max}}$$

$$F_{bra} \leq F_{bra_{max}} \tag{101}$$

$$a_{bra} \leq a_{bra_{max}}$$

6.6 Optimisation algorithms

6.6.1 Algorithm selection

When considering the optimistaion algorithm selection, there are hundreds of algorithms can be applied to solve optimistaion problems. As two well-known algorithms, Genetic Algorithms is created earlier, but Particle Swarm Optimisation becomes more attactive for continuous optimistaion [120]. However, for those problem like course scheduling, GA can find the result faster, although the PSO can find a better fitness result with longer optimisation time [121]. The PSO gets higher accurancy and speed during analysing pavement management activities [122]. However, there are some railway research applied GA to solve railway scheduling problems and get good performance [123, 124]. PSO is noted for its simplicity and efficiency, with fewer parameters to adjust, making it easier to implement. It's particularly effective for continuous problem spaces. GA, on the other hand, is highlighted for its robustness and effectiveness in a wide range of problem types, including discrete, combinatorial problems. GA's crossover and mutation operations are effective for exploring diverse solution spaces, making it versatile for different optimisation challenges [120]. Brute force method is a exhaustive search and it can grarantee the best result but time costy [119]. In the case study of

this thesis, PSO, GA, and Brute force method would be analysis and try to applied to solve the cost optimisation problem.

6.6.2 Optimisation variables

6.6.2.1 Definition of variables

The optimal variables in this thesis are battery pack power P_{BP}, HFC power P_{FC}, new electrified regular route length L_{NE}, and new electrified tunnel length L_{TE}. In these four variables, P_{BP} and P_{FC} present the train's conversion. They represent the new train's power distribution in battery packs and HFCs. L_{NE} and L_{TE} are related to route rebuilding which has a considerable cost impact due to its high infrastructure fees. Besides that, a more extended electrified section means the train can get more highly efficient, high-power overhead wire electricity. That can influence the train's operation performance with the different design of the other two variable factors. Hence, the energy cost is finally different.

Regarding the route rebuilding variables, it is supposed that Part 1 is the existing electrified route, whereas Parts 2 to 8 are not electrified, as Figure 51 shows. When a train operates on an existing or newly electrified route, it can gain energy from the overhead line. Because electrification projects typically extend from the currently electrified route, new electrification starts from the currently electrified part to the terminal. In this optimisation, the length of the yellow part is to be optimised. These parts are electrified, including the regular route of Parts 2, 4, and 7 and the tunnels of Parts 3 and 5. Part 6 (tunnel) and Part 8 (regular route) remain unelectrified.

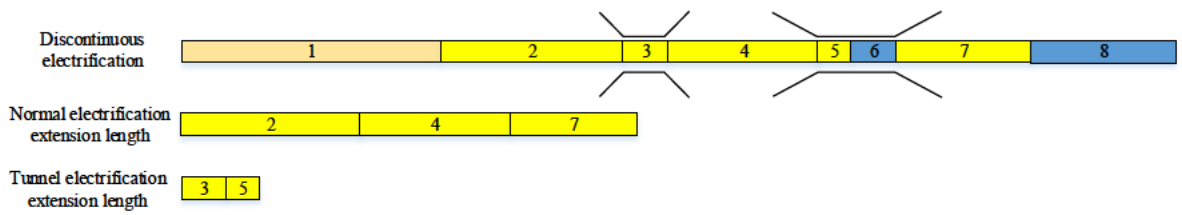

Figure 51 Electrification variables

6.6.2.2 Fitness function

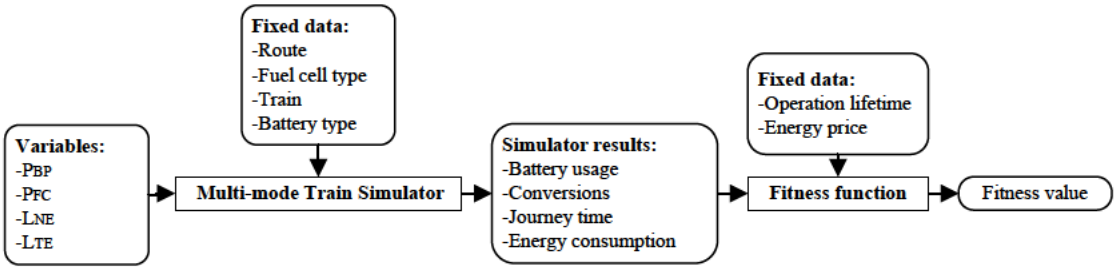

Figure 52 Calculation of fitness value

The evaluation method combines a multi-mode train simulator and a fitness function block. Figure 52 shows the inputs and outputs of the evaluation. The multi-mode train simulator is shown in detail in Section 6.4. Equation (102) gives the fitness function, including the total cost and the journey time factor (TF). The total cost is the money spent on conversion, rebuilding, and future operating costs in the units of GBP. Besides that, TF shows the profit or penalty due to journey time difference in Equation (103) with the same units of GBP. The aims of this redesign research are optimisation the overall cost and keep the journal time less than maximum time limit T_{target}. If the journey time T_j exceeds the maximum time limit, a time penalty is applied. However, the time profit is varied according to the optimisation requirement. If the optimisation recommends reducing journey time, κ_{profit} is negative and set as a greater absolute value. For those optimisations which require no obvious journey time changes, κ_{profit} can set as 0 or positive.

$$f(P_{BP}, P_{FC}, L_{NE}, L_{TE}) = TF + C_{total} \tag{102}$$

$$TF = \begin{cases} \kappa_{profit} \times (T_j - T_{target}) & if\ T_j < T_{target} \\ \kappa_{penalty} \times (T_j - T_{target}) & if\ T_j > T_{target} \end{cases} \tag{103}$$

where T_{target} is the target journey time, κ_{profit} is the time profit coefficient for earliness, and $\kappa_{penalty}$ is the time penalty coefficient for tardiness. If the final State of Charge (SOC) of the battery pack is lower than the initial level, it will require more time to recharge the battery pack back to its initial energy level, the same level as when the train started. That extra time is also considered as journey time except for operation time T_{op}.

$$T_j = T_{op} + \frac{\Delta E_{BP}}{P_{BP\_ch}} \tag{104}$$

6.6.2.3 Constraints and adjustment

As the optimising variables, the four variables $(P_{BP}, P_{FC}, L_{NE}, L_{TE})$ have their constraints. The minimum value of each variable is set as 0, whereas the maximum constraint of the battery pack is 1000 kW and that of the HFC is 2240 kW; the regular route and tunnel rebuilding lengths are set as the length of the simulated unelectrified route. If the updated plan variables exceed the constraints, the value of the variable $\overrightarrow{X_{i+1}^n}$ will be set as the edge (maximum or minimum) value and the variables' change rate $\overrightarrow{V_{i+1}^n}'$ is the opposite, to avoiding exceeding the constraint again.

$$\overrightarrow{V_{i+1}^n}' = -\overrightarrow{V_{i+1}^n} \tag{105}$$

6.6.2.4 Stop condition

The typical stop condition for the optimisation algorithm is to set the maximum number of generations. The optimisation stops once the generation reaches the maximum iteration. However, researchers usually set extremely high maximum iterations because of the unpredicted heuristic approaches. Hence, the widely used stop condition is set as a convergence coefficient. It starts counting when the temporary optimal meets the convergence rate condition

as a flag. Once the convergence flag reaches the maximum convergence generation, the program executes the optimisation result and stops. Determining the optimal plan found condition depends on changes of the best fitness value. If the best fitness value changes, the rate $CR_{fitness}$ over several iterations is less than the convergence coefficient, and the optimisation program can be stopped.

$$CR_{fitness} = \frac{f_{new\ best} - f_{old\ best}}{f_{old\ best}} \qquad (106)$$

6.6.3 Particle swarm optimisation

Particle Swarm Optimisation (PSO) is an optimisation algorithm developed to simulate bird movement [125]. Adaptations include an adaptive PSO with multiple methods and a kernel support vector machine based PSO to enhance convergence speed and exploration capabilities [126, 127]. This research utilises a simple adaptive PSO to determine the optimal result. Figure 53 shows the optimisation flow chart.

Step 1: A set of railway rebuilding plans with variables initialised by random values and related modelling data are input to the optimisation program.

Step 2: Those railway rebuilding plans are simulated based on a railway route and evaluated by the fitness function.

Step 3: The results are ranked according to their fitness value, and the overall best plan and individual best plan are recorded.

Step 4: If the overall best plan meets the stop condition, it will be sent to Step 6. Otherwise, all plans are sent forward to Step 5.

Step 5: All plans need to be updated according to the PSO's updating method. Besides that, new plans out of the variables' range need to be adjusted and then sent back to Step 2 with those plans located inside the range.

Step 6: Output the best plan.

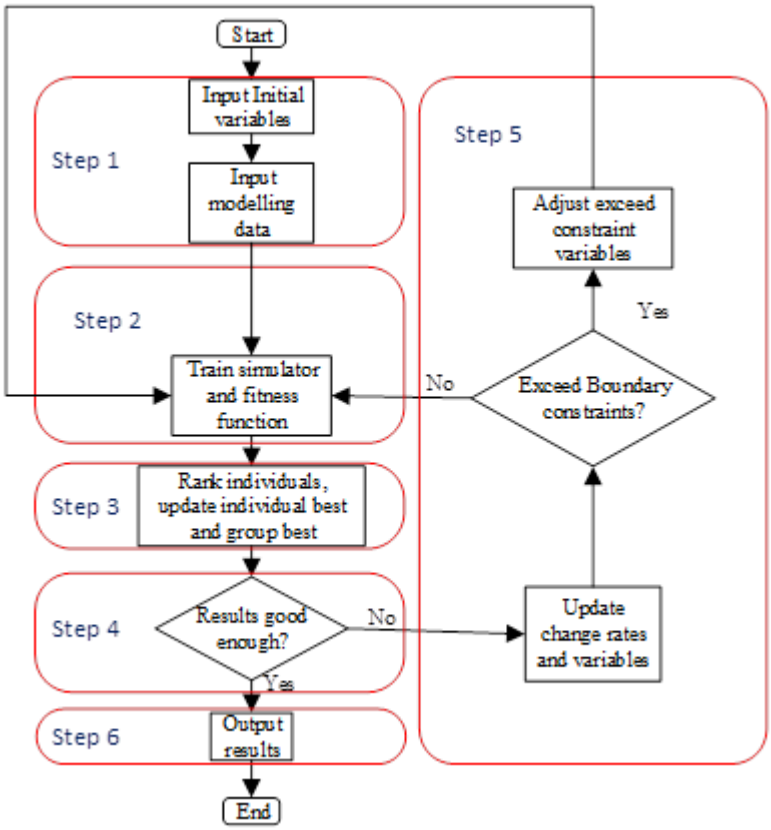

Figure 53 Flow chart of the optimisation

6.6.3.1 Initialisation

For any heuristic algorithm, initialisation is the first and essential step in the optimisation operation. It more or less influences the convergence of the results. In the case of manual set initialisation, if almost all the initialised variables are located near the local optimal point, the final optimal results will be converged at the local optimal point when the algorithm's exploration capacity is not high enough. Alternatively, when all the initialised variables are

concentrated at points away from the global optimal point, the optimisation algorithm needs more time to find the optimal point. To avoid these situations, a bigger and sufficiently dispersed initial population are applied in the PSO of this thesis.

6.6.3.2 Variables update

The basic variable optimisation principle is demonstrated in Figure 54. Updating the variables' change rate in each iteration, as shown in Equations (107) and (108), depends on the last change rate inertia $\omega\overrightarrow{V_{(\iota)}^{(n)}}$, cognitive component $c_1 \times r_1 \times \left(\overrightarrow{X_{\iota best}^{n}} - \overrightarrow{X_{\iota}^{n}}\right)$, and social component $c_2 \times r_2 \times \left(\overrightarrow{X_{\iota best}} - \overrightarrow{X_{\iota}^{n}}\right)$ which are related by the difference to the individual best point and group best point, respectively.

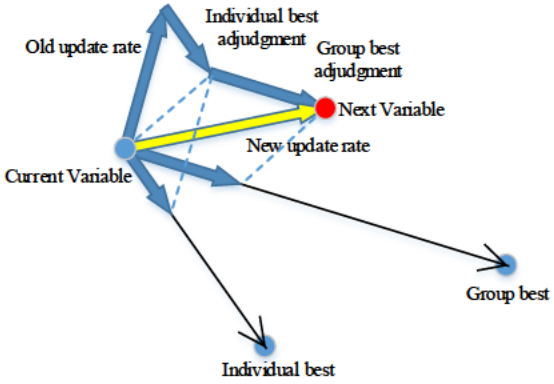

Figure 54 Individual update

$$\overrightarrow{V_{(\iota+1)}^{(n)}} = \omega\overrightarrow{V_{(\iota)}^{(n)}} + c_1 \times r_1 \times \left(\overrightarrow{X_{\iota best}^{n}} - \overrightarrow{X_{\iota}^{n}}\right) + c_2 \times r_2 \times \left(\overrightarrow{X_{\iota best}} - \overrightarrow{X_{\iota}^{n}}\right) \quad (107)$$

$$\overrightarrow{X_{\iota+1}^{n}} = \overrightarrow{X_{\iota}^{n}} + \overrightarrow{V_{\iota}^{n}} \times 1 \quad (108)$$

6.6.4 Genetic algorithms

Holland found and introduced Genetic Algorithms (GA) in the 1970s [128]. This computer approach solves the optimisation problem by determining the global maximum or least digital twin results. The five steps of the Simple GA method are initialising the populations, computing the fitness value of each population, selecting required populations, crossover, mutation, and then repeating the selection, crossover, and mutation in order to find the optimal results [129]. Apart from the phases outlined above, when optimal local outcomes are readily trapped in particular instances, an additional migration step can be added to the progress. Naturally, genes are classified into two types: dominant and recessive genes.

The Simple GA mimics a natural gene in that the chromosomal arrays are binary coded by 1 and 0, respectively, indicating dominant and recessive genes. A single variable can be defined by a long piece of the chromosomal array coded by binary. Apart from the dominant and recessive genes, there are several other critical criteria to consider, such as chromosomal length, population size, and others. A variable's precision is determined by its chromosomal length. The accuracy of the variable is doubled for each additional chromosomal region. All the individuals in each generation are called the population. The bigger the population, the greater the likelihood of achieving the worldwide ideal answer, but it takes longer to run a whole generation [130].

6.6.4.1 Initialisation

As with PSO initialisation, all initials are assigned random values. While the changed GA differs from the Simple GA, all random values in the altered GA are decimal float values that comprise both an integer and a fraction. For better performance and less storage memory, real number coding will take the place of binary coding in this thesis.

6.6.4.2 Fitness function changes

Based on the characteristics of a GA that it can only find the maximum fitness value, the fitness function in Section 6.6.2.2 is not well-fitted for GA optimisation. The fitness function needs to be altered as Equation (109) in this situation. At the same time, the convergence rate also needs to upgrade to a new value, as shown in Equation (110).

$$f'(P_{BP}, P_{FC}, L_{NE}, L_{TE}) = \frac{1}{f(P_{BP}, P_{FC}, L_{NE}, L_{TE})} \quad (109)$$

$$CR'_{fitness} = \frac{CR_{fitness}}{1 - CR_{fitness}} \quad (110)$$

6.6.4.3 Variables update

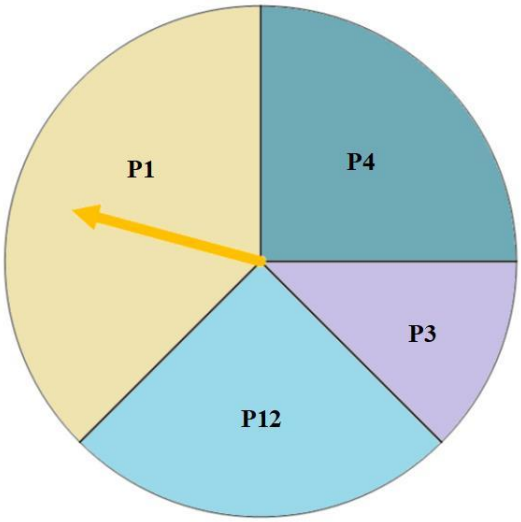

Figure 55 Roulette wheel selection

As seen in *Figure 55*, the roulette wheel selection approach is used in this thesis. There is a flaw in the fundamental wheel selection strategy: probability selection may prevent the fittest chromosome from being picked. Thus, by replacing a random 5% of the total population with

elites in each generation, the best appropriate individuals dubbed the elite can have a greater probability of attending crossover operation. it is devised a method for grading selection intensity [131]. This selection approach can increase the likelihood of poor individuals joining crossover during premature optimisation, to avoid being trapped in the optimal local solution. The selection procedure involves choosing which chromosomes to reproduce, and the possibility of each potential plan is different depending on their fitness value, as shown in Equation (111).

$$P_i = \frac{f(x)}{\sum_1^N f(x)} \qquad (111)$$

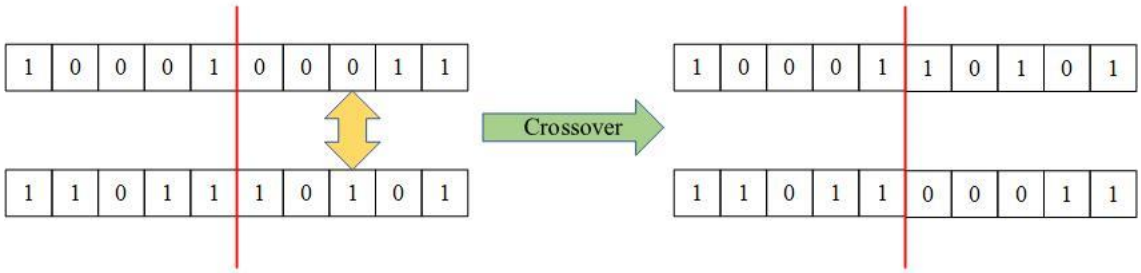

Figure 56 Single-point crossover

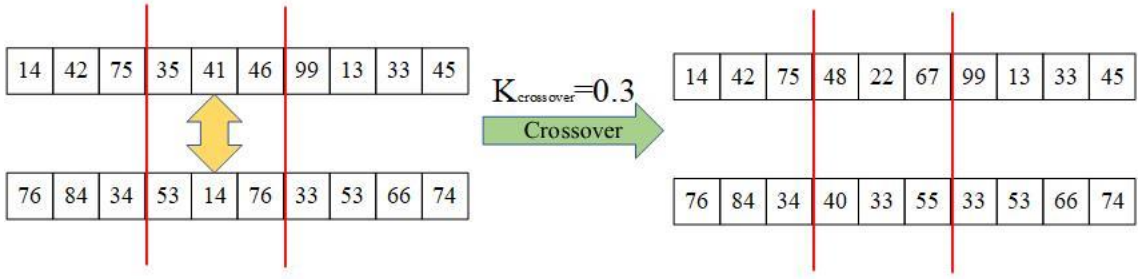

Figure 57 Double-point crossover for real number coding

Following selection, the next step is process crossover. Different from the single-point binary crossover shown in Figure 56, the crossover approach employed in this thesis is known as double-point real-number crossover (Figure 57). Double-point crossover swaps those components between two distinct random points, unlike single-point crossover. Each individual has $P_{crossover}$ changes to operate crossover. GA chooses two random different indices, and the chromosome between these two indices will be altered. The changes in this thesis are also different from those in other research. Assuming there is a random crossover coefficient $K_{crossover}$ at the range of 0 to 1 for every crossover, the variables undertaking crossover will be changed to the new value following the rule below:

$$V_{(i+1)}^{(n)} = K_{crossover} \times V_{(i+1)}^{(n)} + (1 - K_{crossover}) \times V_{(i+1)}^{(n)}$$
$$V_{(i+1)}^{(n+1)} = (1 - K_{crossover}) \times V_{(i+1)}^{(n+1)} + K_{crossover} \times V_{(i+1)}^{(n+1)} \quad (112)$$

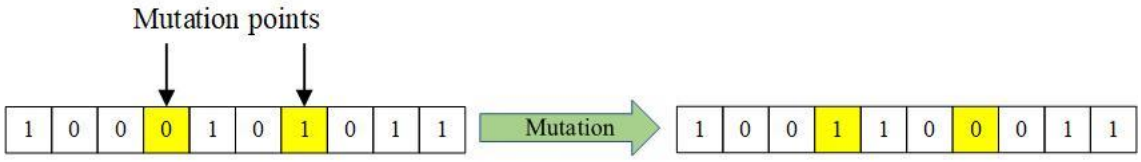

Figure 58 Mutation

In the process illustrated by Figure 58. mutation acts as a search operator for discovering new genes by flipping specific chromosomal bits from 0 to 1 or vice versa. This mechanism introduces new variable values into the optimisation process, helping to prevent the solution from getting stuck in a local optimum. For example, if the fourth and seventh genes of a chromosome undergo mutation, the chromosome might change to a sequence like 1001100011. However, as this thesis employs real number coding instead of binary coding, mutation cannot

be simply applied to switching between 1s and 0s. Therefore, a novel approach to mutation is introduced in this thesis. Here, the gene element (variable) erases its original data, and a new variable value is randomly selected from within the predetermined minimum and maximum values. This innovative method addresses the limitation that real numbers cannot use the traditional mutation operation, thereby eliminating the risk of an exploratory deficit due to the absence of mutation operations. An example of the new mutation is shown in Figure 59.

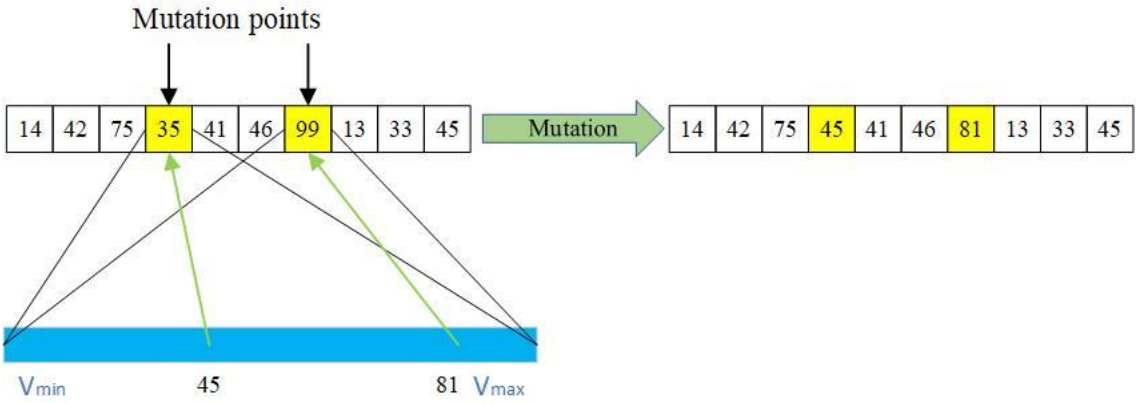

Figure 59 Individual without crossover mutation

It is occasionally challenging to investigate genes just by mutation. Nonetheless, migration may be used to optimise GA. In comparison to mutation, migration brings more random genes into the optimisation process. Completely fresh individuals take the place of the poor performers. This is also an opportunity to import a large number of genes that have never been seen before. However, this approach is likely to significantly reduce the fitness function due to unpredictability, similar to mutation. In this thesis, migration takes place in parallel with other operation. This operation would create some new individuals and replace some bad performance individuals with those new individuals. The GA flow chart is shown in Figure 60. For better convergence, there is no migration at the early stage of optimisation, but when the convergence flag is more significant than a set value.

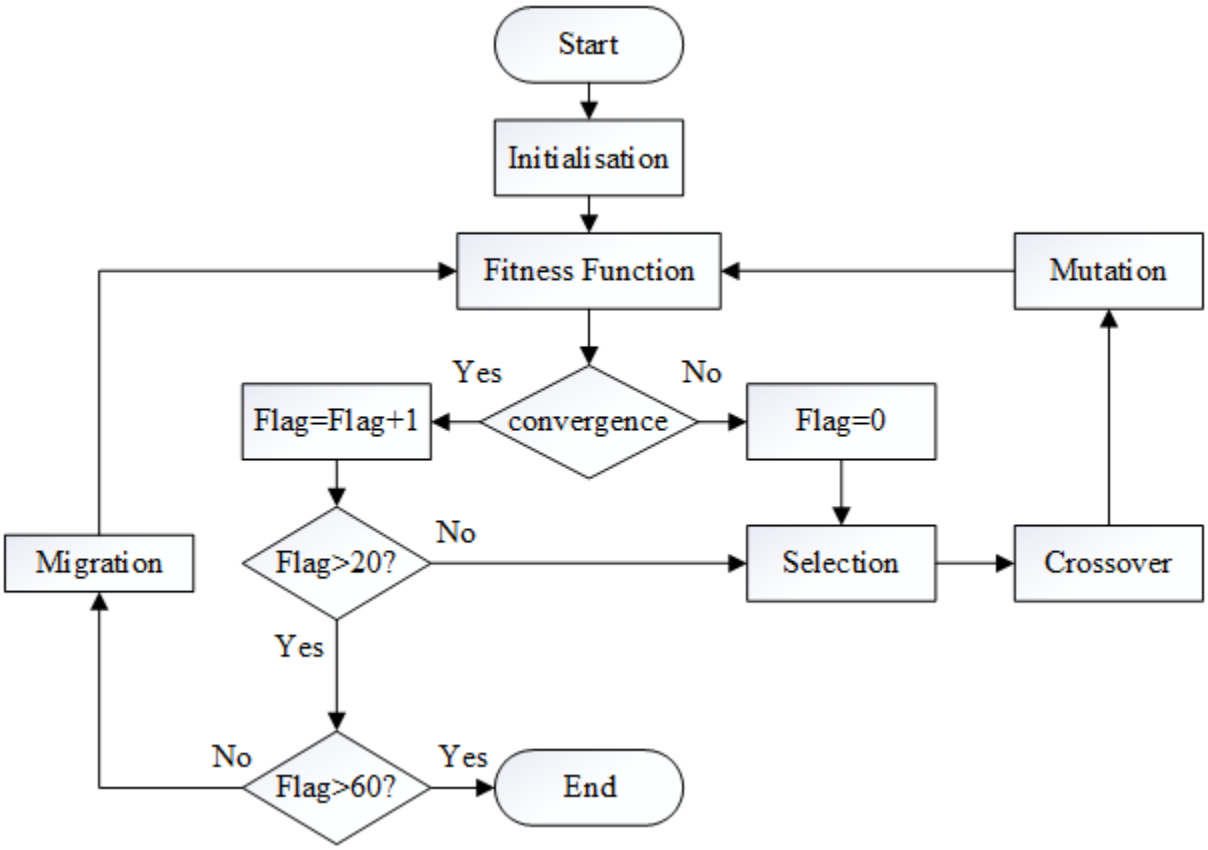

Figure 60 GA flow chart

6.6.5 Brute force

Additionally, the Brute Force approach is referred to as an exhaustive search method. It is a simple approach that expresses and assesses all available options [119]. It is a precise method for optimising a limited number of viable choices but is unsuitable for large-scale optimisation problems.

6.7 Discontinuously electrified route case study

6.7.1 Route selection

The selected simulation route is from London St. Pancras to Leicester (158.54 km), part of the Midland Main Line, with six intermediate stations, as shown in Table 15. The black line shows line speed restrictions. The first half of the route, with a total length of 79.46 km from London St. Pancras station to Bedford station, is electrified. Besides that, there are 11 tunnels located

on the rest of the route, which is not electrified [86, 87]. A two-direction operation is considered to obtain more accurate optimisation results; from the start station, trains operate to the terminal station and then run back.

Eleven tunnels on the unelectrified route are difficult and costly to electrify. Except for Sharnbrook Tunnel (1.7 km), most tunnels are less than 200 m long. In comparison to the Severn Tunnel (7 km), which has a high priority for electrification on the Great Western Main Line, Sharnbrook Tunnel is a relatively short tunnel. However, due to its unique placement on the crest of a hill, train speed is significantly reduced while travelling through the tunnel. The κ_{profit} for this route is zero since the study's objective is to determine the ideal plan with the fewest possible modifications to the travel duration. At the same time, $\kappa_{penalty}$ is set at £40 per minute of delay [132, 133].

Table 15 Station locations [86]

Station	Location [km]
London St. Pancras station	0.00
Luton Airport Parkway	46.78
Luton	48.38
Bedford	79.46
Wellingborough	104.22
Kettering	115.22
Market Harborough	132.68
Leicester	158.54

Table 16 Tunnel location, length, and speed limit [86]

Tunnel	Location [km]	Length [m]	Speed limit [km/h]
Bromham Viaducts (River Ouse)	81.44	140	176
Clapham Viaducts (River Ouse)	83.16	120	176
Oakley Viaducts	85.38	120	176
Milton Ernest Viaducts	86.74	160	176
Radwell Viaducts	87.93	130	176
Sharnbrook Viaducts	89.92	180	176
Sharnbrook Tunnel (Slow line only)	94.40	1701	80
Irchester Viaducts (River Nene)	102.00	140	176
Wellingborough Viaducts (River Ise)	103.42	120	128
Knighton Viaduct	155.8	80	128
Knighton Tunnel	156.84	95	128

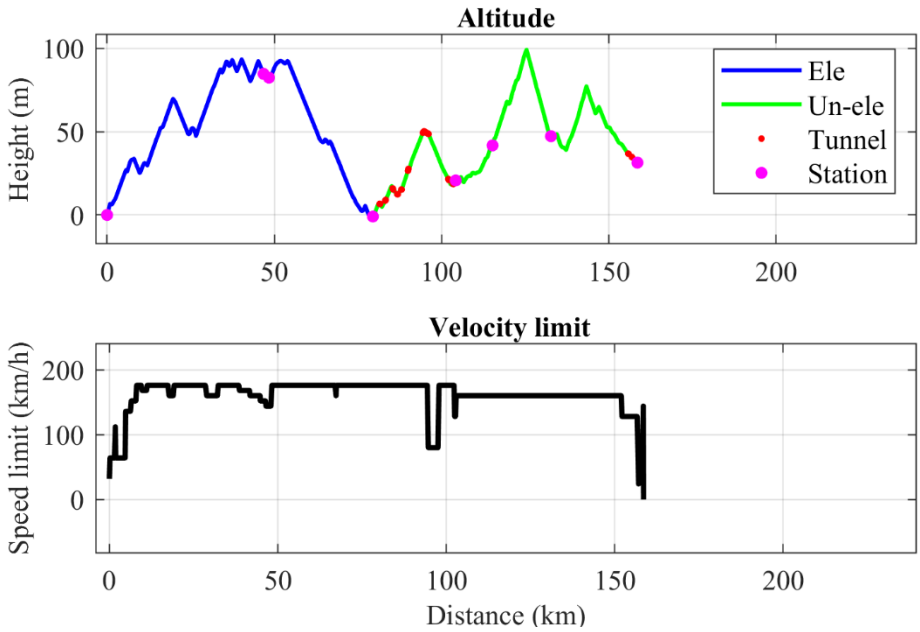

Figure 61 Line altitude, stations, and speed limit from St. Pancras to Leicester [86]

6.7.2 Comparing operating performance

Table 17 Single-mode train route design plans, energy consumption, and cost

Train and route plan	Weight [tonnes]	Diesel engine power [kW]	P_{BP} [kW]	P_{FC} [kW]	L_{NE} [km]	L_{TE} [km]	Journey time [s]	Traction energy use [kWh]	Fuel energy cost [£]	Energy cost saving
Bench-mark diesel train	214	2240	0	0	0	0	9340.3	2190.6	1116.8	0
Hydrogen train	215.38	0	0	2240	0	0	9346.3	2196.1	1682.4	−50.6%
Full electrification (except tunnels)	190.88	0	0	0	76.11	0	9135.2	2134.6	288.65	74.15%
Full electrification	190.88	0	0	0	76.11	2.97	9116.2	2137.4	289.03	74.12%

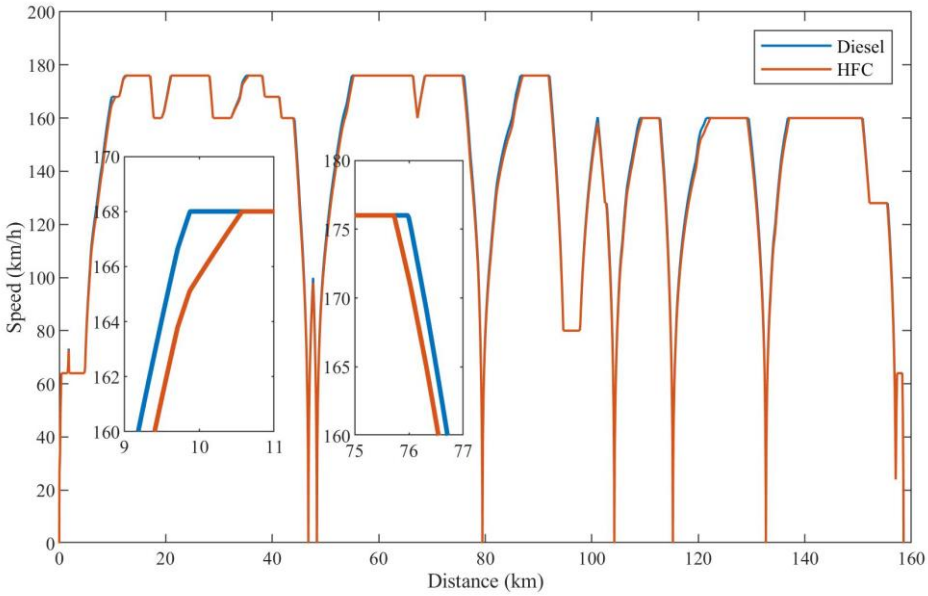

Figure 62 Diesel and HFC train velocity curve from St. Pancras to Leicester

Details for single-mode trains in each run are shown in Table 17. It offers the different parameters related to those optimised variables and the performance of single-mode trains, including diesel, HFC, and electric trains on full electrification with and without tunnel electrification. The performance is almost the same for diesel and HFC trains but there are still some differences. This shows that the HFC train has a journey time 6 s (0.06%) longer than that of the diesel train. Furthermore, the difference in traction energy is 0.25%, less than the 0.64% which is the weight difference. More traction energy is consumed by a hydrogen train, even though better transfer efficiency contributes to 48.67% less fuel energy consumption than for a diesel train. Although the price of hydrogen per kWh is 2.3 times that of diesel, the hydrogen train energy cost for each run is only 50.6% higher than for the diesel train. From Figure 62, it is observed that at any given location, the speed of the diesel train exceeds that of the hydrogen train. This is attributed to the diesel train's ability to alter its speed more rapidly, whether accelerating or decelerating, under the same maximum power supply. During the

acceleration phase, the hydrogen train reaches its power limit earlier than the diesel train. Consequently, its acceleration diminishes as it lacks support for higher power.

The average velocity for both electrification scenarios is higher than for the benchmark diesel train. This is mainly because the electric train is lighter than the others and has greater acceleration power. The energy costs for these two scenarios are nearly the same, saving around 74% compared with the benchmark diesel train. Table 17 also shows that more traction energy is consumed by a hydrogen train than any electric train. Broadly speaking, this is due to a hydrogen train being heavier than other trains, so it needs more energy to propel it forward. In detail, this thesis considers three operation stages during the journey: acceleration, cruising, and braking. The traction energy consumed by the diesel and electric trains is obviously less than for the fuel cell train. Those lighter trains speed up to maximum velocity earlier and enter the cruising stage, demanding less power. The one is less traction forced needed but longer operation, another is more traction force needed but short operation. However, it is hard to compare the energy consumption during the entire cruising stage by qualitative analysis. On the one hand, the HFC train has a shorter cruising time than the diesel train. On the other hand, as said above, the power demand for the fuel cell train in the cruising stage is higher than for the others.

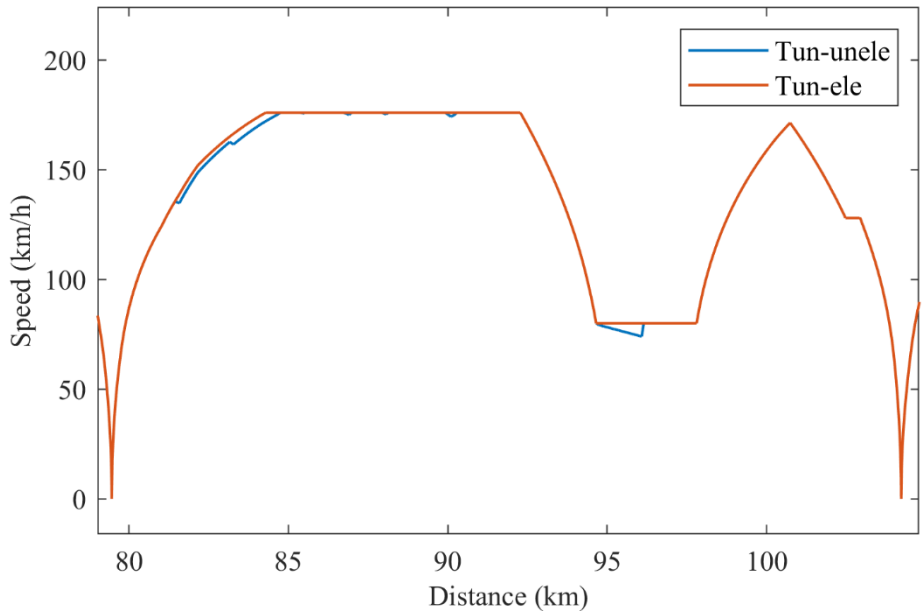

Figure 63 Velocity of electric trains on the fully electrified route (with or without tunnel electrification) between Bedford and Wellingborough

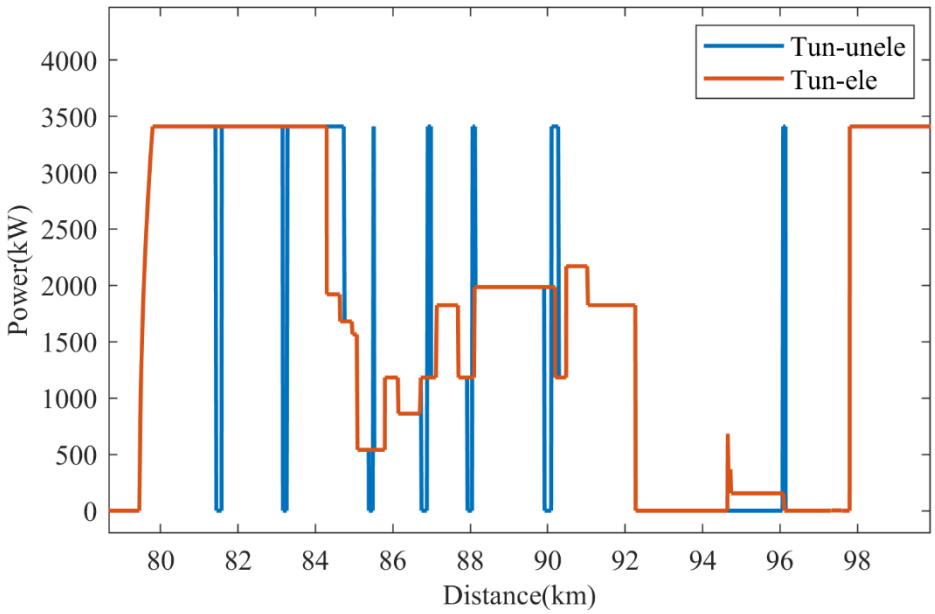

Figure 64 Overhead line power of electric trains on the electrified route between Bedford and Wellingborough

The speed differences between the two electrification scenarios are due to energy support in tunnels. There are nine tunnels located between Bedford and Wellingborough. The train should be in traction mode in the first seven tunnels and braking mode in the other two tunnels before Wellingborough. Velocity drops in unelectrified tunnels as can be seen in Figure 63. However, the drops are not significant. The most significant reduction inside a tunnel is in the Sharnbrook Tunnel, the seventh tunnel, where speed decreases by 6 km/h, from 80 to 74 km/h. Those tiny drops in speed make the journey time in the non-electrified tunnel scenario slightly longer than for the electrified tunnel scenario, by less than 19 s as shown in Table 17. Although the electric train without tunnel electrification are 19 seconds slower than the full electrification electric train, it is still 24 seconds faster than the benchmark train. Due to speed drops in tunnels, after leaving the unelectrified tunnel and connecting with an overhead line, the train gains maximum power instead of balanced cruising power as shown in Figure 64 and then speeds up to the balance speed as shown in Figure 63.

6.7.3 Optimal train and algorithm comparison

6.7.3.1 Comparison of optimisation processes

As the variables and constraints described in Section 6.6.2 show, the optimisation's accuracy requirement is high. The battery and HFC precision are set as 1 Watt, and for the route rebuilding length for both regular routes and tunnels, the precision is set as 1 metre. According to the maximum and minimum constraints and the precisions above, there are around 860 million possible solutions in this optimisation. It cost around 2 seconds to compute one return journey from London St. Pancras to Leicester. Hence, it takes over 54 years to complete the entire plan with the Brute Force algorithm and it is definitely impossible for an optimisation study. In this case, only PSO and GA are employed in this study. The optimisation progress is shown in Figure 65:

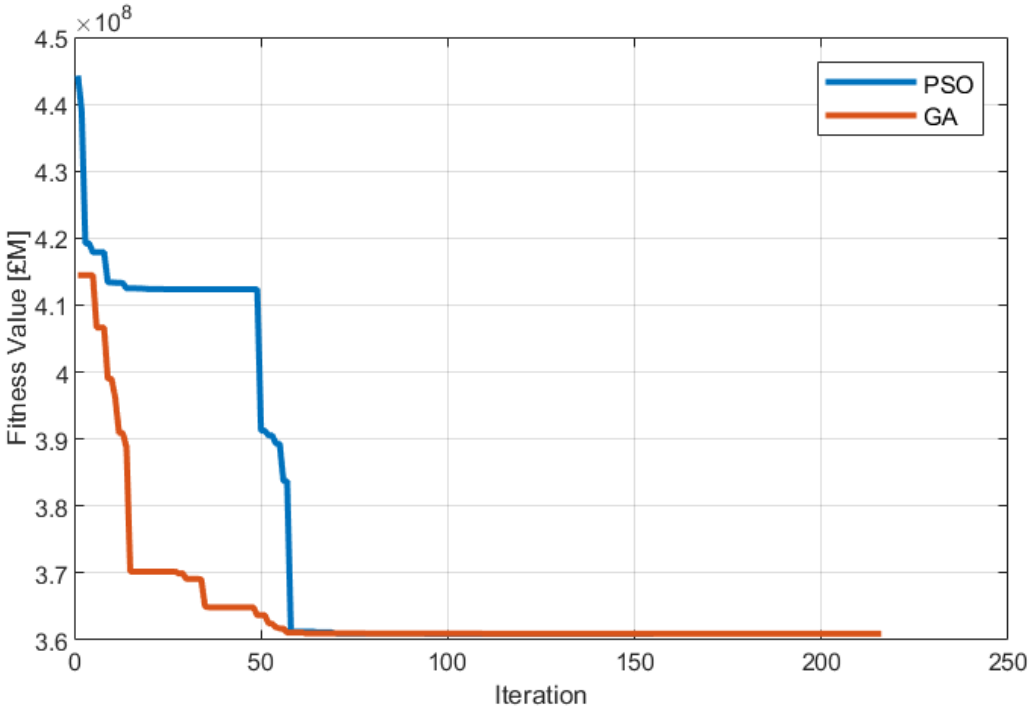

Figure 65 Optimisation progress

The figure above illustrates that both the Genetic Algorithm (GA) and Particle Swarm Optimisation (PSO) strategies can converge on the fitness function, yielding similar results. In this optimisation, GA converges faster than PSO. However, PSO stopped at 155 iterations, which is quicker than GA's 215 iterations, even when the same stopping conditions were applied. Moreover, there is a slight difference in the optimisation results of the two algorithms, with a variance of only 0.00166% based on the PSO result. By GA, the resulting fitness value is 360,925,000, while by PSO, it is 360,919,000. This indicates that the local optimum solution presents challenges for GA optimisation. The next section will describe the optimum plan generated by the PSO algorithm.

6.7.3.2 Analysis of optimisation results

Figure 66 shows the velocity curve of the optimal train for a two-direction run. According to the result optimised by adaptive PSO, the optimal train has an 800 kW battery pack installed

onboard without any HFC. Besides that, the electrification of the normal route is extended for another 53.35 km before Market Harborough without any extra electrification for the tunnels. At the beginning of the electrified route, the battery pack starts charging from the overhead line from an SOC of 20%, the initial SOC. It releases energy in the non-electrified tunnels to keep the traction system in operation as shown in Figure 67. The route is still unelectrified between Market Harborough and Leicester. There is a self-traction system on the train so that the train can run back using the fuel cell and battery pack. The final journey time is 9340 s, the same as for the diesel train. The train operation is not getting slower because the delay penalty is too high, and the energy cost saving cannot cover the time penalty.

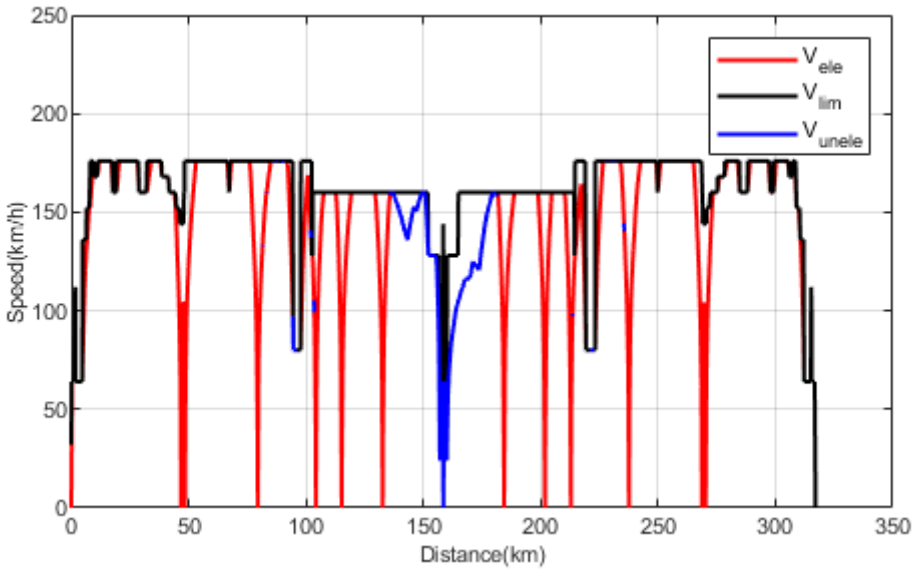

Figure 66 Velocity of the optimal train in up and down directions

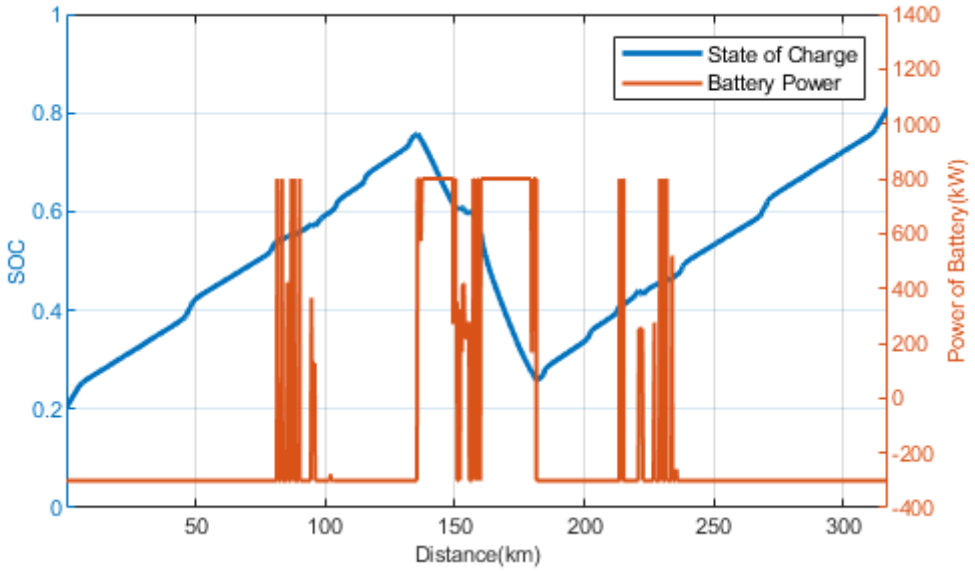

Figure 67 Optimal train battery pack SOC

Due to the absence of a fuel cell, the optimal train relies solely on electricity from the overhead line and its battery. Observing Figure 67 and Figure 68, it's clear that the battery pack consistently charges during the electrified route, but never charged over 0.93 state of charge. Almost all the SOC status are between 20% to 80%, keeping the battery on fast constant current charging stage. Within the tunnel between Bedford and Market Harborough, the train's traction system draws energy from the battery pack, leading to a decrease in SOC. However, upon exiting the tunnel, the battery begins to charge again. As the train approaches the terminal station, traveling on an unelectrified route, the SOC of the battery pack declines more rapidly due to the long distance powered solely by the battery. Nevertheless, the train engages electrical braking before arriving at the station. In Figure 68, it is evident that while operating between 150 km and 158 km, the battery remains in a charging state for most of the time. Subsequently, it resumes charging from the overhead line once it returns to the electrified route. At the completion of the entire route, the battery pack is charged to a high level.

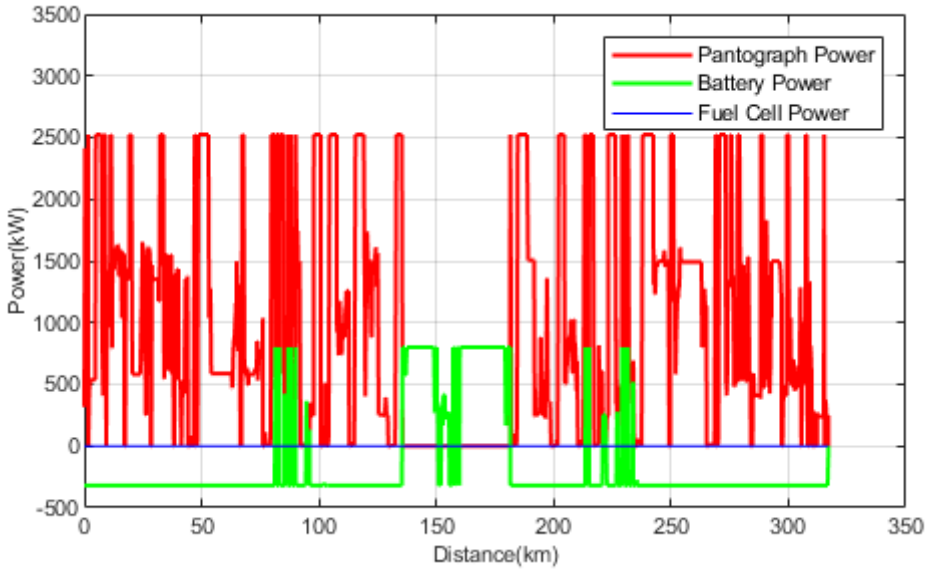

Figure 68 Optimal train battery pack and pantograph power

Table 18 Optimisation results

Train/route plan	**Initial cost [£M]**	**Lifetime energy cost [£M]**	**Replacement cost [£M]**	**Time penalty [£M]**	**Fitness value [£M]**	**Cost saving**
Benchmark diesel train	0	554.37	0	0	554.37	0
Hydrogen train	9.36	835.15	5.99	2.00	852.50	−53.78%
Full electrification (except tunnels)	275.92	143.29	0	0	419.20	24.38%
Full electrification	365.02	143.48	0	0	508.49	8.28%
Optimal train	194.02	160.47	1.87	4.56	360.92	34.90%

Table 18 shows the cost detail and fitness value for all scenarios. The HFC train has the lowest initial cost in the list of converted trains as there are no route rebuilding fees; The HFC train has a high energy cost because of the high price of hydrogen and the energy consumption, although it uses less fuel energy than a diesel train. Moreover, the extra weight of the HFC train produces its time penalty even with the same power output. Because of the lighter train bodyweight, the two full electrification scenarios take less time and are faster than the diesel

trains. Although the train performance is almost the same, there is a considerable cost difference between the two electrification scenarios. From a cost point of view, train conversion cost and energy cost are nearly the same. However, investment in tunnel electrification is too expensive: 65.71% of the total cost of the route with no tunnel electrification is for electrification infrastructure; that percentage for full electrification, including tunnels, is even higher at 71.69%. The extra cost of tunnel electrification, extending the normal double-track route for another 25 km, is around £89 million. The route for the optimal train is still discontinuously electrified. Hence the initial cost is smaller than for full electrification. Also, its energy cost is not much higher than for the full electrification scenarios, so the total cost and fitness value are extremely low on the list. Hence, these three plans with electrification have a much higher initial cost, but the energy cost is relatively low, so the total cost is less than for the hydrogen train.

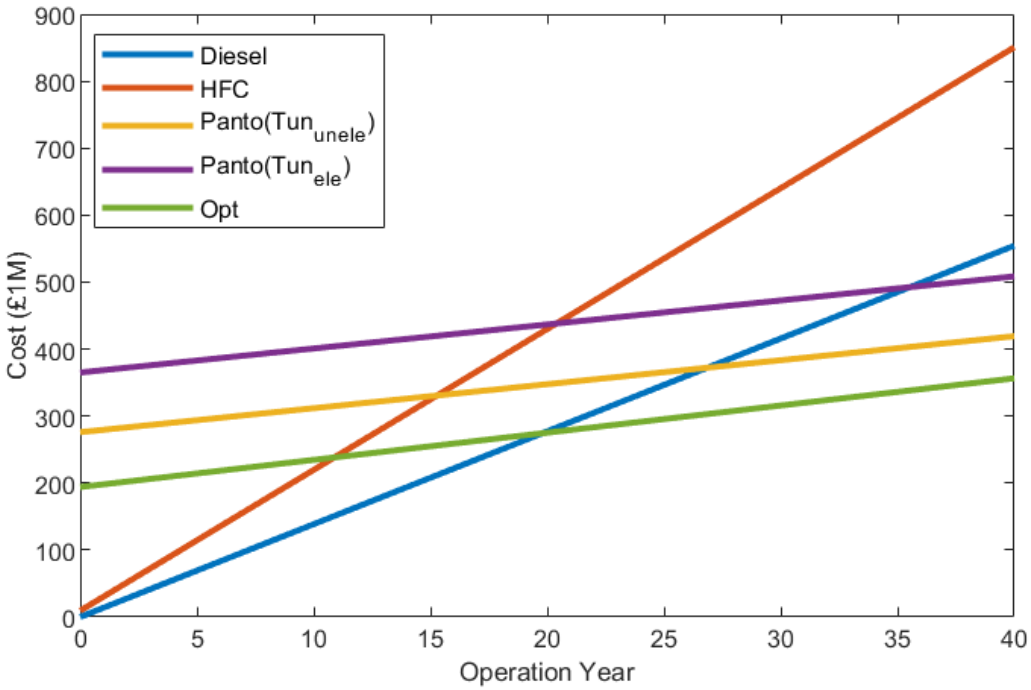

Figure 69 Total cost without energy price change in 40 years

Figure 69 shows the cost accumulation of the different scenarios over the entire 40 years. Calculating costs using current energy prices, the optimal train is the most economical after 20 years of operation. Diesel fuel is currently much cheaper than hydrogen, so the annual operation cost, including energy and maintenance costs, for a diesel train is less than for an HFC train. The initial investment cost for electrification is also too high, though the subsequent energy cost is much lower than for a fuel train.

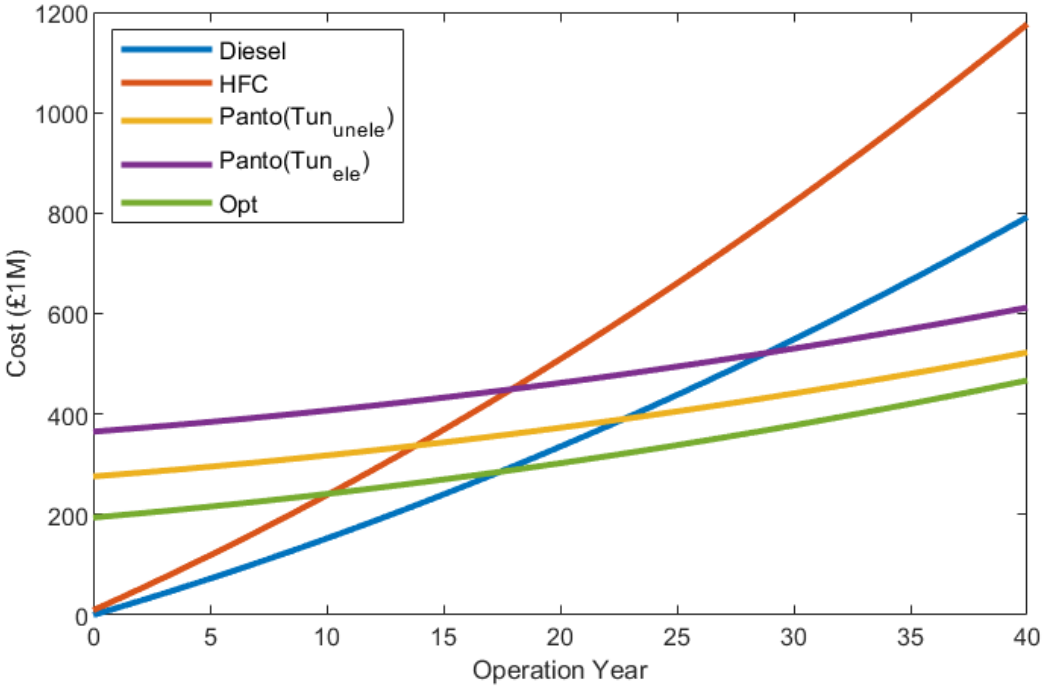

Figure 70 Total cost with energy price changes in 40 years

Table 19 Final cost after energy price changes

Train	**Final cost [£M]**
Benchmark diesel train	792.19
Hydrogen train	1176.2
Full electrification (except tunnels)	522.59

Full electrification	612.02
Optimal train	472.14

From 1996 to 2020, diesel prices in the UK increased from £0.58 per litre to £1.25 per litre, whereas electricity prices have risen about 6% per year since 2000 [77-79]. According to a prediction study, hydrogen prices have only increased by 2.2% annually since 2015[81]. To unify the start year of each kind of energy price change rate, the energy base price is chosen as 2020. In this situation, diesel, electricity, and hydrogen price change rates are 2.2%, 3.7%, and 2%, respectively. After considering the fuel price change, the cost accumulation is shown in Figure 70, and the estimated final cost of each scenario is listed in Table 19. Even though hydrogen has the lowest energy rise during the following years, its absolute fitness value is exceptionally high, 19% higher than the benchmark diesel train. The main reason is that the base hydrogen fuel price limits the HFC train economically. According to the price prediction, hydrogen fuel is £0.54 per kWh, whereas diesel fuel is £0.24 per kWh after 40 years. Although electricity has a higher price increase rate, the two scenarios with extended electrification did not profit less than before the energy price changes due to low energy consumption. At the same time, the optimal train which redesigned according to the optimisation result is still the best among those trains—40.4% less cost than the diesel train.

6.7.4 Optimisation combined with energy price changes

In the previous optimisation strategy, published in the journal paper ‘Cost optimization of multi-mode train conversion for discontinuously electrified routes’, the optimising fitness function is separated from the energy changes. The author has added the energy price changes into the fitness function as the final cost function in this section. Furthermore, it has been optimised by the PSO method. Figure 71 shows the progress of optimisation, and the new result

shows that the previous optimal solution is still optimal after considering the energy price changes in the fitness function.

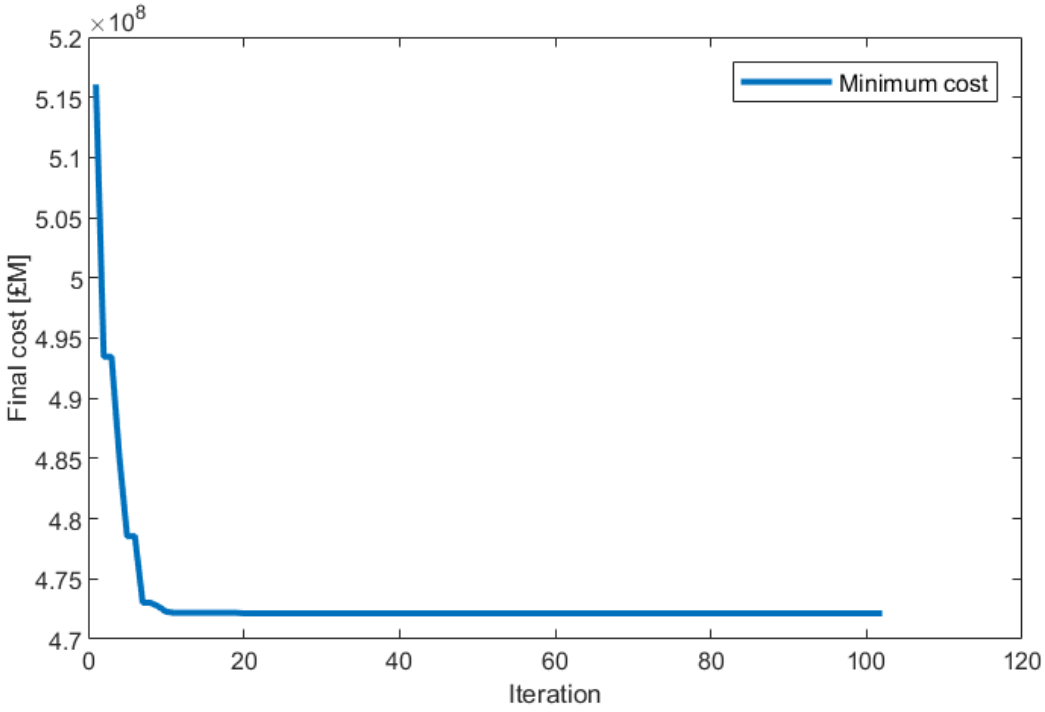

Figure 71 PSO final cost optimisation after price changes

6.7.5 Future probability of HFC trains

The foremost hindrance to the widespread use of Hydrogen Fuel Cell (HFC) trains lies in the lofty cost of hydrogen fuel. To render HFC trains a feasible component in an optimal multi-mode transport framework, it is imperative to curtail hydrogen fuel prices to about 74.07% of their existing value. Achieving a 29% reduction in these costs might yield advantages surpassing those offered by electrification, thus spotlighting the important need for diminishing the expenses associated with hydrogen fuel for the adoption of HFC trains.

6.8 Conclusion

This chapter explores the cost-effective optimisation of multi-mode trains on routes with intermittent electrification. It investigates various strategies for power supply under different

operational conditions. This section utilises advanced optimisation methods, including Particle Swarm Optimisation and Genetic Algorithms, to identify the most economical approaches. A case study is included to demonstrate these techniques in a practical context, providing a comparative analysis of different optimisation strategies and their outcomes. This case study of the transformation of Class 222 trains and route reconstruction from London St. Pancras to Leicester has been conducted. The comparison between different energy powered train evaluation can validate that the ideal train conversion and route reconstruction plan cost 34.9% less than the ecologically damaging diesel train with a stable energy price. After accounting for changes in energy prices, electric trains are more competitive in low-energy scenarios, while fuel trains will experience a significant rise in energy expenses. The optimal train achieves a cost saving of 40.4%. Because tunnel electrification is prohibitively expensive compared to that of conventional track, there is now no need to electrify small tunnels. If the introductory price of hydrogen can be reduced considerably, the HFC train can be competitive with other ways of upgrading. Other variables such as differences in traffic demand and headway, and traffic management will be addressed as optimisation variables in future studies. This chapter underscores the uniqueness of the research by applying these complex algorithms to a tangible railway scenario, contributing novel insights into cost-effective strategies for railway decarbonisation.

7 Conclusion, contributions and future work

7.1 Conclusions

This paper has made a journey through many different areas of railway system decarbonisation, which is a very important topic in engineering nowadays. Each chapter has built upon the last, contributing valuable insights into sustainable railway transportation. From developing new simulation tools to conducting economic analyses, these chapters collectively offer a full understanding of the challenges and possibilities in modern railway systems. The summaries that follow provide overview of chapters, highlighting the significant findings and advancements made.

Chapter 3 introduces a significant advancement with the development of the Train Performance Simulator (TPS). This tool, key for simulating various railway power systems like diesel engines, hydrogen fuel cells, and battery packs, enhances understanding of their operational dynamics. The TPS's detailed simulations provide important insights into the efficiency and environmental impact of these power systems. Its ability to accurately model different power sources marks a obvious leap in railway system analysis, offering a robust platform for future sustainable railway transport research.

Chapter 4 shows the economic aspects of upgrading railway power systems. The chapter outlines the total costs and the methodologies for their determination, linking the research to practical financial scenarios. A case study on cost assessment and energy cost analysis provides tangible examples of the economic implications of green power technologies in railways. This economic evaluation is essential in understanding the financial viability of adopting sustainable railway technologies, balancing economic considerations with environmental benefits.

Chapter 5 presents an in-depth sensitivity analysis using local (LSA) and global (GSA) methods. The analysis is vital in identifying key parameters that significantly affect railway

power system performance and efficiency. A case study comparing sensitivity levels between overhead line and hydrogen fuel cell trains pinpoints critical parameters for future optimisation. This rigorous sensitivity analysis is a major contribution to railway system optimisation, identifying essential parameters that influence system performance and guiding future enhancements in railway power system design.

Chapter 6 focusing on the optimisation of multi-mode railway trains, this chapter discusses the impact of different energy consumption modes on system efficiency and cost-effectiveness. The multi-mode train energy management system approach analysed here is key to understanding the complexities of optimising systems that incorporate various power technologies. This approach to optimisation demonstrates a deep understanding of the interactions between different power supply methods, guiding future efforts towards more cost-effective and efficient railway systems.

In summary, this thesis makes a meaningful contribution to the field of engineering, particularly in sustainable railway systems. The research across these chapters not only deepens theoretical understanding but also presents practical approaches and tools that can be applied in railway scenarios. The work in this thesis paves a path for future innovations in railway decarbonisation, setting a foundation for ongoing research and development. As we look forward, the findings and methodologies outlined in this work will prove invaluable for future engineering efforts aimed at making railway transportation more sustainable and efficient.

7.2 Main contributions and innovations

This thesis introduces several significant contributions and innovations in the field of sustainable railway transportation, specifically in the context of decarbonisation. Chapter 3 presents a major advancement with the development of the TPS, a tool that innovatively integrates multiple power systems for railway modelling. This chapter's contribution is the key

in enhancing the simulation of complex modern trains and their various power systems, including diesel engines, hydrogen fuel cells, and battery packs.

Chapter 4 contributes by establishing a detailed framework for assessing the economic impact of railway power system upgrades, integrating theoretical models with practical scenarios through a case study. This approach effectively bridges the gap between theoretical economic analysis and tangible applications, providing a nuanced understanding of the economic implications of greener railway systems.

In Chapter 5, the focus shifts to a detailed sensitivity analysis of railway parameters. The chapter contributes by using local and global sensitivity analysis methods to identify key factors influencing railway power system performance. The innovation here lies in the comparative case studies that apply these methods, offering deep insights into the relative impacts of different power technologies and aiding in the identification of critical parameters for system optimisation.

Chapter 6 addresses the optimisation of multi-mode railway trains, significantly contributing to cost-effective modernisation strategies. The chapter is obvious for its innovative application of adaptive particle swarm optimisation techniques in a practical case study. This approach demonstrates the effectiveness of optimisation techniques in railway systems and provides valuable insights into potential energy savings and efficiency gains.

Collectively, these chapters advance the field of railway engineering by providing new tools, methods, and insights that enhance the understanding, analysis, and optimisation of railway power systems. The thesis represents a significant contribution to the pursuit of sustainable and efficient railway transportation.

7.3 Recommendations

There are five recommendations according to the overall research:

- **Development of Multi-Mode Train Simulator:** Advance railway technology by developing a multi-mode train simulator for accurate calculations of energy consumption and effective management of power systems in various operational scenarios.
- **Incorporation of Economic Analysis:** Integrate thorough economic analyses, focusing on long-term expenses including replacement of diesel parts, installation of new power systems, and maintenance, to comprehend the financial implications of transitioning to green power in trains.
- **Utilisation of Advanced Optimisation Methods:** Use advanced optimisation techniques like the Genetic Algorithm and Particle Swarm Optimisation for optimal electrification lengths and power system capacities, reducing costs and enhancing eco-friendliness in railway systems.
- **Adoption of Various Green Power Technologies:** Adopt a range of green power technologies, such as electrification, hydrogen fuel cells, and batteries, to achieve obvious cost reductions and environmental benefits, as illustrated in the case study from London St. Pancras to Leicester.
- **Future Potential of Hydrogen-Powered Trains:** Acknowledge the future role of hydrogen-powered trains in decarbonisation strategies, considering their cost-effectiveness may improve with the declining price of hydrogen.

7.4 Limitations

Simulation Model Realism Limits: The TPS, though a significant development in the study, may not perfectly mirror the full complexity of actual train operations. Practical railway

environments involve numerous unpredictable factors like varying weather conditions, track irregularities, and unexpected operational challenges. These elements can be difficult to replicate accurately in a simulation, leading to potential gaps between simulated outcomes and real-world performance. Also, some of the assumed data are not fit well the practical train retraction. This limitation is important as it may affect the direct applicability of the simulation results to actual railway systems.

Economic Analysis Boundaries: The economic analysis provided in the thesis, while comprehensive, is constrained by its scope and the assumptions made. Economic predictions are inherently uncertain and can be influenced by a range of external factors not fully captured in the study. These factors include fluctuating market conditions, changes in government policies affecting the railway sector, and unforeseen advancements in railway technology that could alter cost structures. Thus, while the economic analysis offers valuable insights, its long-term applicability might be limited by these changing external conditions.

Sensitivity Analysis Scope: The sensitivity analysis conducted is an essential part of understanding the dynamics of railway power systems. However, this analysis might be limited by the selection of parameters and the range of conditions tested. In the real world, railway systems are influenced by a vast array of factors, including highly dynamic operational conditions and evolving technological landscapes. As such, the sensitivity analysis might not account for all possible variables or future developments in railway technology, which could impact the robustness of the conclusions drawn.

Generalisability of Research Findings: The research, particularly the case studies like the one focusing on the route from London St. Pancras to Leicester, might have limited applicability in different geographical or operational contexts. Railway systems vary greatly across regions due to differences in infrastructure, regulatory environments, and user demands.

Therefore, the findings and recommendations of the thesis, while highly relevant to the studied contexts, might not be directly transferable to other railway systems with different characteristics or in different countries. Plus, when analysing senstivity index of tram, the only method to analysis train upgrading is to suppose the electric tram was diesel-powered. However, it is not as good as analysing a initial diesel tram.

Rapid Technological Evolution: The railway industry is experiencing rapid technological advancements, particularly in the areas of power systems and sustainable energy sources. While the thesis provides a snapshot of the current state of technologies like battery efficiency and hydrogen fuel cells, these technologies are evolving at a fast pace. This rapid development could potentially make some of the study's findings less relevant over time, as newer, more efficient technologies emerge. Staying abreast of these technological changes is important for ensuring the long-term relevance of the research.

Data and Methodological Constraints: The research may also face limitations related to the data used and the chosen methodological approaches. The availability and accuracy of data are important for sound analysis, and any limitations in data quality can impact the study's conclusions. Furthermore, the methodologies employed, including the assumptions and models used, might have their constraints, which could affect the reliability and validity of the research outcomes.

7.5 Suggestions for future work

To solve or break those limitations in previous section, there are some suggestions for future work:

Improving Simulation Realism: Future work could look at making the TPS more like real life. This means adding more varied weather, different track conditions, and unexpected

situations into the simulation. The goal is to make the simulation results closer to what happens on real trains.

More Flexible Economic Models: Later studies might develop economic models that better handle changes over time, like shifts in the market, new government policies, and advances in technology. Using models that can predict future economic trends would make the economic analysis stronger and more adaptable.

Broader Sensitivity Analysis: It would be good to include more factors in the sensitivity analysis. Future research could explore more variables and different kinds of operational scenarios, especially with new technologies coming in. This would make the sensitivity analysis more thorough and useful.

Wider Range of Case Studies: To make the findings more widely applicable, future studies could use case studies from different places and with different types of railway systems. This would help understand how the findings work in various situations and under different rules.

Keeping Up with Technology Changes: Ongoing research should keep an eye on the latest in railway power technologies, like batteries and hydrogen fuel cells. Future work could focus on how new and emerging technologies work in real train settings.

Better Data and Methods: Future work should try to get better and more detailed data. Improving how data is collected and looking at more sources can make the research results more accurate and reliable. Also, refining how the research is done, like trying different ways of modelling, could give more detailed and reliable insights.

Working Across Different Fields: Collaborating with experts in other areas like environmental science, economics, and policymaking could add a lot to future research. This

kind of teamwork can give a more complete view of the challenges in making train systems more sustainable.

7.6 Further Research Topics

According to the research in this thesis, there are some topics can be furture reseached:

Enhancing Electrical Energy Storage for Railway Systems: This research would explore improvements in electrical energy storage technologies for railway applications. It would focus on developing advanced battery systems with higher energy densities, better charging capabilities, and longer life spans. The aim is to create storage solutions that are more efficient and durable, tailored to meet the high demands of railway transportation.

Energy Harvesting Technologies in Railway Systems: Investigating the potential of energy harvesting technologies in railways. This topic would focus on the development and integration of systems that can capture and utilise energy from various sources, such as solar panels or kinetic energy from braking systems. The goal is to reduce reliance on external power sources and enhance the overall energy efficiency of railway operations.

Smart Grid Integration in Railway Power Systems: This research would examine how railway systems can be integrated into smart grid networks. It would look into ways for railways to not only draw power from the grid but also contribute back, especially through regenerative braking systems. The study would also consider how railway operations can be optimised for effective load balancing and demand response in the context of a smart grid.

Advanced Battery Management Systems for Hybrid Railway Vehicles: Focusing on the development of sophisticated battery management systems for hybrid trains. This research aims to design Battery Management Systems that optimally control battery charging and discharging,

enhancing the life and efficiency of batteries in hybrid railway vehicles, and ensuring their effective integration with other power sources.

8 References

[1] "National Travel Survey England 2022 Main Results." Department for Transport. https://assets.publishing.service.gov.uk/media/64ef09d0da845100146323f7/nts-2022-factsheet.pdf (accessed 20 Sep, 2023).

[2] D. f. Transport, "Decarbonising Transport Setting the Challenge," 2020. Accessed: 28 August 2021. [Online]. Available: https://assets.publishing.service.gov.uk/media/5fa03423d3bf7f03a7a99151/decarbonising-transport-setting-the-challenge.pdf

[3] E. I. S. Department for Business, "Greenhouse gas reporting: conversion factors 2019," 4 June 2019.

[4] D. f. Transport, "Rail freight transport strategy," 2016.

[5] E. a. I. S. Department for Business, "2020 UK Greenhouse Gas Emissions, Final Figures," 2022.

[6] "IMechE rail report backs hydrogen and electrification combination." https://www.theengineer.co.uk/imeche-report-hydrogen-electrification/ (accessed 2th July, 2020).

[7] R. I. Association, "RIA Electrification Cost Challenge," Railway Industry Association, 2019. Accessed: 17th Dec 2020. [Online]. Available: https://www.riagb.org.uk/RIA/Newsroom/Stories/Electrification_Cost_Challenge_Report.aspx

[8] T. Kamel, Z. Tian, M. Zangiabadi, N. Wade, V. Pickert, and P. Tricoli, "Optimized Localization for the inverting substation to maximize the braking efficiency of the DC railways," in *2021 IEEE 15th International Conference on Compatibility, Power Electronics and Power Engineering (CPE-POWERENG)*, 14-16 July 2021 2021, pp. 1-5, doi: 10.1109/CPE-POWERENG50821.2021.9501220.

[9] S. Su, X. Yan, K. Agbossou, R. Chahine, and Y. Zong, "Artificial intelligence for hydrogen-based hybrid renewable energy systems: A review with case study," *Journal of Physics: Conference Series*, vol. 2208, no. 1, p. 012013, 2022/03/01 2022, doi: 10.1088/1742-6596/2208/1/012013.

[10] E. M. Washing and S. S. Pulugurtha, "Well-To-Wheel analysis of electric and hydrogen light rail," *Journal of Public Transportation*, vol. 18, no. 2, p. 6, 2015.

[11] J. Silmon and S. Hillmansen, "Investigating discontinuous electrification and energy storage on the northern Trans-Pennine route," in *IET Conference on Railway Traction Systems (RTS 2010)*, 13-15 April 2010 2010, pp. 1-9, doi: 10.1049/ic.2010.0019.

[12] A. Hoffrichter, J. Silmon, F. Schmid, S. Hillmansen, and C. Roberts, "Feasibility of discontinuous electrification on the Great Western Main Line determined by train simulation," *Proceedings of the Institution of Mechanical Engineers*, p. 11, 2013, doi: 10.1177/0954409712461341.

[13] Z. Tian, "System energy optimisation strategies for DC railway traction power networks," PhD, Department of Electronic, University of Birmingham, 2017.

[14] H. o. Commons, "Trains fit for the future?," 16 March 2021. Accessed: 30 Oct 2021. [Online]. Available: https://committees.parliament.uk/publications/5179/documents/52006/default/

[15] D. f. Transport, "DecarbonisingTransport A Better, Greener Britain," 2021. Accessed: 2nd Aug 2022. [Online]. Available: https://assets.publishing.service.gov.uk/media/610d63ffe90e0706d92fa282/decarbonising-transport-a-better-greener-britain.pdf

[16] K. Ghoseiri, F. Szidarovszky, and M. J. Asgharpour, "A multi-objective train scheduling model and solution," *Transportation research part B: Methodological,* vol. 38, no. 10, pp. 927-952, 2004.

[17] S. O. S. P. (FNPO), "Traction Decarbonisation Network Strategy – Interim Programme Business Case," 2020. Accessed: 15th Feb 2021. [Online]. Available: https://www.networkrail.co.uk/wp-content/uploads/2020/09/Traction-Decarbonisation-Network-Strategy-Interim-Programme-Business-Case.pdf

[18] P. Salvador, P. Martínez, I. Villalba, and R. Insa, "Modelling energy consumption in diesel multiple units," *Proceedings of the Institution of Mechanical Engineers, Part F: Journal of Rail and Rapid Transit,* vol. 232, no. 5, pp. 1539-1548, 2018/05/01 2017, doi: 10.1177/0954409717737226.

[19] M. Saadat, M. Esfahanian, and M. H. Saket, "Reducing fuel consumption of diesel-electric locomotives using hybrid powertrain and fuzzy look-ahead control," *Proceedings of the Institution of Mechanical Engineers, Part F: Journal of Rail and Rapid Transit,* vol. 231, no. 4, pp. 406-418, 2017/04/01 2016, doi: 10.1177/0954409716631010.

[20] A. Pyper and P. S. Heyns, "Evaluating a distributed regenerative braking system for freight trains," *Proceedings of the Institution of Mechanical Engineers, Part F: Journal of Rail and Rapid Transit,* vol. 233, no. 8, pp. 844-856, 2019.

[21] L. Liudvinavičius and V. Jastremskas, "Modernization of Diesel-electric Locomotive 2M62 and TEP-70 Locomotives with Respect to Electrical Subsystem," *Procedia Engineering,* vol. 187, pp. 272-280, 2017/01/01/ 2017, doi: https://doi.org/10.1016/j.proeng.2017.04.375.

[22] S. D'Arco, L. Piegari, and P. Tricoli, "Comparative Analysis of Topologies to Integrate Photovoltaic Sources in the Feeder Stations of AC Railways," *IEEE Transactions on Transportation Electrification,* vol. 4, no. 4, pp. 951-960, 2018, doi: 10.1109/TTE.2018.2867279.

[23] T. Din, Z. Tian, K. Li, S. Hillmansen, and C. Roberts, "Operation and energy evaluation of diesel and hybrid trains with smart switching controls," *Control Engineering Practice,* vol. 116, p. 104935, 2021, doi: 10.1016/j.conengprac.2021.104935.

[24] "Austria's ÖBB completes three-month hydrogen train passenger trials." https://www.railway-technology.com/news/austria-obb-hydrogen-train-testing-trials/ (accessed 28th Nov, 2021).

[25] A. Hoffrichter, S. Hillmansen, and C. Roberts, "Conceptual propulsion system design for a hydrogen-powered regional train," *IET Electrical Systems in Transportation,* vol. 6, no. 2, pp. 56-66, 2016, doi: 10.1049/iet-est.2014.0049.

[26] S. Reimann, F. Jost, and P. Gratzfeld, "Multiphysics Simulation of a Battery Electric Train Operation," presented at the TRA2020 Book of Abstracts, 2020.

[27] M. A. Hannan, M. M. Hoque, A. Mohamed, and A. Ayob, "Review of energy storage systems for electric vehicle applications: Issues and challenges," (in English), *Renewable Sustainable Energy Rev,* Review vol. 69, pp. 771-789, 2017, doi: 10.1016/j.rser.2016.11.171.

[28] Ş. İ *et al.*, "Energy Management of a Smart Railway Station Considering Regenerative Braking and Stochastic Behaviour of ESS and PV Generation," *IEEE Transactions on Sustainable Energy,* vol. 9, no. 3, pp. 1041-1050, 2018, doi: 10.1109/TSTE.2017.2759105.

[29] J. A. Aguado, A. J. S. Racero, and S. d. l. Torre, "Optimal Operation of Electric Railways With Renewable Energy and Electric Storage Systems," *IEEE Transactions on Smart Grid*, vol. 9, no. 2, pp. 993-1001, 2018, doi: 10.1109/TSG.2016.2574200.

[30] C. Wu, W. Zhang, S. Lu, Z. Tan, F. Xue, and J. Yang, "Train Speed Trajectory Optimization With On-Board Energy Storage Device," *IEEE Transactions on Intelligent Transportation Systems*, vol. 20, no. 11, pp. 4092-4102, 2019, doi: 10.1109/TITS.2018.2881156.

[31] V. A. Kleftakis and N. D. Hatziargyriou, "Optimal Control of Reversible Substations and Wayside Storage Devices for Voltage Stabilization and Energy Savings in Metro Railway Networks," *IEEE Transactions on Transportation Electrification*, vol. 5, no. 2, pp. 515-523, 2019, doi: 10.1109/TTE.2019.2913355.

[32] Z. Yang, Z. Yang, H. Xia, and F. Lin, "Brake Voltage Following Control of Supercapacitor-Based Energy Storage Systems in Metro Considering Train Operation State," *IEEE Transactions on Industrial Electronics*, vol. 65, no. 8, pp. 6751-6761, 2018, doi: 10.1109/TIE.2018.2793184.

[33] N. Ghaviha, M. Bohlin, C. Holmberg, and E. Dahlquist, "Speed profile optimization of catenary-free electric trains with lithium-ion batteries," *Journal of Modern Transportation*, vol. 27, no. 3, pp. 153-168, 2019/09/01 2019, doi: 10.1007/s40534-018-0181-y.

[34] t. H. o. Commons, "Rail infrastructure investment: Government and Office of Rail and Road Responses to the Committee's Fourth Report," 19 September 2018 2018. Accessed: 13th 10 2019. [Online]. Available: https://publications.parliament.uk/pa/cm201719/cmselect/cmtrans/1557/155702.htmwww.parliament.uk/transcom

[35] M. S. A. Chowdhury, K. A. A. Mamun, and A. M. Rahman, "Modelling and simulation of power system of battery, solar and fuel cell powered Hybrid Electric vehicle," in *2016 3rd International Conference on Electrical Engineering and Information Communication Technology (ICEEICT)*, 22-24 Sept. 2016 2016: IEEE, pp. 1-6, doi: 10.1109/CEEICT.2016.7873126.

[36] T. Din and S. Hillmansen, "Energy consumption and carbon dioxide emissions analysis for a concept design of a hydrogen hybrid railway vehicle," *IET Electrical Systems in Transportation*, vol. 8, no. 2, pp. 112-121, 2018, doi: 10.1049/iet-est.2017.0049.

[37] M. Walters, A. Kuhlmann, and J. Ogrzewalla, "Fuel cell range extender for battery electric vehicles," in *2015 International Conference on Electrical Systems for Aircraft, Railway, Ship Propulsion and Road Vehicles (ESARS)*, 3-5 March 2015 2015: IEEE, pp. 1-6, doi: 10.1109/ESARS.2015.7101509.

[38] D. W. Gao, C. Mi, and A. Emadi, "Modeling and Simulation of Electric and Hybrid Vehicles," *Proceedings of the IEEE*, vol. 95, no. 4, pp. 729-745, 2007, doi: 10.1109/JPROC.2006.890127.

[39] A. S. Abdelrahman, Y. Attia, K. Woronowicz, and M. Z. Youssef, "Hybrid Fuel Cell/Battery Rail Car: A Feasibility Study," *IEEE Transactions on Transportation Electrification*, vol. 2, no. 4, pp. 493-503, 2016, doi: 10.1109/TTE.2016.2608760.

[40] M. Handwerker, J. Wellnitz, and H. Marzbani, "Comparison of hydrogen powertrains with the battery powered electric vehicle and investigation of small-scale local hydrogen production using renewable energy," *Hydrogen*, vol. 2 (2021), no. 1, pp. 76-100, 2021, doi: https://doi.org/10.3390/hydrogen2010005.

[41] O. Madovi, A. Hoffrichter, N. Little, S. N. Foster, and R. Isaac, "Feasibility of hydrogen fuel cell technology for railway intercity services: a case study for the Piedmont in

North Carolina," *Railway Engineering Science,* vol. 29, no. 3, pp. 258-270, 2021/09/01 2021, doi: 10.1007/s40534-021-00249-8.

[42] J. P. Torreglosa, P. García, L. M. Fernández, and F. Jurado, "Predictive Control for the Energy Management of a Fuel-Cell–Battery–Supercapacitor Tramway," *IEEE Transactions on Industrial Informatics,* vol. 10, no. 1, pp. 276-285, 2014, doi: 10.1109/TII.2013.2245140.

[43] G. Meng, C. Wu, B. Zhang, F. Xue, and S. Lu, "Net Hydrogen Consumption Minimization of Fuel Cell Hybrid Trains Using a Time-Based Co-Optimization Model," *Energies,* vol. 15, no. 8, p. 2891, 2022. [Online]. Available: https://www.mdpi.com/1996-1073/15/8/2891.

[44] T. J. Harrison, W. J. B. Midgley, R. M. Goodall, and C. P. Ward, "Development and control of a rail vehicle model to reduce energy consumption and carbon dioxide emissions," *Proceedings of the Institution of Mechanical Engineers, Part F: Journal of Rail and Rapid Transit,* vol. 235, no. 10, pp. 1237-1248, 2021/11/01 2021, doi: 10.1177/0954409721993632.

[45] M. Li, M. Li, G. Han, N. Liu, Q. Zhang, and Y. Wang, "Optimization Analysis of the Energy Management Strategy of the New Energy Hybrid 100% Low-Floor Tramcar Using a Genetic Algorithm," *Applied Sciences,* vol. 8, no. 7, p. 1144, 2018. [Online]. Available: https://www.mdpi.com/2076-3417/8/7/1144.

[46] t. C. t. E. B. s. Railway, "Written evidence submitted by the Campaign to Electrify," May 2019. Accessed: 12th May 2021. [Online]. Available: https://committees.parliament.uk/writtenevidence/103103/html/

[47] ORR. "Rail Infrastructure and assets statistics." https://dataportal.orr.gov.uk/statistics/infrastructure-and-emissions/rail-infrastructure-and-assets/infrastructure-on-railways-table-252/ (accessed 10th May, 2023).

[48] Z. Tian, N. Zhao, S. Hillmansen, C. Roberts, T. Dowens, and C. Kerr, "SmartDrive: Traction Energy Optimization and Applications in Rail Systems," *IEEE Transactions on Intelligent Transportation Systems,* vol. 20, no. 7, pp. 2764-2773, 2019, doi: 10.1109/TITS.2019.2897279.

[49] Z. Tian *et al.*, "Energy evaluation of the power network of a DC railway system with regenerating trains," *IET Electrical Systems in Transportation,* vol. 6, no. 2, pp. 41-49, 2016, doi: 10.1049/iet-est.2015.0025.

[50] X. Zhao, B. Ke, and K. Lian, "Optimization of Train Speed Curve for Energy Saving Using Efficient and Accurate Electric Traction Models on the Mass Rapid Transit System," *IEEE Transactions on Transportation Electrification,* vol. 4, no. 4, pp. 922-935, 2018, doi: 10.1109/TTE.2018.2851785.

[51] X. Wang, Y. Luo, Y. Zhou, Y. Qin, and B. Qin, "Hybrid energy management strategy based on dynamic setting and coordinated control for urban rail train with PMSM," *IET Renewable Power Generation,* vol. 15, no. 12, pp. 2740-2752, 2021.

[52] D. Iannuzzi and P. Tricoli, "Speed-Based State-of-Charge Tracking Control for Metro Trains With Onboard Supercapacitors," *IEEE Transactions on Power Electronics,* vol. 27, no. 4, pp. 2129-2140, 2012, doi: 10.1109/TPEL.2011.2167633.

[53] A. Fernández-Rodríguez, A. P. Cucala, and A. Fernández-Cardador, "An Eco-Driving Algorithm for Interoperable Automatic Train Operation," *Applied Sciences,* vol. 10, no. 21, p. 7705, 2020. [Online]. Available: https://www.mdpi.com/2076-3417/10/21/7705.

[54] X. Wang, T. Tang, S. Su, X. Liu, and T. Ma, "Energy-efficient operation of multi-trains for metro systems with considering the regenerative energy," in *2018 International*

Conference on Intelligent Rail Transportation (ICIRT), 12-14 Dec. 2018 2018, pp. 1-5, doi: 10.1109/ICIRT.2018.8641563.

[55] K. Wang, H. Hu, J. Chen, J. Zhu, X. Zhong, and Z. He, "System-Level Dynamic Energy Consumption Evaluation for High-Speed Railway," *IEEE Transactions on Transportation Electrification*, vol. 5, no. 3, pp. 745-757, 2019, doi: 10.1109/TTE.2019.2934942.

[56] Z. Tian, P. Weston, N. Zhao, S. Hillmansen, C. Roberts, and L. Chen, "System energy optimisation strategies for metros with regeneration," *Transportation Research Part C: Emerging Technologies*, vol. 75, pp. 120-135, 2017/02/01/ 2017, doi: https://doi.org/10.1016/j.trc.2016.12.004.

[57] G. Zhang, Z. Tian, P. Tricoli, S. Hillmansen, Y. Wang, and Z. Liu, "Inverter Operating Characteristics Optimization for DC Traction Power Supply Systems," *IEEE Transactions on Vehicular Technology*, vol. 68, no. 4, pp. 3400-3410, 2019, doi: 10.1109/TVT.2019.2899165.

[58] M. Schenker, T. Schirmer, and H. Dittus, "Application and improvement of a direct method optimization approach for battery electric railway vehicle operation," *Proceedings of the Institution of Mechanical Engineers, Part F: Journal of Rail and Rapid Transit*, vol. 235, no. 7, pp. 854-865, 2021, doi: 10.1177/0954409720970002.

[59] C. Streuling, J. Pagenkopf, M. Schenker, and K. Lakeit, "Techno-Economic Assessment of Battery Electric Trains and Recharging Infrastructure Alternatives Integrating Adjacent Renewable Energy Sources," *Sustainability*, vol. 13, no. 15, p. 8234, 2021. [Online]. Available: https://www.mdpi.com/2071-1050/13/15/8234.

[60] B. Mellitt, C. J. Goodman, and R. I. M. Arthurton, "Simulator for studying operational and power-supply conditions in rapid-transit railways," *Proceedings of the Institution of Electrical Engineers*, vol. 125, no. 4, pp. 298-303. [Online]. Available: https://digital-library.theiet.org/content/journals/10.1049/piee.1978.0075

[61] A. Hoffrichter, P. Fisher, J. Tutcher, S. Hillmansen, and C. Roberts, "Performance evaluation of the hydrogen-powered prototype locomotive 'Hydrogen Pioneer'," *Journal of Power Sources*, vol. 250, pp. 120-127, 2014/03/15/ 2014, doi: https://doi.org/10.1016/j.jpowsour.2013.10.134.

[62] S. Farhad and A. Nazari, "Introducing the energy efficiency map of lithium-ion batteries," *International Journal of Energy Research*, vol. 43, no. 2, pp. 931-944, 2019, doi: https://doi.org/10.1002/er.4332.

[63] ORR. "Passenger Rail Usage Statistics." https://dataportal.orr.gov.uk/statistics/usage/passenger-rail-usage/passenger-journeys-table-125/ (accessed 2nd June, 2022).

[64] ORR. "Freight Rail Usage Statistics." https://dataportal.orr.gov.uk/statistics/usage/freight-rail-usage-and-performance/freight-moved-table-137-1/ (accessed 2nd June, 2022).

[65] O. R. Infrastructure, "Rail infrastructure and assets 2019-20," 2020. Accessed: 3rd Sep 2021. [Online]. Available: https://dataportal.orr.gov.uk/media/1842/rail-infrastructure-assets-2019-20.pdf

[66] H. Umarji, "Calculation of parameters of overhead power lines," *dostupno na https://fenix. tecnico. ulisboa. pt/downloadFile/395137455925/Resumo_ingles. pdf, preuzeto*, vol. 23, 2000.

[67] J. R. Carson, "Wave propagation in overhead wires with ground return," *The Bell System Technical Journal*, vol. 5, no. 4, pp. 539-554, 1926.

[68] A. Mariscotti and P. Pozzobon, "Measurement of the internal impedance of traction rails at audiofrequency," *IEEE Transactions on Instrumentation and Measurement*, vol. 53, no. 3, pp. 792-797, 2004.
[69] M. Vinţan, P. Mihu, and I. Borlea, "AC power lines impedances computational methods," *Journal of Sustainable Energy*, vol. 2, no. 2, 2011.
[70] T. Vu Phan and J. Tlusty, "The calculated methods of a frequency-dependent series impedance matrix of overhead transmission lines with a lossy ground for transient analysis problem," in *Large Engineering Systems Conference on Power Engineering, 2003*, 7-9 May 2003 2003, pp. 159-163, doi: 10.1109/LESCPE.2003.1204697.
[71] A. Payne, "THE AC RESISTANCE AND INDUCTANCE OF RAILS," 05/04 2021.
[72] Z. Tian *et al.*, "Modeling and simulation of DC rail traction systems for energy saving," in *17th International IEEE Conference on Intelligent Transportation Systems (ITSC)*, 8-11 Oct. 2014 2014, pp. 2354-2359, doi: 10.1109/ITSC.2014.6958067.
[73] A. M. Eltamaly, Y. Sayed, A.-H. M. El-Sayed, and A. N. A. Elghaffar, "Optimum power flow analysis by Newton raphson method, a case study," *Ann Fac Eng Hunedoara*, vol. 16, no. 4, pp. 51-58s, 2018.
[74] T. Kulworawanichpong, "Simplified Newton–Raphson power-flow solution method," *International journal of electrical power & energy systems*, vol. 32, no. 6, pp. 551-558, 2010.
[75] Z. He, L. Fang, D. Guo, and J. Yang, "Algorithm for power flow of electric traction network based on equivalent circuit of AT-fed system," *Xinan Jiaotong Daxue Xuebao/Journal of Southwest Jiaotong University*, vol. 43, pp. 1-7, 02/01 2008.
[76] T. Kamel *et al.*, "Development of a smart hybrid drive system with advanced logistics for railway applications," *International Journal of Hydrogen Energy*, 2023/02/17/ 2023, doi: https://doi.org/10.1016/j.ijhydene.2023.01.293.
[77] "Wholesale Electricity Price Guide." https://www.businesselectricityprices.org.uk/retail-versus-wholesale-prices/ (accessed 20 Nov, 2019).
[78] I. Tiseo. "Average price of diesel fuel in the United Kingdom (UK) from January 2015 and September 2019 (in pence per liter)." https://www.statista.com/statistics/299552/average-price-of-diesel-in-the-united-kingdom/ (accessed 15 Dec, 2019).
[79] M. Grubb and P. Drummond, "UK Industrial Electricity Prices: Competitiveness in a low carbon world," 2018.
[80] W. Evans. Energy Trends and Prices statistical release: 29 September 2022 [Online] Available: https://www.gov.uk/government/statistics/energy-trends-and-prices-statistical-release-29-september-2022
[81] N. A. Al-Mufachi and N. Shah, "The role of hydrogen and fuel cell technology in providing security for the UK energy system," *Energy Policy*, vol. 171, p. 113286, 2022/12/01/ 2022, doi: https://doi.org/10.1016/j.enpol.2022.113286.
[82] G. Smith. "How Long Do Trains Last?" https://vehiclehelp.com/how-long-do-trains-last/ (accessed 07th September, 2022).
[83] T. S. P. a. E. K. Scott F. Gorman, "The 'use-by date' for lithium-ion battery components," *Philosophical transactions of the royal society A*, 2019, doi: https://doi.org/10.1098/rsta.2018.0299. Royal Society.
[84] X. Xu, Z. Li, and N. Chen, "A Hierarchical Model for Lithium-Ion Battery Degradation Prediction," *IEEE Transactions on Reliability*, vol. 65, no. 1, pp. 310-325, 2016, doi: 10.1109/TR.2015.2451074.

[85] K. Das and R. Kumar, "Electric vehicle battery capacity degradation and health estimation using machine-learning techniques: a review," *Clean Energy*, vol. 7, no. 6, pp. 1268-1281, 2023, doi: 10.1093/ce/zkad054.
[86] Bridge and Mike, *Railway Track Diagrams Book 4 Midlands & North West*. 2013.
[87] Brailsford and Martyn, *Railway Track Diagrams Book 2: Eastern*. 2016, pp. 1, 27.
[88] "Midland Main Line Upgrade Plan – Bedford to Kettering." https://www.networkrail.co.uk/running-the-railway/our-routes/lne-and-em/midland-main-line-improvement-programme/bedfordtokettering/ (accessed 30 April, 2019).
[89] R. FORD. "EAST MIDLANDS IC125 DILEMMA." https://www.modernrailways.com/article/east-midlands-ic125-dilemma (accessed 20 October, 2023).
[90] Z. Tian, P. Weston, S. Hillmansen, C. Roberts, and N. Zhao, "System energy optimisation of metro-transit system using Monte Carlo Algorithm," in *2016 IEEE International Conference on Intelligent Rail Transportation (ICIRT)*, 23-25 Aug. 2016 2016, pp. 453-459, doi: 10.1109/ICIRT.2016.7588768.
[91] "Diesel QSK19-Series." https://www.cummins.com/g-drive-engines/diesel-qsk19-series (accessed 24 March, 2018).
[92] P. Varma. "British Rail Class 222." https://alchetron.com/British-Rail-Class-222 (accessed 14 November, 2022).
[93] Z.-M. Yao, Z.-Q. Qian, R. Li, and E. Hu, "Energy efficiency analysis of marine high-powered medium-speed diesel engine base on energy balance and exergy," *Energy*, vol. 176, pp. 991-1006, 2019/06/01/ 2019, doi: https://doi.org/10.1016/j.energy.2019.04.027.
[94] B. E. AG. "EVB1 - HV - Battery (16 kWh / 400 V or 14 kWh / 350 V)." https://www.brusa.biz/_files/drive/05_Sales/Datasheets//BRUSA_DB_EN_EVB1.pdf (accessed 18 May, 2018).
[95] I. Perin, G. R. Walker, and G. Ledwich, "Load Sharing and Wayside Battery Storage for Improving AC Railway Network Performance With Generic Model for Capacity Estimation—Part 2," *IEEE Transactions on Industrial Electronics*, vol. 65, no. 12, pp. 9459-9467, 2018, doi: 10.1109/TIE.2018.2818641.
[96] Q. Li *et al.*, "A State Machine Control Based on Equivalent Consumption Minimization for Fuel Cell/ Supercapacitor Hybrid Tramway," *IEEE Transactions on Transportation Electrification*, vol. 5, no. 2, pp. 552-564, 2019, doi: 10.1109/TTE.2019.2915689.
[97] M. A. Cusenza, S. Bobba, F. Ardente, M. Cellura, and F. Di Persio, "Energy and environmental assessment of a traction lithium-ion battery pack for plug-in hybrid electric vehicles," *Journal of Cleaner Production*, vol. 215, pp. 634-649, 2019/04/01/ 2019, doi: https://doi.org/10.1016/j.jclepro.2019.01.056.
[98] J.-S. Kim, D.-C. Lee, J.-J. Lee, and C.-W. Kim, "Optimization for maximum specific energy density of a lithium-ion battery using progressive quadratic response surface method and design of experiments," *Scientific Reports*, vol. 10, no. 1, p. 15586, 2020/09/24 2020, doi: 10.1038/s41598-020-72442-4.
[99] L. Goldie-Scot. "A Behind the Scenes Take on Lithium-ion Battery Prices." https://about.bnef.com/blog/behind-scenes-take-lithium-ion-battery-prices/ (accessed 9th Dec, 2020).
[100] "Prices of fuels purchased by manufacturing industry." https://www.gov.uk/government/statistical-data-sets/prices-of-fuels-purchased-by-manufacturing-industry (accessed 14 October, 2020).

[101] J. Stones. "ICIS Quarterly European Hydrogen Markets Q1 2023 Update." https://www.icis.com/explore/resources/news/2023/05/10/10883512/icis-quarterly-european-hydrogen-markets-q1-2023-update/ (accessed 19th August, 2023).
[102] D. S. Satyapal. "Hydrogen and Fuel Cells Overview." DLA Worldwide Energy Conference. https://www.energy.gov/eere/fuelcells/downloads/hydrogen-and-fuel-cells-overview (accessed 20 April, 2018).
[103] X.-j. Gao, H. True, and Y.-h. Li, "Sensitivity analysis of the critical speed in a railway bogie system with uncertain parameters," *Vehicle System Dynamics*, pp. 1-21, 2019, doi: 10.1080/00423114.2019.1674345.
[104] Hui Shi, Zhen You, Zhiming Feng, and Y. Yang, "Identifying the Critical Risks in Railway Projects Based on Fuzzy and Sensitivity Analysis: A Case Study of Belt and Road Projects," *Sustainability*, vol. 11, no. 22, p. 14, 2019. [Online]. Available: https://ideas.repec.org/a/gam/jsusta/v11y2019i22p6187-d283989.html.
[105] S. Gupta, P. Mahajan, and R. Garg, "Sensitivity model of energy consumption by railway electric locomotive," in *2015 Annual IEEE India Conference (INDICON)*, 17-20 Dec. 2015 2015, pp. 1-5, doi: 10.1109/INDICON.2015.7443489.
[106] M. Šíra, A. P. Cucala, A. Fernández-Cardador, and A. Fernández-Rodríguez, "Sensitivities and uncertainties of eco-driving algorithm estimating train power consumption," in *2020 Conference on Precision Electromagnetic Measurements (CPEM)*, 24-28 Aug. 2020 2020, pp. 1-2, doi: 10.1109/CPEM49742.2020.9191703.
[107] P. Mahajan, R. Garg, and P. Kumar, "Sensitivity analysis of pantograph-catenary system model," in *2012 IEEE 5th India International Conference on Power Electronics (IICPE)*, 6-8 Dec. 2012 2012, pp. 1-4, doi: 10.1109/IICPE.2012.6450475.
[108] Y. Liu, Z. Yang, F. Lin, and H. Yang, "Energy Loss Analysis of the Stationary Battery-Supercapacitor Hybrid Energy Storage System," in *2019 IEEE Vehicle Power and Propulsion Conference (VPPC)*, 14-17 Oct. 2019 2019, pp. 1-6, doi: 10.1109/VPPC46532.2019.8952184.
[109] Y. Deng *et al.*, "Simulation-based sensitivity analysis of energy performance applied to an old Beijing residential neighbourhood for retrofit strategy optimisation with climate change prediction," *Energy and Buildings*, vol. 294, p. 113284, 2023/09/01/ 2023, doi: https://doi.org/10.1016/j.enbuild.2023.113284.
[110] I. M. Sobol′, "Global sensitivity indices for nonlinear mathematical models and their Monte Carlo estimates," *Mathematics and Computers in Simulation*, vol. 55, no. 1, pp. 271-280, 2001/02/15/ 2001, doi: https://doi.org/10.1016/S0378-4754(00)00270-6.
[111] J. Morio, "Global and local sensitivity analysis methods for a physical system," *European Journal of Physics*, vol. 32, p. 1577, 10/05 2011, doi: 10.1088/0143-0807/32/6/011.
[112] I. Dimov and R. Georgieva, "Monte Carlo algorithms for evaluating Sobol' sensitivity indices," *Mathematics and Computers in Simulation*, vol. 81, pp. 506-514, 11/01 2010, doi: 10.1016/j.matcom.2009.09.005.
[113] C. Chéron, M. Walter, J. Sandor, and E. Wiebe, "European railway energy roadmap: towards 2030," 2011.
[114] D. f. Transport, "Rail Environment Policy Statement On Track for a Cleaner, Greener Railway," 2021.
[115] J. Baker. "Will the UK ever get electrification back on track?" https://www.railway-technology.com/features/will-uk-ever-get-electrification-back-track/ (accessed 25 Feb, 2019).

[116] Y. Zhang, Z. Tian, C. Roberts, S. Hillmansen, and M. Chen, "Cost optimization of multi-mode train conversion for discontinuously electrified routes," *International Journal of Electrical Power & Energy Systems*, vol. 138, p. 107993, 2022/06/01/ 2022, doi: https://doi.org/10.1016/j.ijepes.2022.107993.
[117] A. Kluth, *Rail Industry Decarbonisation Taskforce FINAL REPORT TO THE MINISTER FOR RAIL*. 2019.
[118] "Long Term Passenger Rolling Stock Strategy for the Rail Industry," 2018. Accessed: 5 Sep 2020. [Online]. Available: https://www.raildeliverygroup.com/files/Publications/2018-03_long_term_passenger_rolling_stock_strategy_6th_ed.pdf
[119] N. Zhao, "Railway traffic flow optimisation with differing control systems," University of Birmingham, 2013.
[120] V. Kachitvichyanukul, "Comparison of three evolutionary algorithms: GA, PSO, and DE," *Industrial Engineering and Management Systems*, vol. 11, no. 3, pp. 215-223, 2012.
[121] D. R. Ramdania, M. Irfan, F. Alfarisi, and D. Nuraiman, "Comparison of genetic algorithms and Particle Swarm Optimization (PSO) algorithms in course scheduling," *Journal of Physics: Conference Series*, vol. 1402, no. 2, p. 022079, 2019/12/01 2019, doi: 10.1088/1742-6596/1402/2/022079.
[122] N. R. Tayebi, F. M. Nejad, and M. Mola, "Comparison between GA and PSO in Analyzing Pavement Management Activities," *Journal of Transportation Engineering*, vol. 140, no. 1, pp. 99-104, 2014, doi: doi:10.1061/(ASCE)TE.1943-5436.0000590.
[123] V. Salim and X. Cai, "A genetic algorithm for railway scheduling with environmental considerations," *Environmental modelling & software*, vol. 12, no. 4, pp. 301-309, 1997.
[124] P. Tormos, A. Lova, F. Barber, L. Ingolotti, M. Abril, and M. A. Salido, "A genetic algorithm for railway scheduling problems," *Metaheuristics for scheduling in industrial and manufacturing applications*, pp. 255-276, 2008.
[125] Y. Shi and R. C. Eberhart, "Empirical study of particle swarm optimization," in *Proceedings of the 1999 Congress on Evolutionary Computation-CEC99 (Cat. No. 99TH8406)*, 6-9 July 1999 1999, vol. 3, pp. 1945-1950 Vol. 3, doi: 10.1109/CEC.1999.785511.
[126] M. Hu, T. Wu, and J. D. Weir, "An Adaptive Particle Swarm Optimization With Multiple Adaptive Methods," *IEEE Transactions on Evolutionary Computation*, vol. 17, no. 5, pp. 705-720, 2013, doi: 10.1109/TEVC.2012.2232931.
[127] B. Son, J. Kim, J. Kim, Y. Kim, and S. Jung, "Adaptive Particle Swarm Optimization Based on Kernel Support Vector Machine for Optimal Design of Synchronous Reluctance Motor," *IEEE Transactions on Magnetics*, vol. 55, no. 6, pp. 1-5, 2019, doi: 10.1109/TMAG.2019.2902935.
[128] J. H. Holland, *Adaptation in Natural and Artificial Systems: An Introductory Analysis with Applications to Biology, Control and Artificial Intelligence*. MIT Press, 1992.
[129] T. E. Davis and J. C. Principe, "A Markov chain framework for the simple genetic algorithm," *Evolutionary computation*, vol. 1, no. 3, pp. 269-288, 1993.
[130] C. Dongchao, "Study of construction strategies for test paper based on genetic algorithm," in *2011 International Conference on E-Business and E-Government (ICEE)*, 2011: IEEE, pp. 1-4.
[131] D. Feng, F. Wang, and Y. Ma, "Improvement of selection and crossover strategy in genetic algorithm," *Computer Engineering*, vol. 34, pp. 189-191, 2008.

[132] B. Fan, C. Roberts, and P. Weston, "A comparison of algorithms for minimising delay costs in disturbed railway traffic scenarios," *Journal of Rail Transport Planning & Management*, vol. 2, no. 1, pp. 23-33, 2012/11/01/ 2012, doi: https://doi.org/10.1016/j.jrtpm.2012.09.002.
[133] B. Fan, "Railway traffic rescheduling approaches to minimise delays in disturbed conditions," University of Birmingham, 2012.